MASTER IN BIOCHEMISTRY AND MOLECULAR AND CELL BIOLOGY RESEARCH FOCUS

Study of the putative role of HIF-1alpha and BNIP3L in the biology of mitochondria in Brucella abortus-infected cells

Martin, Lisa

Award date:
2022

Awarding institution:
University of Namur

Faculté des sciences

STUDY OF THE PUTATIVE ROLE OF HIF-1 ALPHA AND BNIP3L IN THE BIOLOGY OF MITOCHONDRIA IN *Brucella abortus*-INFECTED CELLS

Mémoire présenté pour l'obtention du grade académique de master en Biochimie et Biologie Moléculaire et Cellulaire

Martin Lisa

January 2022

Faculté des sciences

STUDY OF THE PUTATIVE ROLE OF HIF-1 ALPHA AND BNIP3L IN THE BIOLOGY OF MITOCHONDRIA IN *Brucella abortus*-INFECTED CELLS

Mémoire présenté pour l'obtention du grade académique de master en Biochimie et Biologie Moléculaire et Cellulaire

Martin Lisa

January 2022

Université de Namur
FACULTE DES SCIENCES
Secrétariat du Département de Biologie
Rue de Bruxelles 61 - 5000 NAMUR
Téléphone: + 32(0)81.72.44.18 - Téléfax: + 32(0)81.72.44.20
E-mail: joelle.jonet@unamur.be - http://www.unamur.be

Study of the putative role of HIF-1alpha and BNIP3L in the biology of mitochondria in *Brucella abortus*-infected cells

MARTIN Lisa

ABSTRACT :

Brucella abortus are facultative intracellular pathogen, causing Brucellosis, known for their interactions and the subversion of multiple organelles in infected host cells, including mitochondria. The mitochondrion is a dynamic organelle that plays a central role in the cell, involving ATP production, cellular immunity, many syntheses and degradation pathways, regulation of calcium homeostasis and the integration of life-or-death signals. These important roles of mitochondria in the regulation of many biological processes also make the mitochondria an important target for pathogens. *B. abortus* is able to corrupt several functions of the mitochondria to its advantage. Indeed, a glycolytic shift, the fragmentation of the mitochondrial population and induction of mitophagy are observed in both myeloid and non-myeloid *B. abortus*-infected cells. More recently, in the host laboratory, a nuclear accumulation of HIF-1α correlated with Parkin translocation have been observed in *Brucella*-infected HeLa cells or macrophages. In addition, at 48 h post-infection (p.i) time, the induction of mitophagy correlates with the expression of the HIF-1α-target gene encoding BNIP3L was demonstrated.

The major aim of the master thesis was therefore to better understand the putative role of these molecular actors/effectors (HIF-1α, Parkin and BNIP3L) in the induction of mitochondrial fragmentation and/or mitophagy in *B. abortus*-infected HeLa and macrophages.

In this work, we observed a decrease in CFU numbers in macrophages in which HIF-1α is stabilised by a chemical hypoxia ($CoCl_2$ treatment) when the stabilisation of the transcription factor occurs prior to or during the early phase of infection. These observations suggest that the entry and/or survival of the bacteria may be disrupted even if the response is not observed for HeLa infected cells. We also show that the translocation of Parkin in the nucleus of *Brucella*-infected cells is not a robust phenotype while a knock-down of BNIP3L expression in *B. abortus*-infected HeLa cells prevent, at least partially, but significantly, the fragmentation of mitochondria observed in *Brucella*-infected cells. A protective effect of BNIP3L expression silencing was also observed on *B. abortus*-induced mitophagy as assessed by a decreased co-localisation between LC3 and TOM20 in *B. abortus*-infected HeLa cells. Finally, we focused on the erUPR response potentially involved in the upregulation of autophagic/mitaphagic pathways. We found that activation of the IRE1 pathway occurs in HeLa cells infected with *B. abortus* at 24 and 48 h p.i. However, the use of siRNA directed against IRE1 did not have any effect on the induction of BNIP3L nor on mitochondrial fragmentation induced by *B. abortus* in HeLa cells.

In conclusion, in this work, we showed that the mitochondrial fragmentation and mitophagy triggered by *Brucella* during its intracellular trafficking in the host cells might be mediated by BNIP3L but not Parkin.

Mémoire de master 120 en biochimie et biologie moléculaire et cellulaire

Janvier 2022

Promoteur: Thierry Arnould

Co-promotteur : Xavier De Bolle

Université de Namur
FACULTE DES SCIENCES
Secrétariat du Département de Biologie
Rue de Bruxelles 61 - 5000 NAMUR
Téléphone: + 32(0)81.72.44.18 - Téléfax: + 32(0)81.72.44.20
E-mail: joelle.jonet@unamur.be - http://www.unamur.be

ETUDE DU ROLE PUTATIF DE HIF-1ALPHA ET BNIP3L DANS LA BIOLOGIE DES MITOCHONDRIES DE CELLULES INFECTEES PAR *BRUCELLA ABORTUS*

MARTIN Lisa

RÉSUMÉ :

Les *Brucella abortus* sont des pathogènes intracellulaires facultatifs, responsables de la brucellose, connus pour leurs interactions et la subversion de multiples organelles dans les cellules hôtes infectées, y compris les mitochondries. La mitochondrie est un organite dynamique qui joue un rôle central dans la cellule, impliquant la production d'ATP, l'immunité cellulaire, de nombreuses voies de synthèse et de dégradation, la régulation de l'homéostasie du calcium et l'intégration des signaux de vie ou de mort. Les mitochondries sont impliquées la régulation de nombreux processus biologiques qui font de la mitochondrie une cible privilégié pour les agents pathogènes. *B. abortus* est capable de corrompre plusieurs fonctions de la mitochondrie à son avantage. En effet, un changement glycolytique, la fragmentation du réseau mitochondriale et l'induction de la mitophagie sont observés dans les cellules myéloïdes et non myéloïdes infectées par *B. abortus*. Plus récemment, dans le laboratoire de recherche d'accueil, une accumulation nucléaire de HIF-1α corrélée à la translocation de Parkin ont été observées dans les cellules HeLa ou les macrophages infectés par *Brucella*. De plus, à 48 h post-infection (p.i), l'induction de la mitophagie corrélée à l'expression du gène cible de HIF-1α codant BNIP3L a été démontrée.

L'objectif majeur de ce mémoire était donc de mieux comprendre le rôle putatif de ces acteurs/effecteurs moléculaires (HIF-1α, Parkin et BNIP3L) dans l'induction de la fragmentation mitochondriale et/ou de la mitophagie dans les HeLa et les macrophages infectés par *B. abortus*.

Dans ce travail, nous avons observé une diminution du nombre de UCF dans les macrophages dans lesquels HIF-1α est stabilisé par une hypoxie chimique (traitement au $CoCl_2$) lorsque la stabilisation du facteur de transcription intervient avant ou pendant la phase précoce de l'infection. Ces observations suggèrent que l'entrée et/ou la survie des bactéries peuvent être perturbées même si cette réponse n'est pas observée pour les cellules HeLa infectées par *B. abortus*. Nous montrons également que la translocation de la Parkin dans le noyau des cellules infectées par *Brucella* n'est pas un phénotype robuste tandis qu'un knock-down de l'expression de BNIP3L dans les cellules HeLa infectées par *B. abortus* prévient, au moins partiellement, mais de manière significative, la fragmentation des mitochondries observée dans les cellules infectées par *Brucella*. Un effet protecteur de l'inhibition de l'expression de BNIP3L a également été observé sur la mitophagie induite par *B. abortus*, comme l'indique la diminution de la co-localisation entre LC3 et ATPs-β dans les cellules HeLa infectées par *B. abortus*. Enfin, nous nous sommes concentrés sur la réponse erUPR potentiellement impliquée dans la régulation à la hausse des voies autophagiques/mitaphagiques. Nous avons constaté que l'activation de la voie IRE1 se produit dans les cellules HeLa infectées par B. abortus à 24 et 48 h p.i. Cependant, l'utilisation de siRNA dirigé contre IRE1 n'a eu aucun effet sur l'induction de BNIP3L ni sur la fragmentation mitochondriale induite par B. abortus dans les cellules HeLa.

En conclusion, dans ce travail, nous avons montré que la fragmentation mitochondriale et la mitophagie déclenchées par Brucella pendant son trafic intracellulaire dans les cellules hôtes pourraient être médiées par BNIP3L mais pas par la Parkin.

Mémoire de master 120 en biochimie et biologie moléculaire et cellulaire

Janvier 2022

Promoteur: Thierry Arnould

Co-promotteur : Xavier De Bolle

REMERCIEMENT

C'est en arrivant au bout de ces 10 mois que l'on arrive à prendre un peu de recul pour observer tout ce beau chemin parcouru. Il n'a certes pas toujours été bien plat mais c'est ce qui en fait sa beauté. Tout au long de ce cheminement, j'ai été accompagné par de belles personnes qui laisseront à tout jamais une trace indélébile.

Je souhaite tout d'abord remercier l'ensemble des professeurs de l'URBC pour l'accueil chaleureux au sein de leur laboratoire. Je tiens également à remercier tout particulièrement mon promoteur Thierry Arnould pour ses conseils précieux, ses nombreuses corrections, son soutien, ses encouragements et son exigence scientifique qui m'ont permis d'évoluer dans le monde de la recherche bien plus que ce que je n'aurai pu imaginer en commençant. Je tiens à remercier également mon co-promoteur Xavier De Bolle, pour m'avoir accueilli dans son labo en URBM.

Aucun merci ne pourra être à la hauteur, pour remercier Jérémy Verbeke, mon tuteur. Il a pu m'accompagner tout au long de ce parcours avec une extrême gentillesse, une générosité et une disponibilité sans faille. Il nous a fait découvrir le magnifique monde de la recherche, nous a transmis son savoir en toute humilité et nous a merveilleusement soutenu tout au long de ce parcours. J'espère avoir été à la hauteur de tes attentes. Merci pour tout.

Ensuite, la team *Brucella* ne serait pas une team sans mon super, fidèle compatriote, collègue et ami Youri Fayt. Il a été d'une aide et d'un soutien précieux tout au long de ce mémoire. Je tiens également à le féliciter pour son travail, sa détermination et ses innombrables lectures d'articles qui m'ont toujours beaucoup impressionnée. Nous avons formé une belle équipe de choc, alors merci.

J'aimerai ensuite remercier l'ensemble des Doctorants pour leur soutien, leur conseil mais également tous ses moments partagés tout au long de ce mémoire. Ces moments de sérieux, ou non, ont contribués à rendre ce mémoire beaucoup plus pétillant. Merci plus particulièrement à Damien, Myriame, Sébastien, Karim, Marino, Joëlle, Giacomo.

Un mémoire n'est pas un mémoire sans son équipe de mémorants !! Mes chers amis, vous avez été d'un soutien sans faille, de réel pilier lors de ces 10 mois. Je voudrais vous remercier pour ces moments de sérieux, ces moments de rire ou de fou rire, de joie, de stress, … que nous avons traversé ensemble.

Merci à ma chère petite Louise, ma wild woman, pour nos moments bouffe, introspection, voyage, … Tu es une personne magnifique et on n'en aura pas fini de sitôt. Je compte encore sur toi pour nous entrainer dans des soirées ou voyages de folie !

Merci à ma belle Amandine, ma fashionista, pour nos moments d'échange, nos fous rire et tes nombreux conseils. Tu nous as apporté folie et rire pour notre plus grand bonheur alors ne t'arrête jamais de briller, de rire et d'avoir la tête dans les étoiles.

Merci à Ines, ma belle force tranquille, pour ton apaisement, ta joie et ta bonne humeur ! Ensemble nous avons affronté les nombreuses procédures du Canada, une autre belle épreuve. Jamais je ne pourrai oublier ton immense gentillesse.

Merci à Manon et ses nombreux pulls à papy, toujours d'un style incroyable ! Tu as été tellement courageuse, sans jamais baisser les bras et toujours d'un soutien indéfectible. Tu es une merveilleuse personne.

Merci à Coline, pilote pour Düsseldorf, bien que tes chevilles n'aient pas toujours été en grande forme sur ce mémoire, tu n'as jamais rien lâché et tu as également pu te confronter aux douces formalités du Canada. On s'y retrouve là-bas avec ton beau sourire et ta joie de vivre.

Merci à Thomas, mon accompagnateur pour la bouffe et le café, pour nos belles discussions, ton incroyable sens de l'humour et tes attentions tout au long de ce mémoire ! Tu es quelqu'un de formidable alors ne l'oublie pas.

J'aimerai également remercier l'ensemble du staff technique pour l'aide qu'ils nous ont apporté tout au long de ce mémoire. Et peut-être également plus particulièrement Dorian pour nous échanges lors des temps de midi. Un labo sans vous tourne beaucoup moins bien. Alors merci pour tout.

Je me dois également de remercier l'ensemble des membres de l'URBM qui m'ont accueilli au sein de leur labo et également au sein de BL3.

Et finalement un tout grand merci à ma petite famille, pour le soutien tout au long de ce mémoire. Sans eux ces 10 mois auraient été bien plus compliqué. Merci à mes parents, mes sœurs, mes grands-parents et également mon amoureux pour avoir été à mes côtés tout du long.

TABLE DES MATIERES

LIST OF ABBREVIATIONS

A

Activated macrophages (M-1)

Activating transcription factor 6 (ATF6)

Adherent and invasive E. coli (AIEC)

AIM receptors (AIM2)

Alternatively activated macrophages (M-2)

Apoptosis-associated speck-like protein containing a CARD (ASC)

Aspect ratio (AR)

Autophagic BCV (aBCV)

Autophagy activating molecule regulated by Beclin 1-, protein 1 (AMBRA1)

Autophagy genes (ATG)

B

BAB1_0678 (BspA)

BAB1_0678 (BspA)

BAB1_0712 (BspB)

BAB1_0847 (BspC)

BAB1_1948 (BspF)

B-cell lymphoma 2 (BCL2

BCL2 interacting protein 3-like (BNIP3L)

BCL2-interacting protein (BNIP)

Breast cancer susceptibility gene 1 (BRCA1)

Breast cancer susceptibility gene 1 (BRCA1) gene (NBR1)

Brucella species (Brucella spp)

Brucella-containing vacuole (BCV).

Brucella Toll/Interleukin-1 Receptor (TIR)-domain-containing proteins (Btp)

C

Carbonyl cyanide 4-(trifluoromethoxy) phenylhydrazone (FCCP)

Carcinoembryonic antigen-related (CEA) Cell Adhesion Molecule 6 (CEACAM6),

Casein kinase II (CKII)

Coat Protein complex II (COPII)

Conserved oligomeric Golgi (COG)

D

Dentritic cells (DC)

Disulfide isomerase (PDI)

Dynamin-Related Protein 1 (Drp1)

E

Early endosome antigen-1 (EEA-1)

Endoplasmic reticulum (ER) exits sites (ERES)

Endoplasmic reticulum (ER)

Endosomal BCV (eBCV)

Endpoint/branch-point ratio (EBR)

Eostrogen related receptor α (ERRα)

ER quality control (ERQC)

ER-associated degradation (ERAD)

ER-to-Golgi intermediate compartment (ERGIC)

erUPR (Endoplamic Reticulum Unfolded Protein Response)

Erythropoietin (EPO)

F

FK506 binding protein 8 (FKBP8)

FUN14 domain-containing protein 1 (FUNDC1)

FYVE 1 domain (DFCP1)

G

γ-aminobutyric acid receptor-associated proteins (GABARAPs)

Glucose transporter 1 (GLUT1)

Glyceraldehyde-3-phosphate deshydrogenase (GAPDH)

Glycosylphosphatidylinositol (GPI)

GTPase-activating protein (GAP)

Guanylate-binding protein (GBPs)

H

Homocysteine-inducible ER stress protein (Herp)

Homotypic fusion and protein sorting complex (HOPS)

Hypoxia-inducible factor 1 (HIF-1)

Hypoxic response element (HRE)

I

i-AAA protease (YME1L)

Inducible nitric oxide synthase (iNOS)

Inhibitor of nuclear factor kappa-B kinase E/ TANK binding kinase 1 (IKKE/TBK1)

Inner mitochondrial membrane (IMM),

Inositol-requiring protein 1α (IRE1α)

Interacting with PhosphoInositides (WIPIs)

Interferon (INFs)

Interleukin (IL)

Interleukine-1 receptor-accosiated kinase 4 (IRAK4)

J

Janus Kinase 2 (JAK2

Jun N-terminal kinase (JNK)

JUN N terminal kinase (JNK)

K

Knock down (KD)

Knock-out (KO)

L

LC3 interaction region (LIR)

Light Chain-3 (LC3)

Lipopolysaccharide (LPS)

Lysosomal-associated membrane protein 1 and 2 (LAMP-1/2)

M

M-AAA protease (OMA1)

Matrix targeting signal (MTS)

Mitochondria-Associated ER Membranes (MAMs)

Mitochondrial contact site and Cristae Organizing System (MICOS)

Mitochondrial dynamics proteins of 49 kDa (MiD49)

Mitochondrial fission 1 protein (FIS1)

Mitochondrial fission factor (MFF)

Mitochondrial intermembrane space (IMS)

Mitochondrial permeability transition pore (mPTP)

Mitochondrial protein of 18 kDa (MTP18)

Mitochondrial transcription factor (TFAM)

Mitogen-activated protein kinase (p38 MAPK)

Mouse embryo fibroblast (MEF)

Mitochondrial DNA (mtDNA)

Myeloid differentiation primary response gene 88 (MyD88)

N

Natural Killer (NK)

Neonatal rat ventricular myocytes (NRVMs)

Nicotinamide adenine dinucleotide (NADH)

Nitric oxide syn- thase (NOS)

Nitrite oxide reductase (NorD)

NOD-like receptor family (NLRP3)

Normal Human Epidermal Keratinocytes (NHEKs)

Nuclear domain 10 protein 52 (NDP52)

Nuclear factor-κB (NF κB)

Nuclear factor erythroid 2 related factor 2 (NRF2)

O

Optic atrophy 1 (OPA1)

Optineurin (OPTN)

Outer mitochondrial membrane (OMM)

Oxidative phosphorylation (OXPHOS)

Oxygen pressure (PO2)

Pathogen- or damage-associated molecular patterns (PAMPs or DAMPs)

Phosphatidyl inositol 3 phosphate (PI3P)

Phosphatidylcholine (PC)

phosphatidylethanolamine (PE)

polymorphonuclear cells (PMN)

Post-infection (p.i)

Post-transfection (p.tr.)

Post-treatment (p.t)

Prohibitin 2 (PHB2)

Proliferator-activated receptor-γ co-activator 1α (PGC1)

Protein kinase RNA-like ER protein Kinase (PERK)

PTEN-induced putative kinase 1 (PINK1)

PX-478 (S-2-amino-3-[4-N,N,-bis(2-chloroethyl)amino] phenyl propionic acid N-oxide dihydrochloride)

R

RB1 inducible coiled-coil protein 1 (FIP200)

Rab2 interacting conserved protein A (RicA)

Reactive oxygen species (ROS)

Replicative BCV (rBCV)

S

Sarco-/endoplasmic reticulum (SR/ER)

Secretion associated ras-superfamily gene1 (SAR1)

Signal transducer and activator of transcription 1 (STAT1)

Signalling Intermediate in Toll (ESCIT)

Single guide RNA (sgRNA)

Small interfering RNA (siRNA)

Soluble N-éthylmaleimide-sensitive-factor Attachment protein Receptor (SNAREs)

Stimulator of IFN genes (STING)

Stress-induced mitochondrial hyperfusion (SIMH)

Superoxide dismutase (enzymes found in the mitochondria (SOD2) or in the cytosol (SOD1))

Superoxide dismutase (SOD)

Synaptosomal- associated protein 29 (SNAP29)

Syntaxin 17 (STX17)

T

TAX1-binding protein 1 (TAX1BP1)

TBC domain family member 15 (TBC1D15)

Thioredoxin-interacting protein (TXNIP)

Third sgRNA (sgRNA3)

Toll-Like Receptors (TLRs)

TNF receptor-associated factor 6 (TRAF6)

Toll/IL-1R domain-containing adapter inducing IFN-B (TRIF)

Toll/Interleukin-1 receptor (TIR)

Transcription factor, the inositiol requiring enzyme 1 (IRE1)

Translocase of the outer membrane (TOM)

Transmembrane domain (TM)

Tricarboxylic acid (TCA)

Tumor Necrosis Factor (TNF)-

Type IV secretion system (T4SS)

U

UDP-N-acetylglucosamine (GlcNAc)

Unc-51-like kinase complex (ULK1)

Unfloding Protein Response (UPR)

Unspliced X box-binding protein 1 (XBP1u)

V

Vacuolar protein 34 (VPS34)

Vascular Epithelium Growth Factor (VEGF)

Vacuolar protein (VPS)

Vesicular and tubular clusters (VTC)

Vesicular transport factor (p115)

Voltage-dependent anion channels (VDACs)

W

WD-repeat protein Interacting with PhosphoInositides (WIPIs)

Y

YPT-interacting protein 1A (Yip1A)

Introduction and Objectives

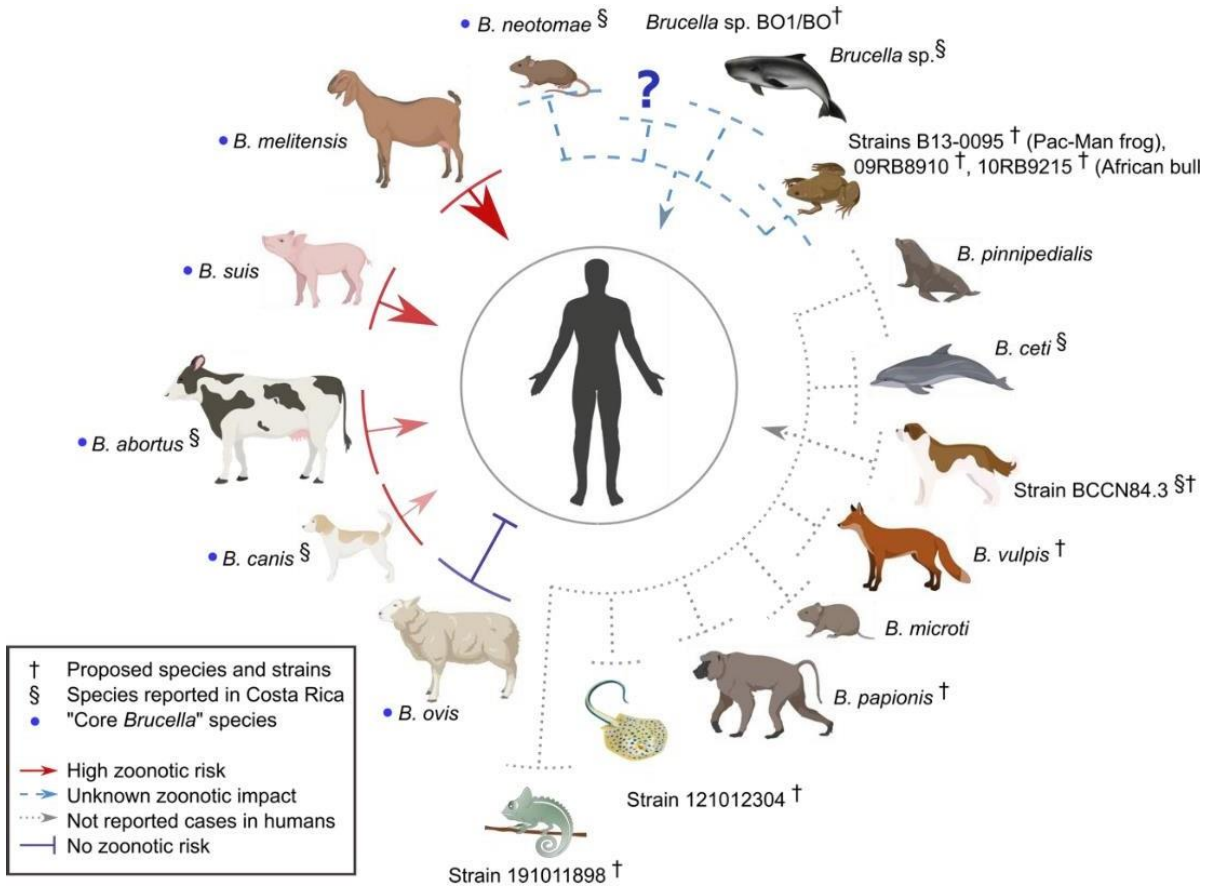

Figure 1: Zoonotic potential of various *Brucella* species (Suárez-Esquivel et al., 2020).
The potential to induce zoonosis varies according to the species of *Brucella* that may be encountered by humans. The arrows indicate the risk of zoonosis, and the size of the arrow indicates the probability of catching it. Each species is linked to its preferred or presumed preferred host.

1 INTRODUCTION

1.1 Bacteria of the genus *Brucella*

1.1.1 Taxonomy

Bacteria of the genus *Brucella* belong to the Proteobacteria phylum. This name refers to the Greek name "protean" which means “first”. It is also related to the shape-shifting god Proteus, which is a nice coincidence(Suárez-Esquivel et al., 2020). This phylum contains 5 classes including the class of Alpha-proteobacteria in which *Brucella* are found. This class consists of bacteria that differ both in shape, lifestyle, and metabolic capacity. Lifestyles can vary from free-living, commensal, endosymbiotic to opportunistic and intracellular pathogens of eukaryotic cells. One of the great characteristics of this class is that it is intimately related to all complex forms of life as it possessed the ancestor of the mitochondrion(Kämpfer et al., 2013).

The Alpha-proteobacteria contain the order of the Rhizobiales. This order contains both bacteria that can fix oxygen when in symbiosis with leguminous plants and bacteria that are pathogenic to animals and plants(Kämpfer et al., 2013). The Brucelleae familly which includes the genera *Pseudochrobactrum*, *Falsochobactrum*, *Ochrobactrum* and *Brucella*. This order is characterised by gram-negative organisms with a form that is close to the bacile. The bacteria are occasionally motile, do not produce spores and have an aerobic respiratory metabolism[2]. Bacteria of the genus *Brucella* were then distinguished by different species based on phenotypic and biochemical analyses as well as by host preference (**Figure 1**). The homogeneity of the *Brucella* genome, which is more than 90% identical between the different species, has made classification challenging and has led to perpetual shuffling both from a species and an intra-species perspective(Garin-Bastuji et al., 2014).

Brucella currently has 12 identified species (*Brucella spp*.) among which 4 are recognised as human pathogens: *Brucella abortus*, *Burcella melitensis*, *Brucella suis* and *Brucella bovis*(Suárez-Esquivel et al., 2020).

These 12 species can be classified into 2 categories: 1) the "most commonly encountered" species: *B. abortus*, *B.melitensis*, *B. suis*, *B. canis*, *B. neotomae*. 2) the newly discovered species: *B. microti*, *B. ceti*, *B. pinnipedialis*, *B. inopinata*, *B. vulpis*, *B. papionis*.

Based on their phenotypic characteristics, host preferences, biochemical or growth characteristics, a taxonomic scheme can be identified and thus allow the classification of bacteria of the genus *Brucella* into different biovars(Kang et al., 2015). For example, *B. abortus* is subdivided into 8 biovars(Neta et al., 2010). A better understanding of the genome of these bacteria will also help to refine this classification.

1.1.2 Bacteriological characteristics

Bacteria of the genus *Brucella* are gram-negative facultative intracellular pathogens. This term refers to the fact that *Brucella spp*. do not depend exclusively on their intracellular habitat for survival, unlike obligate intracellular pathogens. These bacteria are small coccobacilli, which remain individual and measure between 0.6-1.5 µm. These bacteria are not motile, do not sporulate and are non-capsulated bacteria(GŁOWACKA et al., 2018).

Brucella spp multiply in phagocytic cells and non-phagocytic cells. Due to their intracellular cycle, *Brucella* can survive in an acidic environment with low oxygen and nutrient concentrations(GŁOWACKA et al., 2018). They can also survive from a few weeks to a few months in dust, water, abortion tissue, meat, and dairy products(Suárez-Esquivel et al., 2020).

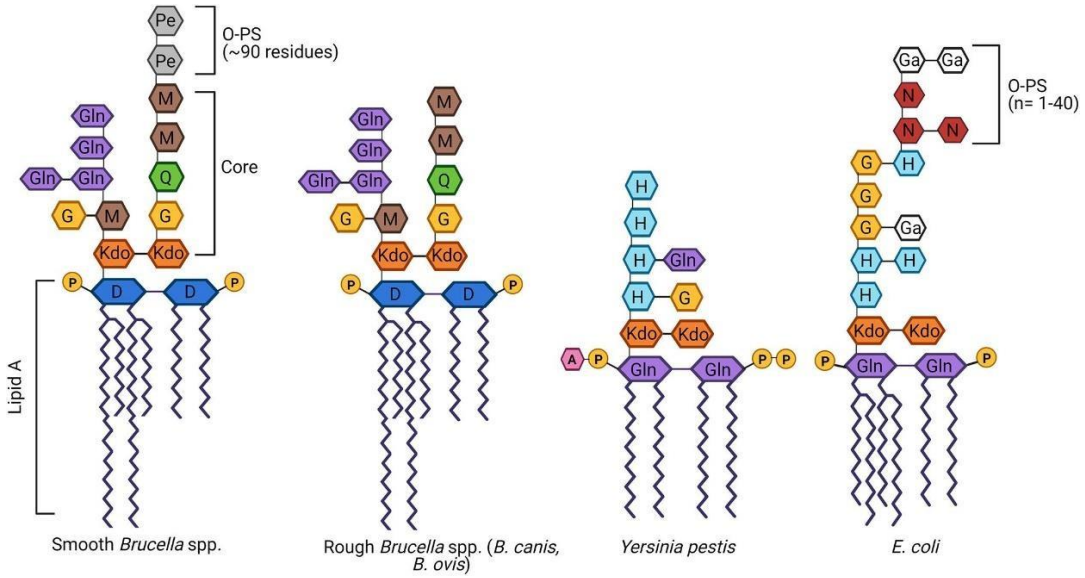

Figure 2: Representation of the structure of lipopolysaccharide (LPS) of *Brucella* spp. compared to other Gram-negative bacteria (Stranahan & Arenas-Gamboa, 2021).
Brucella spp. has two forms of LPS: smooth (S-LPS) and rough (R-LPS). *Brucella* LPS differ from other Gram-negative bacteria mainly through their lipid A which has a very long acyl group chain composed of a diamino-glucose backbone connected to the body by amide bonds. These characteristics lead to lower endotoxicity, in contrast to bacteria such as *E. coli* and *Yersina pestis* that have a much shorter lipid A connected to the body by amide and ester bond and does not have a laterally branched core.

The difference between the smooth and the rough LPS comes respectively from the absence or presence of O-liposaccharides.

D, diamino-glucose; G, glucose; Ga, galactose; Gln, glucosamine; H, heptose; 3-deoxy-D-mannose-2-octulosonic acid, Kdo; M, mannose; N, N-acetylglucosamine; Pe, N-formylperosamine; Q, quinovosamine.

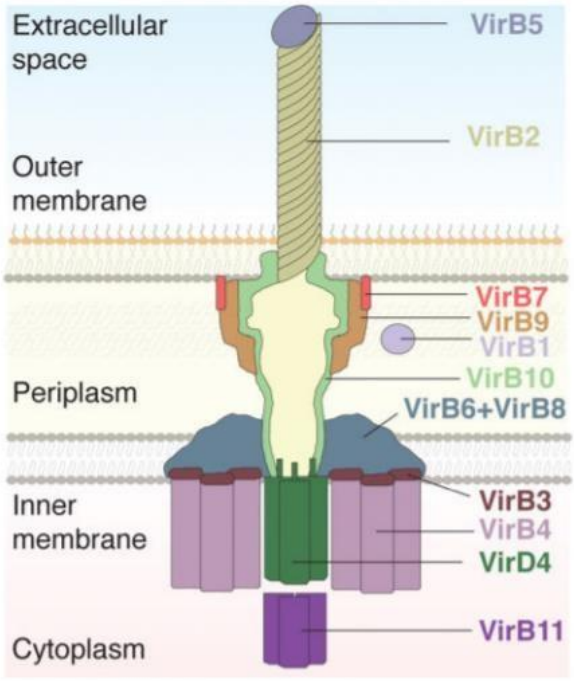

Figure 3: Representation of the structure of type IV secretion (T4SS) (Grohmann et al., 2018). T4SS is a composite structure composed of functional protein modules that can be classified into 4 groups based on their function or subcellular location: i) Cytoplasmic ATPase with VirB4, VirD4 and VirB11, ii) Inner membrane platform component with VirB3, VirB6 and VirB8, iii) Component of the periplasmic body with VirB7, VirB6 and VirB8, and finally iv) Component of the pilus with VirB1 transglycosylase, VirB2 pilin and VirB5 pilus-tip protein. T4SS can be identified as a nanomachine allowing both the specific recognition of a substrate repertoire and the specific delivery of effectors into prokaryotic and eukaryotic cells.

Table 1: *Brucella species,* their preferred host, and the zoonotic potential

Species	Preferred host	Zoonotic potential
Brucella melitensis	Sheep, goat (Ovis spp and Capra spp	High
Brucella abortus	Cattle (Bos taurus and Bos indicus)	Moderate
Brucella suis	Pig (Sus scrofa)	Moderate
Brucella canis	Dog (Canis lupus familiaris)	Mild
Brucella ceti	Dolphin, porpoises, whale (Cetacea)	Mild
Brucella ovis	Sheep (Ovis spp)	No reported infections

One common feature of gram-negative bacteria is the structural element of the outer membrane, lipopolysaccharide (LPS). *Brucella* possess two forms of LPS: smooth LPS (S-LPS) or the rough LPS (R-LPS) as a major surface antigen (**Figure 2**)(Stranahan and Arenas-Gamboa, 2021). The particularity of *Brucella* is that their LPS is unconventional and non-endotoxic and therefore, confers a defence and leads to a modulation of the host's immunity(Cardoso et al., 2006). Species such as *Brucella suis*, *Brucella abortus* and *Brucella melitensis*, which are pathogenic to humans, possess a S-LPS. To go into more details about the LPS produced by Brucella species, we need to look at its composition. LPS is composed of a lipid A that has an oligosaccharide core and an O antigen. The endotoxicity of LPS lies in the composition of this lipid A, which in the case of *Brucella*, is less toxic and less active than for other Gram-negative bacteria(Stranahan and Arenas-Gamboa, 2021).

Another virulence factor found in Brucella is the type IV secretion system (T4SS). This is a multi-protein complex encoded by the VirB operon (**Figure 3**)(GŁOWACKA et al., 2018). The expression of this operon is regulated by quorum sensing which results in the expression of twelve proteins(Foulongne et al., 2002). This multiprotein complex is important for the secretion of bacterial macromolecules and is extremely important for the intracellular life cycle of the bacteria (see section 1.2.3)(Marchesini et al., 2011).

Several proteins such as Superoxide dismutase, Nitrite oxide reductase and catalase will also enable *Brucella* to survive in a hostile environment(GŁOWACKA et al., 2018). Indeed, immune cells set up bactericidal conditions to limit infection such as production of reactive oxygen species (ROS), acidification of endocytic vesicles and production of nitrite(West, Brodsky, et al., 2011). It is therefore necessary for the bacteria to counter or diminish the deleterious effect of these events. The main line of defence for the bacteria will be to limit these bactericidal conditions by enzymatic reactions. Superoxide dismutase (SOD) and catalase as well as alkyl hydroperoxide reductases can be used against ROS. The acidification of the microenvironment during intracellular trafficking will be controlled by urease while the production of nitrite will be detoxified a nitrite oxide reductase (NorD)(GŁOWACKA et al., 2018).

1.2 Brucellosis from the host perspective

Depending on the bacterial species, the preferred host will vary, mainly affecting ruminants for *Brucella abortus*, goat and sheep for *Brucella melitensis*, pig for *Brucella suis.* The host can serve as reservoirs and facilitate the transmission to humans. Again, the different *Brucella species* are not equivalent in terms of the probability of transmission to humans(Suárez-Esquivel et al., 2020)**(Table 1)**.

Brucellosis is one of the most widespread bacterial zoonosis that affects 500 000 people per year and has a huge socioeconomic cost, mainly, in developing countries(Atluri et al., 2011). Indeed, Brucellosis reduces cattle fertility and milk production leading to a decrease in consumable goods in poor countries(G et al., 2006). Brucellosis starts as a debilitating acute infection that can become chronic, consumes resources for the treatment of patients, and reduces the ability of the patient to support their family. In the worst-case scenario, if left untreated by appropriate antibiotic treatment (as no effective human vaccine is currently available), the infection can lead to the death of the patient(Franco et al., 2007).

In the next section, a more precise description of the clinical signs and pathogenicity of *Brucella abortus* will be given.

1.2.1 Clinical signs

1.2.1.1 In ruminants

In ruminants, brucellosis leads to a predominantly reproductive disease (such as infertility or abortion) that affects both females and males, but the bacteria can also affect many other cell types, allowing its escape from the immune system(Neta et al., 2010).

In cattle, the most common route of infection is ingestion of contaminated feed or water. The bacteria will be able to cross the intestinal mucosal barrier to reach the lymph node in which *Brucella* can replicate in macrophages. There will then be a tropism for the reproductive organs of livestock. This tropism is due to the erythritol and steroid hormones which will favour the survival of the bacteria in these tissues, as they will be used as a carbon source(Atluri et al., 2011).

The disease can be divided into three phases; the incubation period, during which no symptoms can be seen, the acute phase which represents the phase of active growth of the bacteria within the tissue, it is at that time that the first signs may appear, and finally the chronic phase, the replication of the bacteria reaches a plateau phase before decreasing. It is also at that time that the symptoms will clearly appear(Mellado et al., 2013; Neta et al., 2010).

Infection in non-pregnant cows is generally asymptomatic. Nevertheless, pregnant females will be prone to placentatis leading to abortions in the last trimester of pregnancy. Several warning symptoms can also be detected in pregnant females; fever, vaginal bleeding, swollen mammary glands and enlarged udders. Significant *Brucella* secretion will also be found in milk, vaginal secretions, and abortion tissue. Calves born from infected cows may be contaminated vertically in 60-70 % of cases either by passage through the uterine tract or by suckling colostrum or milk of infected cows(DÍAZ APARICIO, 2013).

Bulls may also be affected in their reproductive system. Inflammation of the testicles, epididymis and seminal vesicles is often reported. If the inflammation becomes chronic, fibrosis of the testicular parenchyma may occur, leading to infertility(Neta et al., 2010).

1.2.1.2 In humans

Humans can be infected by *Brucella* but are considered as an accidental host or dead-end host in view of the rare human-to-human infections. Brucellosis is highly endemic in the Mediterranean basin, Middle East, Western Asia, Africa, and South America(G et al., 2006). The most common routes of infection in humans are ingestion of contaminated and unpasteurised milk products, inhalation or contact between an open wound and secretions from contaminated animals or abortion waste. Exceedingly rare cases of human-to-human contamination have been observed(de Figueiredo et al., 2015; O'Callaghan, 2020). Brucella penetrate the mucosal barrier and preferentially infect phagocytic cells. These cells can then reach the lymph nodes before a dissemination to the various organs of the body could be observed, with a preference for the organs of the reticuloendothelial system(Moreno & Barquero-Calvo, 2020).

The symptoms of brucellosis will be related to the route of infection, the immune system of the host and the organs affected by the infection. Brucellosis initially causes unspecific symptoms that are like a feverish state. But left untreated, it can become chronic and lead to disabling and debilitating severe symptoms(Franco et al., 2007).

The disease can be divided into three phases. A latency (asymptomatic) phase, which can last 2 to 4 weeks after the inoculation of the bacteria. The acute and sub-acute phases occur

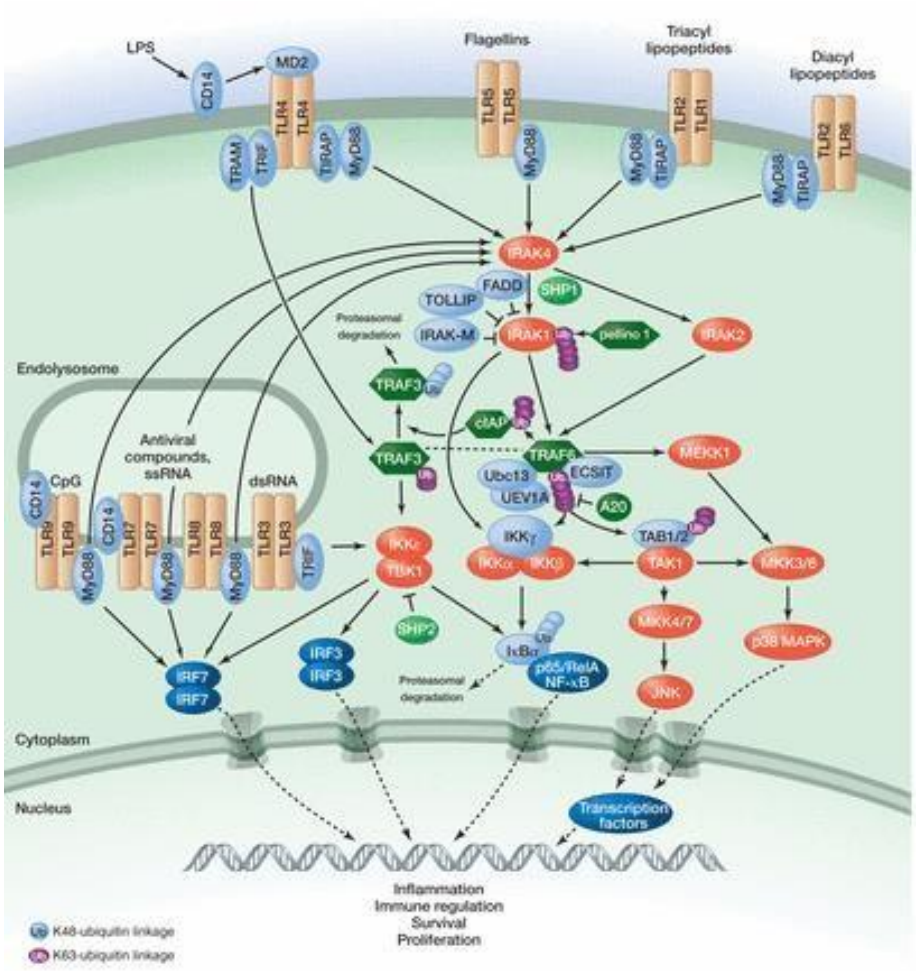

Figure 4: Toll like receptors: organization and signaling pathways (Lim and Staudt, 2013).

Toll like receptors (TLR) are present on dendritic cells, macrophages and plasmacytoid dendritic cells. There are two types of TLRs; TLRs localized in plasma membrane (TLR2, TLR4, TLR5 and TLR11) and other localized in endosomes (TLR3, TLR7 and TLR9). Those found on the surface of endosomes are brought by the ER-localized transporter protein UNC-93B. Some receivers may need adapters like the Toll-interleukin-1 Receptor (TIR) domain-containing adaptor protein (TIRAP) to link MyD88 or TRIF-related adaptor molecule (TRAM) to link TIR Domain-containing Adaptor-inducing Interferon-B (TIRF). MyD88 and TIRF represent the two main signalling pathways of TLR signalling. Recognition of ligand allows the recruitment of a whole series of adapters containing a TIR domain. Myeloid differentiation factor 88 (MyD88) is recruited for each TLR except for TLR3. In the MyD88-dependent pathway, MyD88 recruits the interleukin-1 receptor-associated kinase (IRAK) family of proteins and TNF receptor associated factor 6 (TRAF6). In turn, TRAF6 activates Transforming growth factor-β (TGF-β)-activated kinase 1 (TAK1). The activated TAK1 activates the NF-κB (IκB) kinase (IKK) complex, which activates NFκB subunits. The activated TAK1 also activates the MAPK pathway. These molecules initiate the transcription and translation of various proinflammatory cytokines, chemokines, IFNs and other TLR-inducible genes.

TIRF-dependent signalling pathway is initiated by TLR3 and TLR4. In the TRIF-dependent pathway, TRIF interacts with TRAF3 which is recruiting TBKI and IKKi for the phosphorylation of Interferon Regulatory Factor 3 (IRF3) and IRF7. Phosphorylated IFR3 and IRF7 translocate to the nucleus and initiates the transcription of type I INFs.

in the first 2 months after infection with dissemination of the bacteria within the various organs of the organism(Godfroid et al., 2011). As mentioned, the symptoms are often unspecific with fever, malaise, fatigue, and anorexia. Finally, the chronic phase is declared when symptoms continue beyond 12 months. The symptoms reported during this period are often related to the establishment of the replicative niche of the bacteria within one or more organs. These localised infections can lead to endocarditis, meningoencephalitis, arthritis, orchitis, spondylitis, osteomyelitis, and recurrent febrile conditions(González-Espinoza et al., 2021). Meningoencephalitis and endocarditis can in extreme situations, lead to the death of the patient.

Brucellosis can be treated using two synergistic antibiotics. The antibiotics used are often doxycycline, rifampin, streptomycin (or other aminoglycosides) or trimethoprim-sulfamethoxazole (co- trimoxazole)(Godfroid et al., 2011). It is a treatment that requires high doses over an extended period that does not allow the avoidance of relapse. When focal complications and chronic courses are observed, the use of triple or tetra combinations of antibacterial drugs is required(Atluri et al., 2011).

1.2.2 Immune response

The immune response plays overriding role in *B. abortus* infection, particularly innate immunity. At the start of the infection, innate immunity kicks in and eliminate about 90% of the bacteria(Amjadi et al., 2019). This eviction is both insufficient to counteract the infection and may influence the development of a protective adaptive immunity(Neta et al., 2010). The first cells to recognise the bacteria are neutrophils, macrophages, and dendritic cells (DC). These cells express Toll-Like Receptors (TLRs) which are located both in the plasma membrane or on the endosome TLRs become active through the recognition of conserved components of the micro-organisms, called pathogen-associated molecular patterns (PAMPs)(Kumar et al., 2009; Lim & Staudt, 2013). These components are for example LPS found on the surface of Gram-negative bacteria, peptidoglycans, bacterial genomic DNA which are recognised by TLR4, TLR2 and TLR9, respectively, converging towards the activation of genes that encode pro-inflammatory cytokines or Type I Interferon (INFs) (**Figure 4**)(Neta et al., 2010).

The secretion of these pro-inflammatory molecules first activates the adaptive immunity to fight the infection effectively. Interleukin (IL)-12 stimulates the activation of CD4+ T cells and their differentiation into Th1 (T-cells that induce macrophage activation)(Godfroid et al., 2011). Cytokines also allows the activation of CD8+ T cells. INF, also secreted by Natural Killer (NK) lymphocytes during the infection, is responsible for macrophage activation and restriction of *Brucella* infection(Barrionuevo et al., 2011; Boschiroli et al., 2002; Neta et al., 2008).

A problem encountered during *B. abortus* infection is that the S-LPS produced by the bacteria do not effectively induce the immune system. Indeed, the LPS produced by *Brucella* contains lipid A which is a much longer fatty acid (C28) when compared to other enterobacteria. This characteristic decreases its endotoxic properties and thus reduce its TLR4 immunostimulation(Atluri et al., 2011). In addition to this property, this organism has been able to develop strategies to further hide from the immune system with, for example, its Toll/Interleukin-1 receptor (TIR) domain. This TIR domain interferes with TLR signalling. This results in the inhibition of DC maturation and thus in the absence of secretion of pro-inflammatory cytokines(C et al., 2008; Pei et al., 2012).

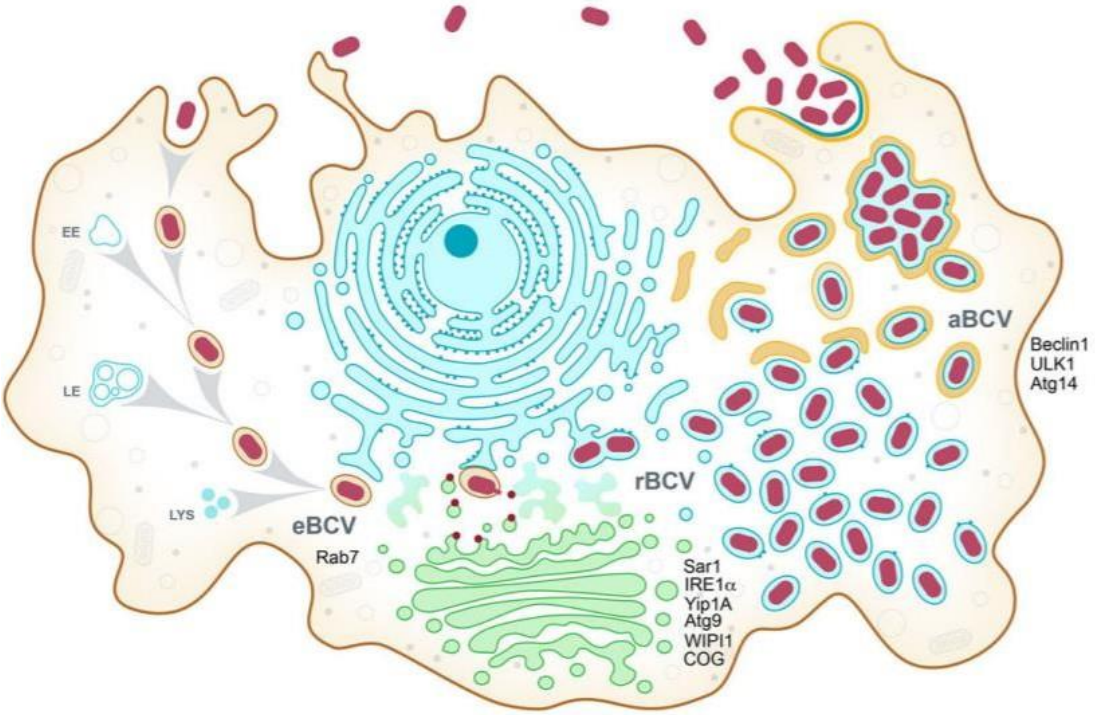

Figure 5: Model of the *Brucella* intracellular cycle in macrophages (Celli, 2019).
Brucella spp are phagocyted inside a membrane bound vacuole in the macrophages. Once inside, the membrane-bound vacuole will undergo endosomal maturation within 8-12 h. Sequential interactions with early, late endosomes, and finally lysosomes allow its acidification and the acquisition of endosomal markers. The endosomal vacuole that contains the bacteria is then named “endosomal *Brucella*-Containing Vacuole” (eBCV). The presence of the small GTPase Rab7 will promote the expression of the VirB type 4 secretion system (T4SS). This secretion system will induce the translocation of effector proteins (in red) that will allow the interaction between eBCV and RE-Golgi. This interaction with “ER exit sites” (ERES) leads to the loss of endosomal markers and the acquisition of ER markers such as Sar1, IREα, ... This membrane conversion is conducive to the establishment within 12-48 h of a replication niche for the bacterium, now called “replicative BCV” (rBCV). The rBCVs will then be captured in autophagic-like membranes that require several autophagic proteins such as Beclin 1, ULK1 and Atg14. This multi-membrane structure completes the intracellular cycle of *Brucella*, leading to the egress of the bacterium. This vacuole is called "autophagic BCV" (aBCV).

Another escape mechanism from the immune system also occurs during the chronic phase of the infection. This mechanism is based on the polarity of macrophages. It is now known that macrophages have two distinct phenotypes identified based on their mode of activation: classically activated macrophages (M-1) and alternatively activated macrophages (M-2). M1 macrophages are differentiated by the influence of Tumor Necrosis Factor (TNF)-ɣ or LPS. This M1 polarisation promotes antimicrobial (production of ROS and Nitric oxide synthase (NOS)) and proinflammatory (expression of IL-6, IL-12 and TNF-α) responses and an amplification of the Th1 response. Whereas M2 macrophages are induced by exposure to IL-4 and IL-13 or through stimulation by immune complexes or TLRs. M2s promote an anti-inflammatory (expression of IL-10) response and a Th2 response (Muraille et al., 2014; Murray, 2017). In addition to having an impact on the response, polarisation leads to a drastic shift in the amino acid, glucose, lipid, and iron metabolism. Indeed, during this chronic phase, a shift in macrophage polarisation may occur. This M1 (inflammatory) macrophages to M2 (anti-inflammatory) macrophages shift will confer the advantage, for the bacteria, of altering the metabolism towards oxidative metabolism as well as reducing the inflammatory response(Xavier et al., 2013). The M2 macrophages allow the bacteria to access a greater quantity of nutrients and promote the establishment of its ER replicative niche.

Finally, the escape from the immune system can also result from the cell type infected by the bacteria. Indeed, in cows *Brucella* mainly and first infect trophoblasts. It has been shown that *B. abortus* can modulate the expression of pro-inflammatory cytokines such as IL-12 and IL-1β during infection. There is a suppression of cytokine expression in the early stages of infection which will only be partially recovered during infection. This mechanism is of course involved in the pathogenesis triggered by *Brucella*(Neta et al., 2008).

1.2.3 Brucella abortus as an intracellular pathogen: features of the intracellular cycle

1.2.3.1 Multi-stage intracellular cycle

Brucella is a facultative intracellular pathogen able to replicate in phagocytic cells such as macrophages, dendritic cells (DC) and neutrophils as well as non-phagocytic cells such as epithelial, fibroblastic, and trophoblastic cells. Phagocytosis of the bacteria is initiated in the lipid raft of the cell and then enclosed in a vacuole, called *Brucella*-containing vacuole (BCV)(Celli, 2019).

Brucella can modulate the intracellular traffic of this vacuole that acquires properties that will be beneficial to its survival, virulence, replication and finally its egress (**Figure 5**)(Celli, 2006).

The BCV initially follows the endosomal pathway, becoming acidified and allowing the bacteria to activate the expression of its virulence factor T4SS. The vacuole then acquires markers, characteristics specific to late endosomes and name of endosomal BCV (eBCV). The vacuole is then diverted from the classical endosomal pathway to form the replicative niche of the bacterium at the entrance of the endoplasmic reticulum (ER). The markers and specificities of the late endosomes present on the vacuole are replaced by markers that are specific to the ER. This change in the nature of the vacuole allows the initiation of replication of the bacteria, thus renaming the vacuole as replicative BCV (rBCV). For the exit of *Brucella abortus*, the vacuole adopts markers and features of the autophagic compartment and was called autophagic BCV (aBCV)(Celli, 2019).

1.2.3.2 Endosomal BCV

The first cells in direct contact with *Brucella* are the macrophages. The bacteria will adhere and invade these cells by its internalisation/phagocytosis. The entry of the bacteria remains somewhat poorly understood and even controversial as several mechanisms of entry have been described. Some studies relate an entry by zipper-like phagocytosis, a transepithelial migration that occurs through apical dome of lymphoepithelial cells(Ackermann et al., 1988) . Other studies show that *B. abortus* can invades macrophages through lipid rafts microdomains. Bacteria swim on the surface of macrophages and these movements allow the internalisation of *Brucella* into macropinosomes that acquire lipid raft-associated molecules such as glycosylphosphatidylinositol (GPI) anchor proteins, GM1 gangliosides and cholesterol(S. Kim et al., 2004). Actin polymerisation also appears to be involved in the internalisation of bacteria by epithelial and phagocytic cells. This actin polymerisation would require the activation of a signalling pathway mediated by Toll like receptor 4 (TLR4) and Janus Kinase 2 (JAK2)(J. J. Lee et al., 2013). The route of entry therefore appears to be variable, dependent on cell type and is still debated in the literature.

Once inside the host cell, *Brucella* are enclosed within a membrane compartment called *Brucella* containing vacuole (BCV)(Celli, 2019). The newly formed BCV matures by sequential interactions with the classical endocytosis pathway. At that moment, the BCV is called eBCV for "endocytic BCV". In a rapid and transient manner, BCV acquires early endosomal markers with Rab 5, GTPase that plays a key role in the maturation of the early endosome into the late endosome(Nagano et al., 2019), and early endosome antigen-1 (EEA-1)(Mu et al., 1995), also an essential player in the maturation and trafficking of early endosomes(Celli, 2019). Indeed, the kinetics of endosomal marker acquisition follows the kinetics observed for a classical phagosome. Within one hour of infection, BCV maturation continues with the acquisition of late endosome markers such as Lysosomal-associated membrane protein 1 and 2 (LAMP-1/2), CD63 and Rab7, also a GTPase involved in a series of events related to intracellular trafficking with for example vesicle formation, transport and fusion, cargo selection and sorting, vesicular traffic in endocytosis, exocytosis and autophagy(Pigino et al., 2012). LAMP-1, a glycoprotein associated with the lysosomal membrane, is retained on the surface of BCV up to 12 h p.i. The maturation of BCV towards the formation of a replicative niche will be marked by an exclusion of LAMP-1, which is a process that is likely initiated when these vacuoles intercept the secretory pathway at endoplasmic reticulum (ER) exit sites (ERES)(Celli, 2019).

The acquisition of these markers is simultaneous with the acidification of the BCV. This acidification is both deleterious for the bacteria (since 90% of the internalized bacteria in a macrophage population is killed between 1 and 4 h p.i) but also essential for the induction of the virulence factor T4SS(Starr et al., 2008). The fusion between the BCV and the lysosome is a subject that has also often been controversial. Initially, no experiments could demonstrate the presence of D-cathepsin, a lysosomal protease, in the lumen of BCV following its fusion with a terminal lysosome(J et al., 1998). It was only afterwards that a live cell imaging was performed to demonstrate the fusion between eBCV and terminal lysosomes. The technique is based on liquid phase labelling of the lysosomes which prevents a detection bias that can occur with the detection of on soluble antigens(Starr et al., 2008).

Although this step may seem counter-intuitive for bacterial survival, it is a necessary step for the bacterium. Indeed, it is the acidification of the vacuole that leads to a signal allowing the induction of T4SS allowing the release of effectors that are essential for the bacteria

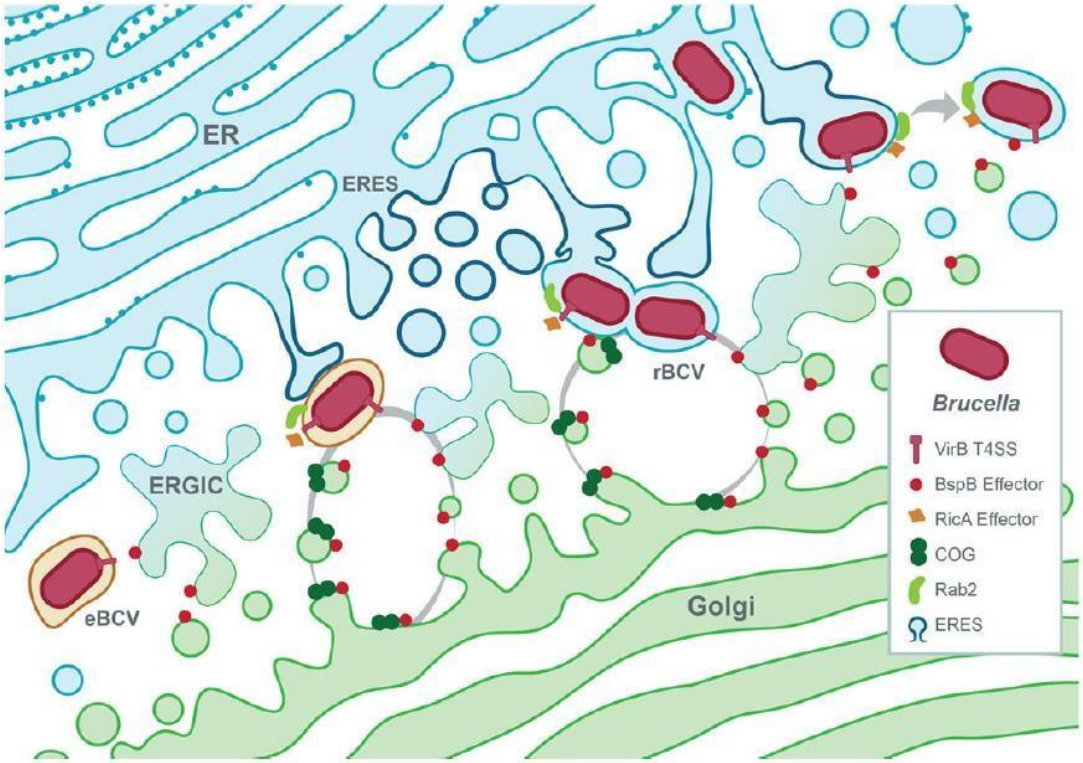

Figure 6: Model of VirB T4SS-dependent biogenesis of the rBCV (Celli, 2019).
The acidification of eBCV allows the expression of T4SS VirB. The secretion system can deliver protein effectors into the host cell and more specifically into the secretory pathway of the cell. The BspB effector is transported from the Golgi membrane by the ER-to-Golgi intermediate compartment (ERGIC) to join and bind the Conserved Oligomeric Golgi (COG) complex. This complex allows the redirection of Golgi-derived vesicles to BCVs. RicA, a second effector, can bind Rab2, a host GTPase, and induce the maturation of eBCV to rBCV. At the same time, eBCV meets ER exit sites (ERES), an upregulation of COP II components is observed as well as an induction of IRE1 and the formation of Yip1-dependent ER-derived vesicles that contribute to rBCV biogenesis.

survival, growth, and replication. The bacteria start to grow during this phase but then will be blocked in the G1 phase as long as they remain at the level of the eBCV(Deghelt et al., 2014).

1.2.3.3 Replicative BCV

In order to continue its intracellular life cycle, *Brucella* must reach a vacuole that allows the establishment of a replicative niche. A conversion of the eBCV into a replicative BCV (rBCV) is therefore necessary. To ensure survival and replication *B. abortus* VirB-dependently diverts intracellular traffic to approach the ER(Celli, 2019). The conversion of eBCV to rBCV will take place at exit sites of the ER. These sites are preferred as they are sites that facilitate ER fusion and fission. This conversion is initiated by secretion associated ras-superfamily gene1 (SAR1), a GTPase that activates Coat Protein complex II (COPII), a protein that allows vacuolation and tubulation of the ER membrane. The vesicle can fuse to allow acquisition of ER proteins on the surface such as calcineurin, calreticulune sec16b and protein disulfide isomerase (PDI)(Celli & Gorvel, 2004; Starr et al., 2008).

The biogenesis of this vacuole first requires maturation in the endosomal pathway and the presence of Rab7. In the early and intermediate stages of vesicle trafficking, the vesicles will be labelled with LAMP1 and Rab7 and then lose these markers and allow replication of the bacteria. A disruption of Rab7 will infer a fusion of the BCV with the endosomal/lysosomal tract and thus interfere with the proper trafficking and maturation of the BCV(Celli et al., 2003).

Rab2 and the glyceraldehyde-3-phosphate deshydrogenase (GAPDH) also appear to be proteins involved in rBCV biogenesis and the replication of *B. abortus*(Fugier et al., 2009). These 2 eukaryotic proteins are normally localised on vesicular and tubular clusters (VTC) and involved in the regulation of VTC membrane traffic between the ER and the Golgi. During *Brucella* infection, Rab 2 and GAPDH are localized on the surface of BCV at 10h p.i.. Their inhibition leads to the absence of replication of the bacteria and the biogenesis of rBCV is interrupted. The biogenesis of rBCV is dependent on VirB as RicA, a bacterial effector that targets Rab2, promote the formation of rBCV(Nkengfac et al., 2012). The role of RicA in Rab2 modulation is not yet well understood as it binds preferentially to a GDP-Rab2 but does not appear to have guanosine exchange activity (**Figure 6**). Nevertheless, it appears that retrograde transport from the ER to the Golgi is essential for the formation of the replicative niche of *B. abortus*(Fugier et al., 2009).

The modulation of cell trafficking and the biogenesis of rBCV is also BAB1_0678 (BspA)-, BAB1_0712 (BspB)- and BAB1_1948 (BspF)-dependent(Myeni et al., 2013). These are substrates for T4SS effectors that interfere with cell trafficking and protein secretion from the host cell. BspB and the coordinated action of BspA, BspB and BspF favour intracellular replication of *Brucella* as they allow inhibition of host cell protein secretion. More exactly, BspB interacts with the conserved oligomeric Golgi (COG) complex(Miller et al., 2017). The complex acts as an interaction centre on Golgi membranes for secretory Rab GTPases, Golgi attachments and Soluble N-éthylmaleimide-sensitive-factor Attachment protein Receptor (SNAREs). COG will thus regulate intra-Golgi and retrograde vesicular trafficking along the secretory pathway providing membranes and functions from the Golgi to the BCV(CN et al., 2017). This decrease in protein secretion and disruption of cell trafficking will also provide an immune advantage as it limits the membrane exposure of immune-related molecules. There will be a retention of class 1 MHC at the Golgi level which also limits the formation of cytotoxic CD8+ T-lymphocytes(Myeni et al., 2013).

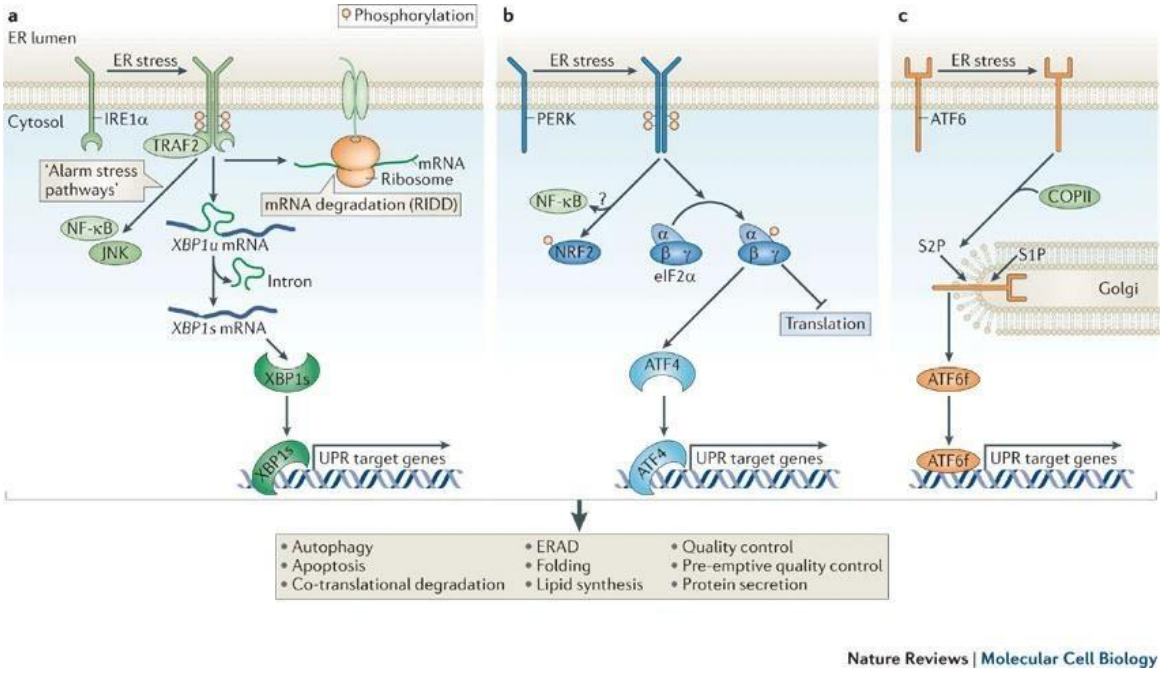

Figure 7: The unfolded protein response (UPR) stress sensors, inositol-requiring protein 1α (IRE1α), protein kinase RNA-like ER kinase (PERK) and activating transcription factor 6 (ATF6) (Hetz, 2012).

The stress sensors IRE1, PERK and ATF6 provide information on the state of folding within the ER to the cytosol or nucleus in order to restore protein folding capacity if necessary. **A)** Upon ER stress, IRE1α dimerises and induces its auto-trans-phosphorylation. This phosphorylation allows the activation of the cytosolic RNAse domain by a conformational change. Active IRE1α processes the mRNA encoding a transcription factor X-box binding protein 1 (XBP1) by excising 26 nucleotides from the intron. The stable and active spliced form of XBP1 translocates into the nucleus to allow upregulation of target genes that encode proteins involved in folding protein, ER-associated degradation (ERAD), protein quality control and phospholipid synthesis. IRE1α can also degrade some mRNA through IRE1-dependent decay (RIDD)-regulation to modulate stress alarm pathways involving c-JUN N-terminal kinase (JNK) and nuclear factor-κB (NFκB). **B)** PERK also dimerises and auto-trans-phosphorylates under ER stress. This phosphorylation leads to its activation and to eukaryotic translation initiator factor 2α (eIF2α) phosphorylation. This protein is involved in the selective translation of mRNA encoding ATF4, a transcription factor controlling pro-survival gene expression by redox balance, amino acid metabolism, protein folding and autophagy. The active form of PERK additionally phosphorylates nuclear factor erythroid 2-related factor 2 (NRF2) involved in redox metabolism. **C)** Under normal conditions, ATF6, which has a transcription factor region in its cytosolic domain, is localized to the ER. However, under ER stress, this protein is translocated to the Golgi by its interaction with COPII. In the Golgi, ATF6 is processed by site 1 protease (S1P) and site 2 protease (S2P), releasing its cytosolic domain fragment (ATF6f). ATF6f is then able to up-regulate genes that encode ERAD and XBP1 proteins.

The hijacking of the ER will not be without consequences for the host cell. *B. abortus* infection activate the Unfloding Protein Response (UPR). This response involves 3 signalling branches: the activation of activating transcription factor 6 (ATF6), a transcription factor, the inositiol requiring enzyme 1 (IRE1), a bifunctional enzyme which functions as both a kinase and an endoribonuclease and Protein kinase RNA-like ER protein Kinase (PERK), a Ser/Thr Kinase (**Figure 7**)(Zhou et al., 2018a). The consequences of the activation of these proteins are to counteract/adapt the cell to ER stress by reorganising its functions, reducing protein synthesis, increasing the expression of chaperones, and increasing autophagy until the stress can be resolved(D & ZA, 2015). Even if still debated in the literature, it is widely accepted that *Brucella* induces UPR mainly the IRE1 pathway out of the three major signalling pathways. Furthermore, the UPR response appears to be beneficial to the bacteria as IRE1α is required for its replication. The link between UPR, rBCV biogenesis and ER exit sites (ERES) may seem confusing, but Yuki Taguchi's team has provided some answers. IRE1 appears to be activated by a protein YPT-interacting protein 1A (Yip1A). Yip1A phosphorylates IRE1 through an IRE1 cluster located at the ERES(Y et al., 2015). This protein is involved in autophagic membrane recruitment recognised by ATG9 and WD-repeat protein Interacting with PhosphoInositides (WIPIs). WIPI proteins are considered to bridge PtdIns3P production and LC3 lipidation which have been identified as necessary for rBCV biogenesis(Proikas-Cezanne et al., 2015).

Brucella use T4SS effectors to promote both the approach of the BCV to the ERES sites and the modulation of intracellular trafficking to allow the BCV to acquire new properties. This change of nature and this membrane exchange carried out at the level of the various organelles of the secretory pathway promote the formation of the *Brucella* replicative niche. The final stage of its intracellular cycle is to leave the host cell to continue its infection in neighbouring cells or tissues(de Jong et al., 2013).

1.2.3.4 Autophagic BCV

The bacterium will have to complete its life cycle by leaving the infected cell in order to start a new infection cycle. Within 48 to 72 h p.i., the BCV will change its nature again(Celli, 2019). The vacuole acquires an enlarged multivesicular structure that carries late endosome markers such as LAMP1. Formation of these multimembrane vesicles requires functions of the canonical autophagy nucleation complexes (composed of vacuolar protein (VPS) 15, VPS34, ATG14 and Beclin1), but not elongation complex (composed of ATG5, ATG7, ATG10, ATG12 and ATG16L), as depletion or removal of Beclin1, Unc-51-like kinase complex (ULK1) and Atg14L, but not Atg5, Atg7, Atg4 or Atg16L, blocked their formation. For that reason, the BCV is called autophagic (aBCV)(Celli, 2015). There is thus a subversion of the classical autophagic pathway which promotes the infection process of *B. abortus*. One of the hypotheses of this subversion involved the UPR and more precisely IRE1α which allowed the formation of autophagosomes in the ER(Deegan et al., 2015; Y et al., 2015). In addition to this a transient production of VirB11, an ATPase known to energise T4SS, was recognised as being necessary for the formation of aBCV and the egress of the bacteria. It is only recently that a clue to the answer has been found. BspL, a type IV protein effector secreted by *Brucella,* was able to bind to homocysteine-inducible ER stress protein (Herp), a component of ERAD, belatedly in the intracellular cycle. Herp is an ER membrane protein that is upregulated during ER stress by all UPR pathways(Kokame et al., 2000). This protein has a significant role in allowing the interaction of ERAD components with their substrate at ER quality control (ERQC) sites(Leitman et al., 2014). The binding between Herp and BspL leads to an over-activation of ERAD which is necessary for a delayed formation of aBCVs allowing an optimal proliferation of the bacteria within the host cell (Luizet et al., 2021). The formation of aBCV is

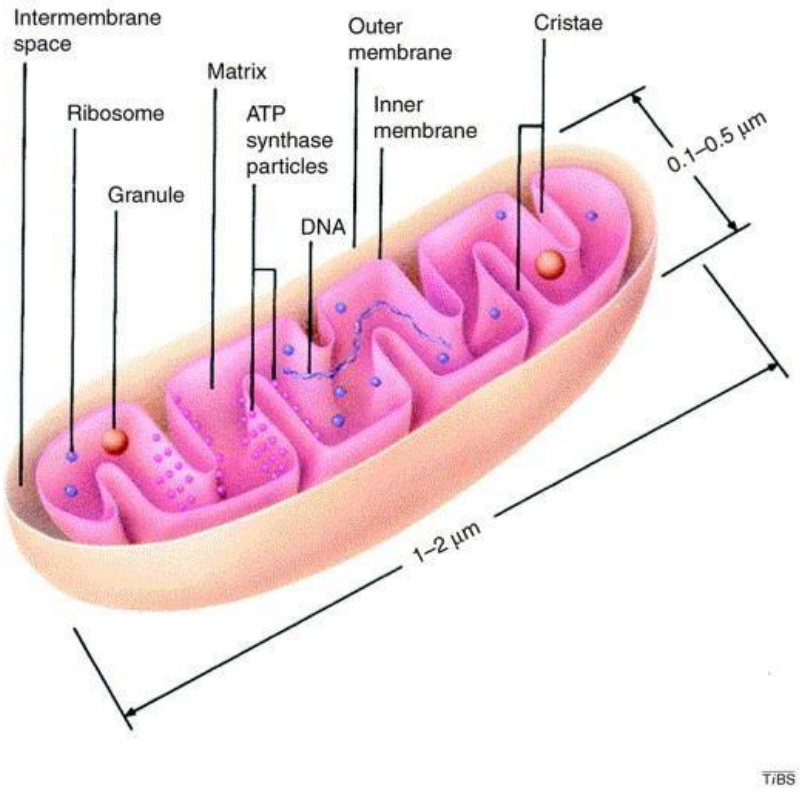

Figure 8: The internal structure of the mitochondria (Frey and Mannella, 2000).
Structure of the mitochondria represented under the Baffle model. This model is the most observed in the literature and is based on the studies of Palades in the 1950s. This model is however not the most complete and can be supplemented by the addition of cristae junctions observed in all higher animals. This 3D visualisation was then confirmed by electron tomography.

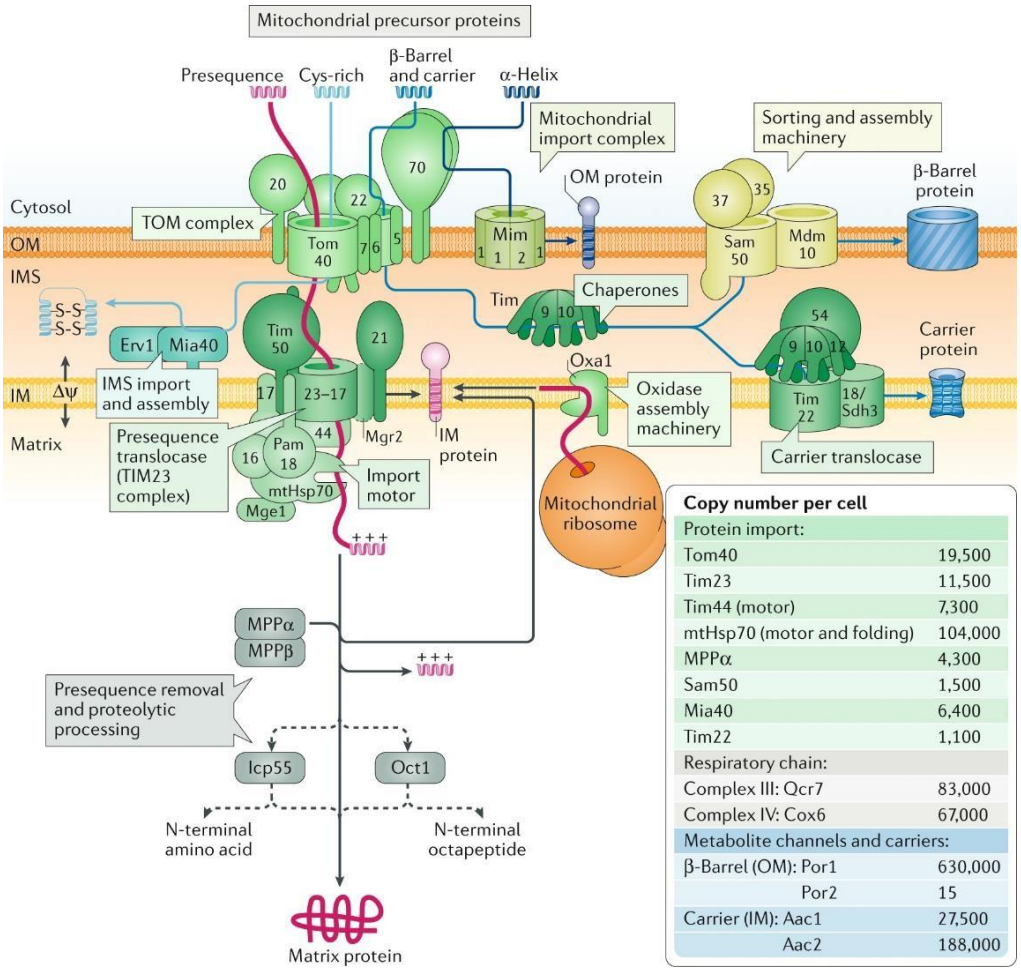

Copy number per cell	
Protein import:	
Tom40	19,500
Tim23	11,500
Tim44 (motor)	7,300
mtHsp70 (motor and folding)	104,000
MPPα	4,300
Sam50	1,500
Mia40	6,400
Tim22	1,100
Respiratory chain:	
Complex III: Qcr7	83,000
Complex IV: Cox6	67,000
Metabolite channels and carriers:	
β-Barrel (OM): Por1	630,000
Por2	15
Carrier (IM): Aac1	27,500
Aac2	188,000

Figure 9: The different import pathways of mitochondrial proteins (Pfanner et al., 2019).
There are 5 major pathways for the import of protein precursors into the mitochondria. The **presequence pathway** is the most studied. The presequence (or MTS; Mitochondrial Targeting Sequence) is a series of terminal amino acids forming a positively charged amphiphilic α-helix. This presequence is recognised by the TOM20 and TOM22 receeptors located at the OMM. These proteins initiate the passage of the presequence through the main protein translocation channel of the outer membrane TOM40 complex. Once the OMM is crossed, the preprotein is engaged to the presequence translocase of the inner membrane (TIM23) located at the IMM. The membrane potential at this level is decisive for the passage of the presequence to the matrix. The positively charged presequence requires a negative membrane potential to activate TIM23 channels and cross the IMM. TIM23 is also associated with presequence translocase-associated motor (PAM) which is itself associated with mitochondrial heat shock protein 70 (mtHsp70s) that allows unidirectional movement of the protein precursor. The presequence is cleaved within the matrix by the mitochondrial processing peptidase (MPP) and processed by different actors to allow its folding (mtHsp70, mtHsp60-10 complex) or its degradation. **Proteins destined for the IMM** can follow 2 distinct routes. Proteins with a hydrophobic sorting signal stop at TIM23 and are redirected to the IMM by Mgr2. Other proteins are brought into the matrix, synthesized on mitochondrial ribosomes and inserted into the IMM by Oxa1. **Proteins characterised by a cysteine motif** are intended for IMS. These proteins first pass the TOM40 complex before being imported and folded via an oxidative mechanism by the mitochondrial intermembrane space import and assembly (MIA) system composed of Mia40 (oxidoreductase) and Erv1 (sulfhydryl oxidase). OMM proteins can be classified into 2 categories: **proteins with α-helical transmembrane segments** that bypass the TOM40 channel to use the mitochondrial import (MIM) channel to be inserted at the outer membrane and the **β-barrel proteins** that are translocated by the TOM complex before being redirected to a small TIM complex localised in the IMS and whose membrane insertion is facilitated by sorting and assembly machinery (SAM).

linked to the exit of the bacteria to continue a new infection cycle. In view of the loss in the bacterial population at the beginning of the infection, it therefore seems advantageous to delay the exit of the bacteria in order to obtain a sufficient bacterial population to allow the durability of the bacteria and the establishment of a new intracellular cycle(Celli, 2019).

In view of the multiple interactions observed between cellular organelles and the bacterium, it was essential to study the impact of *B. abortus* on the central organelles of the cell, the mitochondria. To date, a minority of studies have focused on the interaction between B. abortus and the mitochondrial network of the host cell. Mitochondria play multiple roles within the cell, ranging from energy production to modulation of immunity. In the following, we will focus on the mitochondria, its structure, functions, and those known to be hijacked during infection by *B. abortus* during its intracellular cycle.

1.2.4 Mitochondria: main characteristics and interactions with Brucella

1.2.4.1 Mitochondrial structure and morphology

Mitochondria are dynamic organelles consisting of a double phospholipid membrane into which proteins are inserted. This double membrane will make it possible to define 4 compartments within this organelle; the outer membrane, the intermembrane space, the inner membrane forming the cristae and the matrix (the space created between cristae) (**Figure 8**)(Wai & Langer, 2016a).

The morphology (as well as ultrastructure) and function (bioenergetics and other functions) of mitochondria are closely linked.

The outer mitochondrial membrane (OMM) has a phospholipid-protein ratio of approximatively 50/50 comparable to the one of the plasma membranes. Although this ratio is similar, mitochondria have their own lipid-protein composition. Mitochondria will mainly be composed mainly of phosphatidylcholine (PC) and phosphatidylethanolamine (PE) which constitute 80%. Cardiolipins represent 10 to 15% of membrane phospholipids. The last percentage is made up of sterols and sphingolipids(Horvath & Daum, 2013). The proteins of that membrane are mainly composed of porins allowing the passage of small molecules from the cytoplasm to the intermembrane space(Checchetto & Szabo, 2018). The most abundant protein pores in the OMM are the voltage-dependent anion channels (VDACs) which play a role in the diffusion of metabolites such as Na^+, K^+, Ca^{2+},Cl^-, ATP, succinate and malate across this membrane. Mammals have 3 isoforms of these channels (VDAC1, VDAC2 and VDAC3). Genes encoding these proteins are ubiquitously expressed but their relative expression can vary according to the tissue. In addition to the passage of small molecules, the outer membrane of mitochondria can also be used as a cell signalling platform and contain the complex machinery for import of mitochondrial protein precursors from the cytosol to the matrix (**Figure 9**)(Pfanner et al., 2019). Indeed, out of the 1000 proteins that need for mitochondria biogenesis, only 13 peptides of the respiratory chain are encoded by the mitochondrial DNA. The rest are encoded by nuclear genes, translated in the cytosol and then imported by different mechanisms.

The information required to direct these matrix protein precursors is present as a cleavable sequence at the N terminus. The matrix targeting signal (MTS) of 60-70 amino acids enable the cooperation of the main two mitochondrial preprotein translocases, the translocase of the outer membrane (TOM) complex and the translocase of the inner membrane (TIM23) complex. The TOM complex consists of several proteins such as TOM20 and TOM70 that recognise mitochondrial protein precursors encoded by nuclear genes and allow them to be passed through the TOM40 channels associated with a series of TOM5, TOM6 and TOM7

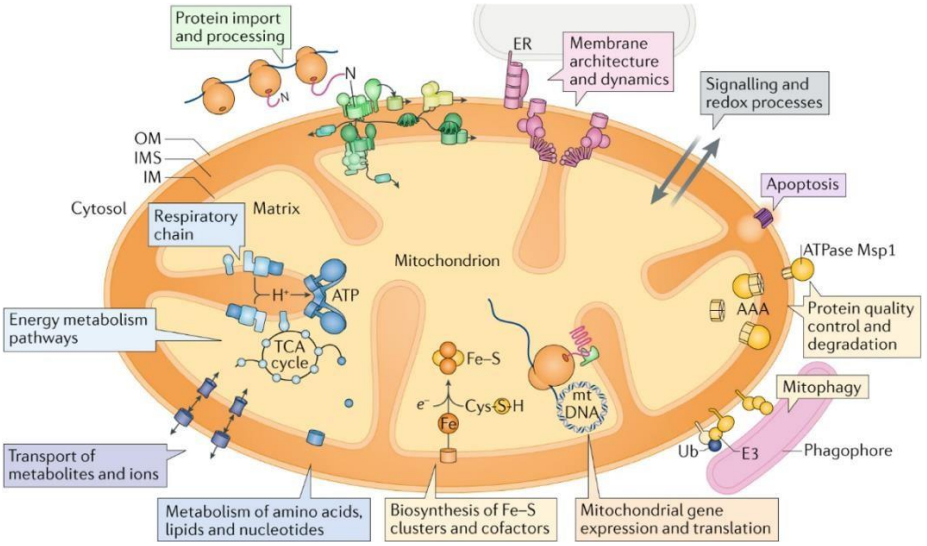

Figure 10: Overview of mitochondrial functions (Pfanner et al., 2019).
A range of functions has been attributed to the mitochondria thanks to the number of proteins and protein complexes that are found in its membranes. The different functions are energy metabolism with respiration and production of ATP; metabolism of amino acids, lipids and nucleotides; biosynthesis of iron–sulfur (Fe–S) clusters and cofactors; expression of the mitochondrial genome; quality control and contribution to the degradation processes including mitophagy and apoptosis; signalling and redox processes; membrane architecture and dynamics. Complexes will also allow the entry and processing of precursors that have been translated by cytosolic ribosomes.
AAA, ATP-dependent proteases of the inner membrane; E3, ubiquitin-protein ligase; ER, endoplasmic reticulum; mtDNA, mitochondrial DNA; TCA, tricarboxylic acid; Ub, ubiquitin.

subunits(Pfanner et al., 2019; Pitt & Buchanan, 2021). However, not all proteins localised to the mitochondria have the MTS. Indeed, proteins located to all other mitochondria compartments contain an internal sequence(Neupert & Herrmann, 2007). The OMM proteins also include proteins that enable the elongation and fusion of mitochondria, such as mitofusin (Mfn) 1 or 2, and proteins that regulate cell death, belonging to the B-cell lymphoma 2 (BCL2) family that contain pro- and anti-apoptotic proteins (see section 1.2.4.2 and 1.2.4.3 for more details). The OMM is also involved in contact sites with other organelles by specific domains called Mitochondria-Associated ER Membranes (MAMs) when mitochondria contact physically and functionally the ER(Kühlbrandt, 2015).

The mitochondrial intermembrane space (IMS) acts as an important separation between the cytosol/IMS and the mitochondrial matrix. The proteins found in the IMS are mainly involved in the assembly of oxidative phosphorylation (OXPHOS) including respiratory chain complexes and Fo-F1 ATPsynthase found in the inner mitochondrial membrane (IMM), the redox regulation for the acquisition of protein conformation as well as protein involved in cell death regulation as AIF, several pro-caspase, endonuclease G, ...(Kühlbrandt, 2015)

The IMM is rich in cardiolipin and form a tight diffusion barrier that allows ions and molecules to pass very selectively (molecule with a MW lower than 1500 daltons). The electron transport chain generates and the permeability control by the IMM generate a mitochondrial membrane potential ranging between -120 and -180 mV. This membrane is also characterised by a high protein/phospholipid ratio as the different complex of the OXPHOS, as well as metabolite transporter, protein machinery involved in mitochondrial protein import or in mitochondrial dynamics are found in the IMM. The large surface/area invagination of the membrane into the matrix are called cristae and are the main site of energy conversion. The morphology of the mitochondrion is highly connected to the efficiency of the bioenergetic function of the organelle(Giacomello et al., 2020).

The mitochondrial matrix is the site of mitochondrial DNA replication, transcription, and mitochondrial protein (encoded by the mitochondrial genome) translation but also the site of numerous enzymatic reactions, notably those involved in the Krebs/TCA cycle(Gray, 2013). Mitochondrial DNA do exist in multiple copies (over a 1000 per cell) and is present in the form of nucleoids, containing mtDNA, the mitochondrial transcription factor (TFAM) and twinkle (a helicase)(Basu et al., 2020; Yan et al., 2019).

1.2.4.2 Mitochondrial functions and their disruption by B. abortus

The role of mitochondria within the eukaryotic cell are numerous, going from ATP production, fatty acid β-oxidation, catabolism of branched amino acid, many syntheses such as steroid hormones, the contribution to the control of cell cycle, the contribution to innate immunity by altered in AMP/ATP ratio, the production of ROS and tricarboxylic acid (TCA) cycle metabolites, the regulation of calcium homeostasis, the integration of programmed cell death signals, and in certain cells types such as hepatocytes, the urea cycle (**Figure 10**)(Kummer & Ban, 2021; Tiku et al., 2020; Weinberg et al., 2015). This section does not aim to review all the functions of mitochondria, but rather to focus on those functions that are impacted by *B. abortus* infection.

1.2.4.2.1 Modulation of energy metabolism

The Krebs/TCA cycle is formed by 8 enzymes that consume and regenerate citrate. Several sources of macromolecules can be catabolized to fuel this cycle, such as carbohydrates, fatty acids, and several ketogenic amino acids such as lysine and leucine. Their catabolism leads

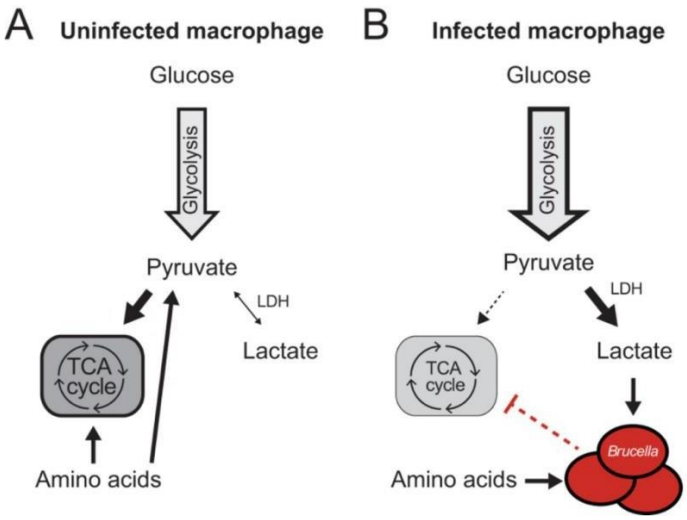

Figure 11: The Warburg shift in host metabolism upon *Brucella* infection (Czyż et al., 2017).
This model suggests that *Brucella*-induced inhibition of tricarboxylic acid cycle (TCA) metabolism prevents the host cell from moving towards amino acid catabolism and shift to lactic acid production.
(A) In uninfected macrophages, glucose is converted to pyruvate via glycolysis and is used, indirectly, by the Krebs cycle as a carbon source (in the form of acetyl-CoA). (B) During infection with *Brucella abortus*, glucose can be converted to pyruvate. Pyruvate is converted to lactate by the lactate dehydrogenase and this metabolite, together with amino acids, are used as a carbon source by the bacteria.

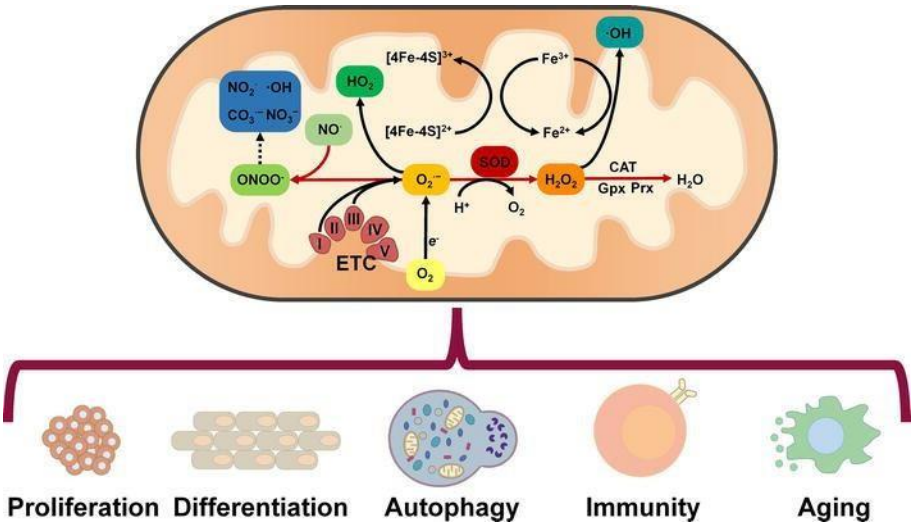

Figure 12: Reaction and transformation of mitochondrial ROS (Choi and Kim, 2019).
The production of ROS comes mainly from the respiratory chain during OXPHOS. The electrons that leak from the respiratory chain (complex I and III) bind to O_2. This reaction results in O_2-which is quickly catalysed by SOD and transformed into H_2O_2. Subsequently, three enzymes CAT, Gpx and Prx convert H_2O_2 into OH-. This reaction is called the Fenton reaction. Another pathway is also possible for O_2. The mitochondria produce nitrite oxide (NO) which reacts with O_2 to form reactive nitrogen oxide species (RNS) such as $ONOO^-$. This reactive species is also capable of forming highly oxidative intermediates. ROS are considered as signalling molecules.

An accumulation of ROS, especially hydroxyl radical (·OH), that overwhelms the antioxidant defences, is deleterious to the cell because it can induce mutations, DNA breaks and aberrant signalling as they react with biomolecules or -SH groups in protein (Diebold and Chandel, 2016).

A controlled production and release of ROS is beneficial and necessary for cell signalling. H_2O_2 is one of the first molecules to be used in cell signalling as it reacts with the cysteine of the redox-sensitive proteins resulting in a change in the conformation and activity of the protein. For cell proliferation and particularly cell survival in hypoxia, ROS induce stabilisation of hypoxia-inducible factor 1 (HIF-1) which is associated with the expression of hundreds of genes. This induction can also take place under non-hypoxic conditions (Patten et al., 2010). However, there
continues to be conflicting evidence in many aspects of HIF-1α regulation by ROS (Chua et al., 2010). Autophagy is also a process that is regulated by the concentration of ROS in the cell. H_2O_2 modulates the activity of the cysteine protease ATG4 allowing to cleave the C-term part of ATG8/LC3 controlling the condensation of the phosphatidyl ethanolamine (PE) on the autophagic receptor. ATG8, in its active form, associates with the autophagosome membrane and promotes its formation (Byun et al., 2009).

ETC, electron transport chain; SOD, superoxide dismutase ; CAT, catalase ; Gpx, glutathione peroxidase; Prx, peroxiredoxin.

to the production of acetyl CoA and then citrate which is then oxidised during the cycle to produce the reducing agents NADH and FADH2 (3 and 1 per cycle respectively)(van der Bliek et al., 2017). These are electron donors for complex 1 and 2 of the respiratory chain, respectively. However, the Krebs/TCA cycle is not only involved in catabolic but also anabolic reactions such as the biosynthesis of amino acids, lipids, and nucleotides. More recently, the Krebs/TCA cycle metabolites such as acetyl Coa, succinate and fumarate have been identified as a tool for intracellular signalling by controlling chromatin modifications, DNA methylation and post-translational modifications of proteins(Martínez-Reyes & Chandel, 2020). It is therefore a central function of the mitochondrion that allows both macromolecule biosynthesis, intracellular signalling, and electron donor generation necessary for oxidative phosphorylation.

Oxidative phosphorylation will therefore initially use electrons from NADH and FADH2 to produce ATP. This process involves the multiprotein complexes of the respiratory chain and the Fo-F1 ATPsynthase inserted in the IMM. The active redox complexes conduct electrons to their final electron acceptor: oxygen. These complexes do not work alone, mobile electron transporters such as coenzyme Q and cytochrome C allow electrons to be transferred from one complex to another. A proton gradient can then be formed at the IMS. The re-entry of these protons in the matrix catalysed by the Fo-F1-ATP-synthase produces ATP(van der Bliek et al., 2017).

This central energy pathway is modulated during infection with *B. abortus.* During chronic infection, an attenuation of the Krebs/TCA cycle, a decrease in amino acid consumption and changes in the localisation of mitochondria can be observed. The normally established oxidative metabolism shift towards glycolytic metabolism in a comparable way to the Warbrug effect observed in cancer cells but also in macrophages activated by *B. abortus* infection. There is a decrease in the metabolism of amino acids in the Krebs cycle, a decrease in the consumption of mitochondrial substrates and an increase in lactate production (**Figure 11**) (Czyż et al., 2017). The metabolic shift is beneficial for *B. abortus*, which can use lactate dehydrogenase to transform lactate as a carbon source (Zhou et al., 2018b).

1.2.4.2.2 Modulation of mitochondrial reactive oxygen species production

Beside their role in energy production, mitochondria are involved in other processes with for example the generation of ROS. It is now widely accepted that, even physiologically mitochondria can use 1-1.5% of the oxygen to produce reactive oxygen species such as $O_2^{(-)}$, by a process, called electron leak. This reactive oxygen species (ROS) is generated at complexes I and III of the electron respiratory chain from the one-electron reduction of oxygen production is enganced when the electron transporters are maintained in their reduced form. The $O_2\cdot$ is rapidly and spontaneously or in a reaction catalysed by superoxide dismutase (enzymes found in the mitochondria (SOD2) or in the cytosol (SOD1)) in H_2O_2 (**Figure 12**)(Shadel & Horvath, 2015). ROS can have several functions depending on their concentrations. An accumulation of ROS (especially hydroxyl radical (.OH)) leads to deleterious effects within cells with mutation induction, DNA breaks and aberrant signalling as they react with biomolecules or -SH groups in protein. However, a regulated production and release of ROS possesses an important and beneficial role in cell signalling related to cell proliferation, survival under hypoxia, cell differentiation, autophagy, and innate immunity (Diebold & Chandel, 2016; Shadel & Horvath, 2015) (for more information refer to **Figure 12**). The involvement of ROS in immunity is of particular interest in the case of *B. abortus* infection(Hu et al., 2019, 2020b).

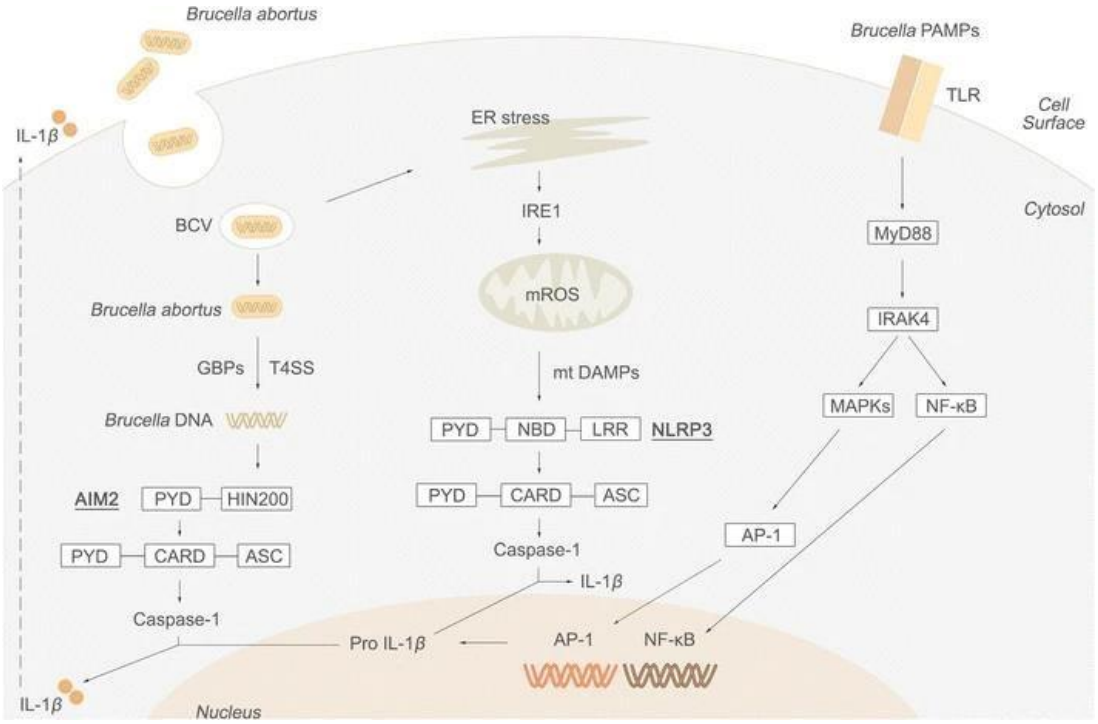

Figure 13: Absent in melanoma 2 (AIM2) and NACHT, LRR, and PYD domains-containing protein 3 (NLRP3) inflammasome activation by *B. abortus* (Marim et al., 2017).
B. abortus can induce inflammasome activation through the presence of PAMPs as, for example, LPS detection by TLR4. This is followed by the activation of NFκB and MAPK signalling pathway which generates the pro-IL-1β form. This form is then matured by caspase 1 to IL-1β as a result of the NLRP3 inflammasome activation. Secondly, ER stress can lead to the activation of the mitochondrial form of NLRP3 but also of the cytoplasmic form with the formation of DAMPs. Finally, *B. abortus* will, during infection, release microbial DNA that is recognised by the AIM2 inflammasome. Activation of the NLRP3 or AIM2 inflammasome leads to activation of caspase 1 and secretion of IL-1β, a pro-inflammatory cytokine that amplifies the B and T cell response.

1.2.4.2.3 Modulation of immunity

As mentioned above, ROS participate in the regulation of cellular immunity by four different mechanisms.

The first axis involves TLR signalling. One study found that the downstream signalling pathway of TLR1,2 and 4 was directly increased in the presence of ROS (West, Brodsky, et al., 2011). This activation of TLRs by ROS is possible through the intermediary of 2 factors, the TLR signalling adaptor TRAF6 which translocate to the mitochondria and activates Evolutionarily conserved Signalling Intermediate in Toll (ESCIT) pathways. The interaction between its proteins at the OMM leads to ubiquitination of ESCIT. ESCIT is then able to regulate the production of ROS that occurs following engagement of TLRs. This pathway also has a role in bacterial clearance with an induction of autophagy(Lim & Staudt, 2013).

The second axis is that the cell during bacterial infection can set up systems that promote ROS production and increase the bactericidal environment of the cell. For example, during bacterial infection, the INFɣ produced can activate oestrogen related receptor α (ERRα) which acts in a coordinated manner with proliferator-activated receptor-γ co-activator 1α (PGC1) for to transcriptionally increase ROS production(Sonoda et al., 2007).

The third axis is the activation of the inflammasome. The inflammasome is a multiprotein complex that can assemble itself in response to two signals: endogenous cytokine production and/or pathogen- or damage-associated molecular patterns (PAMPs or DAMPs). There are several types of inflammasome differentiated by the type of receptors included in the protein complex. It is possible to distinguish 2 large families with the receptors belonging to the AIM receptors (AIM2) and the NOD-like receptor family (NLRP3) (Campos et al., 2019; Marim et al., 2017a). Upon infection with *B. abortus*, several ligands can activate the AIM2 and NLRP3 inflammasome (**Figure 13**).

Upon infection with B. abortus, bacterial DNA is released into the cytoplasm. This DNA is recognised by the sensor protein AIM2, which leads to the activation of caspase 1 and the secretion of IL-1β. The activation of this pathway is also dependent on the transcription factor IRF1 present in DCs. Stimulator of IFN genes (STING) a protein associated with the ER, detects bacterial DNA from *B. abortus* and activates a type 1 IFN response and IRF-1–dependent signaling cascade(Costa Franco et al., 2018). Indeed, IRF and type 1 IFN are required for the expression of guanylate-binding protein (GBPs) which promotes BCV lysis and thus the releasing of bacterial components to the cytoplasm such as DNA to activate in its turn the AIM2 inflammasome(Marim et al., 2017b).

NLRP3 activation depends on 2 main pathways. The first requires PAMP presentation at TLRs which initiates the NFκB signalling pathway and upregulation of NLRP3. The second pathway involves DAMPs. Brucella is known to induce ER stress which activates IRE1α. IRE1α initiates the recruitment of Thioredoxin-interacting protein (TXNIP), a multifunctional protein(Hu et al., 2020a), and NLRP3 to the mitochondrial membrane where it leads to ROS production and pore formation at the mitochondrial membrane. The ROS as well as the mitochondrial content released by the pores serve as DAMPs that have the ability to induce the activation of cytosolic NLRP3 with activation of caspase 1 and secretion of IL-1β(Marim et al., 2017b).

The last axis is the activation of autophagy and its crosstalk between the NLRP3 inflammasome and the ROS production. Mitophagy, a selective autophagy, can occur following bacterial infection to limit DAMP with ROS production and thus limit NLRP3 inflammasome

activation(Biasizzo & Kopitar-Jerala, 2020). This modulation of the inflammasome-induced response can also be induced by *B. abortus*. It was observed, that in *Brucella* containing a functional T4SS, the secretion of IL-1β was decreased(Gomes et al., 2013). BtpA and BtpB effectors can interfere with host cell TLR receptors and thus decrease the induced immune response including inflammasome activation(Coronas-Serna et al., 2020).

1.2.4.2.4 Modulation of programmed cell death

Finally, mitochondria are involved in the induction of programmed cell death, called apoptosis. Apoptosis is divided into two pathways: an intrinsic mitochondrial pathway and an extrinsic receptor-mediated pathway. The intrinsic pathway is induced when a series of stress signals converge on the mitochondria and induce permeabilisation of the outer mitochondrial membrane (OMM). MOMP allows the release into the cytosol of a series of IMM proteins including cytochrome C. Cytochrome C interacts with Apoptotic peptidase activating factor 1 (APAF-1) and induces its oligomerisation which leads to the formation of a structure called the apoptosome. The apoptosome recruits and activates a range of caspases that can induce cell death. MOMPs are also tightly regulated by proteins of the Bcl-2 family. This family includes both pro-apototic (Bac and Bax) and anti-apoptotic (Bcl-2 and Bcl-xL) proteins. When 2 pro-apoptotic proteins homodimerise, they form a proteolipidic channel in the MOM to induce MOMP(Lopez & Tait, 2015).

The modulation of apoptosis induced by *B. abortus* is still unclear and controversial. One study shows that B. abortus induces T cell apoptosis via its lipoprotein l-Omp19 (Velásquez et al., 2012). It has also been observed that B. abortus can release LPS into polymorphonuclear cells (PMN). This LPS leads to an increase in the production of ROS via NADPH oxidase which leads to premature death of PMNs(Barquero-Calvo et al., 2015). However, it has also been shown that B. abortus can induce the expression of A20, an anti-apoptotic protein in macrophages, and thus reduce apoptosis via a decrease in NFκB expression(Wei et al., 2015).

B. abortus therefore induces disturbances within the mitochondria. However, there are still many unexplored avenues regarding this interaction.

1.2.4.3 Mitochondrial dynamics:

The functions of mitochondria are closely dependent on the morphology of the organelle and *vice versa* as the activity of the organelle might affect its morphology. Indeed, there is a complex interrelationship between the morphology of the organelle and their activity, especially for the bioenergetic function(Tilokani et al., 2018). For example, a change in the nutritional requirements of the cell or a response to a stress signal can lead to changes in network connectivity of the mitochondrial fragments through fusion or fission events(Chan, 2020) . Morphological changes can therefore have an important effect on the regulation of ATP production, ROS production, calcium homeostasis, or the regulation and integration of programmed cell death signals(Wai & Langer, 2016b) .

1.2.4.3.1 Fusion:

The fusion of the mitochondrial fragments occurs during an energy demand with an increase in ATP production by promoting oxidative metabolism (Youle et al., 2012). The fusion process can be observed during a decrease in protein synthesis, an induction of autophagy or during a period of fasting with the use of carbon sources such as lipids and proteins (Yoo & Jung, 2018a). Fusion can also occur in response to inhibition of fission, as a protective mechanism of the mitochondria to avoid autophagy, as a consequence of a compensation

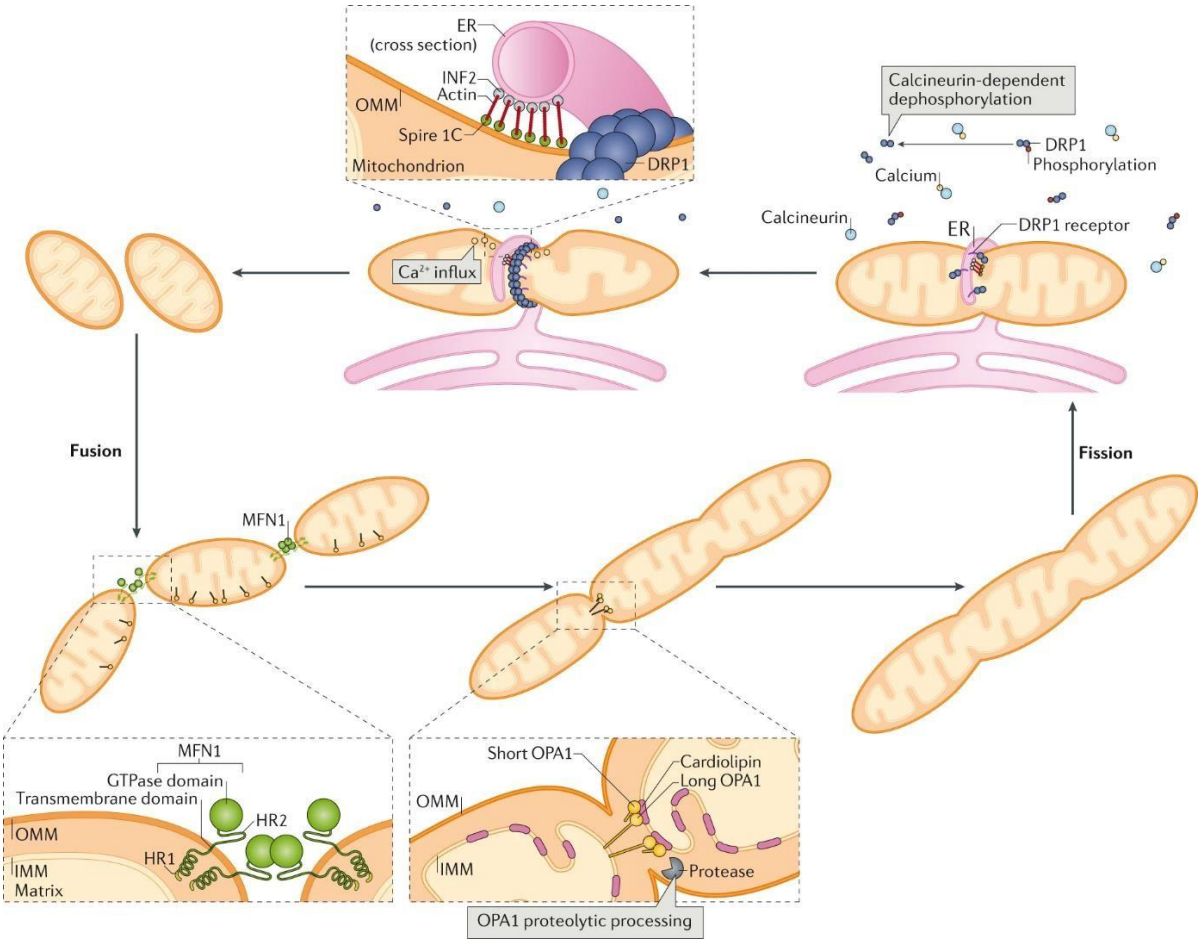

Figure 14: Cooperation between fusion and fission to modulate mitochondrial dynamics (Giacomello et al., 2020).

Fission is initiated by DRP1. This protein, once dephosphorylated by calcineurin, can bind to the mitochondria and more particularly to the sites of ER-induced deformation of the mitochondrial membrane. DRP1 oligomerises and causes membrane constriction via GTP hydrolysis. DRP1 activity is supported by actin polymerisation at the ER-mitochondrial interface through the nucleation of inverted formin 2 (INF2) and formin-binding protein spire 1C. This actin polymerisation initially promotes the deformation of the mitochondrial membrane and thus facilitates the oligomerisation of DRP1 which leads to fission.

Fusion involves 2 GTPases found at OMM and IMM. These proteins are respectively Mfn1 and OPA1. An association in trans of 2 Mfn1 located on 2 fragments of mitochondria will allow their interactions and the hydrolysis of the GTP. This leads to a closing of the membranes and a fusion of the MMOs. For IMM, it is the long form of OPA1 that is required. L-OPA1 can associate in trans with cardiolipins and thus initiate membrane fusion.

between damaged and healthy mitochondria. This ability to bring together and then assemble membranes is dependent on proteins/enzymes found on both the OMM and IMM (Youle et al., 2012).

At the molecular level, two mitofusins (Mfn1 and Mfn2), belonging to the dynamin-related family of large GTPases, regulate fusion at the OMM (**Figure 14**). These enzymes display structures with a high degree of homology including a catalytic GTP binding domain (Giacomello et al., 2020). Although the similarity is high between these proteins, their role seems to differ. Mfn1 has been identified as the main component in the mitochondrial outer membrane fusion process (Sinha & Aradhyam, 2019). The role of Mfn2, in fusion, is still to be clarified as the enzyme seems to be more involved in the interactions between mitochondria and the ER (or other organelles) than just playing a role in the fusion of mitochondria (Giacomello et al., 2020). From a functional point of view, Mfn1 will be able to interact in a homotypic manner after hydrolysis of a GTP and thus, allows the tethering and fusion of the OMM(Wai & Langer, 2016a).

The fusion of the IMM involves optic atrophy 1 (OPA1), another protein of the dynamin-like GTPase anchored family (Gilkerson et al., 2021). The enzyme can exist in 2 forms; L-OPA1, a long form which contains a transmembrane domain at its N-terminal domain and S-OPA, a short and soluble fusion inactive isoform (Landes et al., 2010). During translation OPA1 is imported and inserted at the IMM either via attachment to cardiolipins (found in high concentration at this membrane) or associating with itself. This homotipic association is followed by a GTP-dependent membrane fusion. This fusion is also facilitated by ATP synthase dimerisation and interaction with multisubunit Mitochondrial contact site and Cristae Organizing System (MICOS) assisting in the remodelling of the internal membrane. The short form arises from cleavage at the S1 and S2 site of OPA1, releasing it into IMS. S-OPA1 is obtains by a controlled proteolytic cleavage with one of these 2 proteases: overlapping with the m-AAA protease (OMA1) or the i-AAA protease (YME1L). The difference between these 2 enzymes is not yet well understood but it seems that the expression of OMA1 is increased during various stress conditions such as mitochondrial inner membrane depolarisation, oxidative stress, and hypoxia (Ref) while the abundance of YME1L increases upon a shift from glycolysis to OXPHOS(Ohba et al., 2020). Constitutive cleavage of OPA1 is observed forming a balance between L-OPA1 and S-OPA1. In cases of fusion, it is the L-OPA1 form and more precisely the homotypically associated L-OPA1 form that is found in the IMM(Gilkerson et al., 2021).

Deregulation of these proteins, such as reduced expression of Mfn1/2 or overexpression of OMA1 leading to the soluble form of OPA1, can lead to fragmentation of the mitochondrial network(Giacomello et al., 2020).

1.2.4.3.2 Fission

The fission of the mitochondrial network can occur when there is an excess of nutrients or mitochondrial dysfunction (Giacomello et al., 2020). In response to mitochondrial dysfunction, this process can also occur upstream of mitophagy allowing the isolation of damaged mitochondria (Wai & Langer, 2016a). Dynamin-Related Protein 1 (Drp1) is one of the main proteins involved in OMM fission. It is again, an enzyme of the cytosolic dynamin family (Adachi et al., 2020). There are several Drp1 receptors or recruitment factors that recruit Drp1 to cleavage sites at the OMM. Several of these proteins have been identified: Mitochondrial fission 1 protein (FIS1), Mitochondrial fission factor (MFF), mitochondrial dynamics proteins

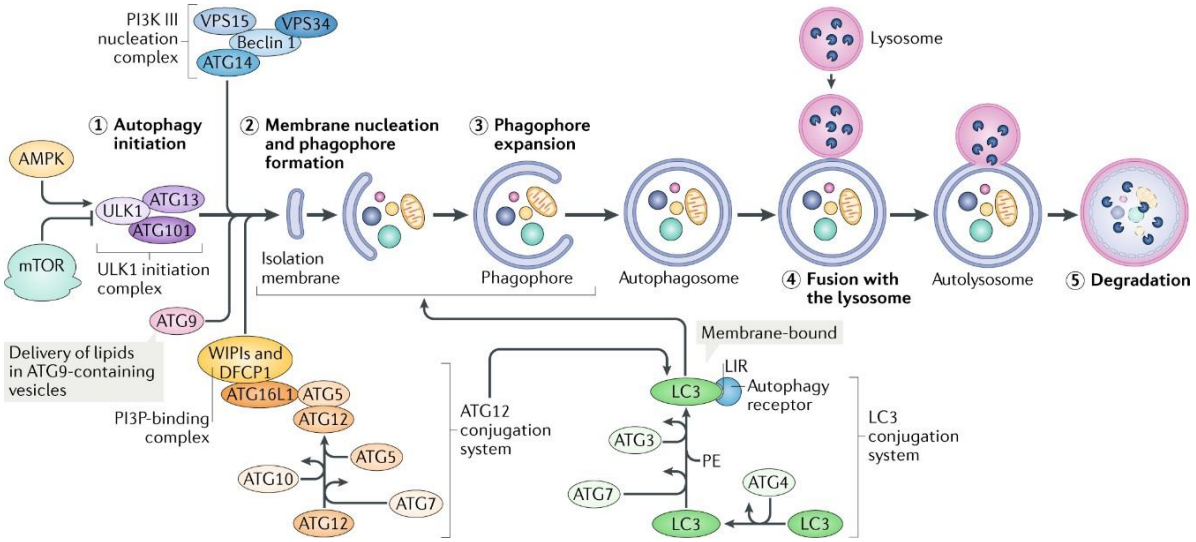

Figure 15: A schematic depicting the process and main regulatory machinery of macroautophagy (Hansen et al., 2018).

Macroautophagy in general will be induced via cellular signals such as damage or stress. The first target of this signal is the Unc-51-like kinase complex (ULK1). This complex is made up of a series of proteins linked to autophagy: ULK1, ATG13, ATG101 and RB1 inducible coiled-coil protein 1 (FIP200). Activation of this complex induces phosphorylation of a second complex essential for nucleation of the double membrane that will form the phagophore, the PI3KIII complex. It is formed by vacuolar protein 34 (VPS34), Beclin 1, ATG14, an autophagy activating molecule regulated by Beclin 1-, protein 1 (AMBRA1) and general vesicular transport factor (p115) which are then able to induce the production of phosphatidyl inositol 3 phosphate (PI3P) at the level of the omegasomes, specific structures of the ER. The membrane input for phagophore formation can have several origins. Membranes come from specific sites in the ER but also from the membranes of organelles such as the Golgi, mitochondria, endosomes or from the plasma membrane via vesicles labelled with the ATG9 protein. This protein is important for the supply of membrane and protein to the double membrane of the phagophore (Dikic and Elazar, 2018; Yang and Klionsky, 2009).

Then, the autophagophore can expand. PI3P found at the membrane can recruit protein effectors including WD-domain phosphoinositide interaction proteins (WIPI) and zinc finger proteins containing the FYVE 1 domain (DFCP1). These effectors are involved in binding to an ATG16L-ATG12-ATG5 protein complex that both promote membrane expansion and enhance ATG3-mediated conjugation to proteins of the ATG8 family (ATG8s). This family includes microtubule-associated light chain 3 (LC3) proteins and γ-aminobutyric acid receptor-associated proteins (GABARAPs) that bind to membrane phosphatidylethanolamine. ATG8s allow the recruitment of cargo during selective autophagy. Indeed, protein aggregates or organelles can harbour receptors with an LC3 interaction region (LIR) domain that allows for the capture of tagged elements during the expansion of this double membrane. This is a marker that can be used in research to identify an induction of autophagy. The LC3 protein has two forms: a soluble form (LC3-I) and a lipid form (LC3-II). Upon induction of autophagy LC3-I converts to LC3-II, the lipid form found at the autophagosome membrane. Labelling of the LC3-II form identifies an induction of this process(Dikic and Elazar, 2018; Johansen and Lamark, 2020; Yang and Klionsky, 2009).

Following the expansion of the phagophore, the vesicle can mature. A loss of ATG proteins from the outer membrane of the autophagosome is observed in favour of a recruitment of the machinery responsible for the approach and fusion with the lysosome. The proteins involved in this process are SNARE proteins such as syntaxin 17 (STX17) and synaptosomal- associated protein 29 (SNAP29). These proteins will allow the binding with the approximation between the 2 membranes via the VAMP8 protein which is found on the lysosome and the homotypic fusion and protein sorting complex (HOPS)(Dikic and Elazar, 2018; Yang and Klionsky, 2009).

of 49 kDa (MiD49) and mitochondrial dynamics proteins of 51 kDa (MiD51) (Giacomello et al., 2020).

The fission sites are localised close to the contact sites between the ER, the mitochondria and the actin cytoskeleton which facilitates the assembly and polymerisation of Drp1 around the mitochondria. The polymer forms a ring which, through hydrolysis of GTP, changes conformation and encloses the mitochondrial membrane until it splits (Adachi et al., 2020). A decrease in membrane recruitment of Drp1 can lead to hyper-fusion of the mitochondrial network.

Two proteins may be involved in the fission of IMM: the S-OPA1 protein and the mitochondrial protein of 18 kDa (MTP18)(Giacomello et al., 2020). The accumulation of S-OPA1 accelerate the fission of the mitochondrial population. This accumulation of S-OPA1 is mediated by activation of the proteases OMA1 and YMEL1 in response to stress or metabolic shift. This form can also be colocalised with components of the fission machinery found at OMM at the contact sites between the ER and the mitochondria (Ohba et al., 2020). MTP18 is an integral protein that maintains the morphology of mitochondria. The function of this protein is not yet well understood but it seems that overexpression induces Drp1 recruitment to the OMM and deletion induces hyper-fusion (Kreymerman et al., 2019) (**Figure 14**).

More recently, contact sites between organelles such as the ER, lysosomes, and mitochondria have been identified as important for the localisation of mitochondrial fission sites (Wong et al., 2018). At the ER level, contact sites with mitochondria are necessary for the initiation of the fragmentation process. Protein players such as Drp1 and its adapters (FIS, MiD49, MiD51) are recruited to these sites. It is also at these sites that actin polymerisation takes place to constrict mitochondrial membranes even before Drp1 polymerisation(Tilokani et al., 2018). For lysosomes, contacts with mitochondria are made possible by RAB7, a small GTPase bound to lysosomal in its GTP-binding form. Subsequently, FIS1 will recruit TBC domain family member 15 (TBC1D15), a GTPase-activating protein (GAP) from RAB7. Hydrolysis GTP at the contact sites controls the regulation of lysosomal morphology as well as mitochondrial fission(Wong et al., 2018).

The dynamic of mitochondria controlled by fission and fusion events is closely linked to mitophagy (Yoo & Jung, 2018a). Indeed, fission allows damaged mitochondria to be separated from healthy mitochondria population and thus facilitates the degradation of a dysfunctional mitochondria by mitophagy(Youle et al., 2012).

1.2.4.4 Mitophagy

Mitophagy is a selective and specific process of macro-autophagy allowing the degradation of damaged mitochondria(Youle and Narendra, 2011). The global mechanisms of mitophagy are therefore relatively comparable to autophagy (**Figure 15)**.

The particularity of mitophagy comes from its selective character which is based on the presence of protein actors found on the surface of the mitochondria to be degraded.

There are different actors, effectors and regulators of mitophagy which can be classified in 2 categories: the ubiquitin-mediated and ubiquitin-independent interactions between Light Chain-3 (LC3) and adapters (Youle & Narendra, 2011).

In the category of ubiquitin-mediated interactions between LC3 and adapters, there is the PTEN-induced putative kinase 1 (PINK1)/Parkin pathway (Narendra et al., 2008). This

pathway will depend on the ubiquitination of mitochondrial membrane proteins and is regulated by presenilin-associated rhomboid-like (PARL) protease. In healthy mitochondria (with high mitochondrial membrane potential (about -180 mV)), PINK1, a Ser/Thr kinase, can be imported and translocate in the IMM where it will be degraded by PARL. In response to a loss (or reduction) of mitochondrial membrane potential, PINK1 is stabilised and accumulates at the OMM. This accumulation leads to the recruitment of Parkin, an E3-ubiquitin ligase (Eiyama & Okamoto, 2015). Parkin is then phosphorylated by PINK1 and activated allowing its E3 ubiquitin ligase activity to promote ubiquitination of mitochondrial membrane proteins such as Mfn1 and Mfn2. Next, ubiquitin-tagged mitochondrial proteins bind LC3, by the intermediates of several LC3-interacting region (LIR)-containing autophagy adapters, such as p62, optineurin (OPTN), neighbour of Breast cancer susceptibility gene 1 (BRCA1) gene (NBR1), nuclear domain 10 protein 52 (NDP52), or TAX1-binding protein 1 (TAX1BP1), and allow the formation of the autophagosome(Y. Chen & Dorn, 2013; Narendra et al., 2008).

In the category of ubiquitin-independent interactions between LC3-adapters, there are several proteins that are directly attached to the mitochondria such as BCL2-interacting protein (BNIP), BCL2 interacting protein 3-like (BNIP3L), FUN14 domain-containing protein 1 (FUNDC1), FK506 binding protein 8 (FKBP8) allowing a direct physical interaction between mitochondria and LC3 proteins.

BNIP and NIX/BNIP3L (these two proteins share 56 % homology) are proteins that contain a Bcl-2 homology domain and a transmembrane domain (TM) at the carboxyl-terminal domain (Ref). Theses protein can be found in a monomeric or dimeric forms. Interactions between two monomers is allowed by the presence of GXXXG motif located in the transmembrane domain connecting the helices of each monomer to be brought together (Lawrie et al., 2010). These interactions, although reversible, can be observed both in the OMM and under detergent conditions, indicating a strong interaction force between the TM domains (Lawrie et al., 2010; Sulistijo et al., 2003a; Sulistijo & MacKenzie, 2006). This TM domain allows the insertion of BNIP and NIX at the mitochondrial and ER membranes. First identified in the regulation of cell death by apoptosis or necrosis via their interference with the respiratory chain or the increase of ROS(Novak et al., 2010), these proteins were also later discovered to play a role in mitophagy(Ding & Yin, 2012). Indeed, BNIP and NIX contain a LIR domain that interacts with LC3 and its homologue GABARAP (Youle & Narendra, 2011). They are thus defined as receptors involved in mitophagy. This interaction between the LC3 family and BNIP3L is also modulated by the dimeric form as the dimerization of BNIP3L increases its affinity to LC3/GABARAP. This form has been identified as a strong initiator of mitophagy(Marinković et al., 2021).

Several signals have been identified as responsible for the induction of BNIP and NIX-dependent mitophagy and hypoxia is one of these inducing signals(Ney, 2015). Upon a decrease in partial oxygen pressure (PO_2), hypoxia-inducible factor 1 (HIF-1), a heterodimeric transcription factor, is stabilised and activated and initiates an adaptive response (Weidemann & Johnson, 2008). This complex consists of both: a constitutively expressed (and degraded) oxygen non-dependent unit and one hypoxia-inducible subunits, HIF-1β or HIF-1α, respectively(Masoud & Li, 2015; Weidemann & Johnson, 2008). In normoxia, HIF-1α will undergo a very rapid degradation mediated by prolyl-hydroxylase domain proteins (PHDs) which allow the hydroxylation of proline residues (Ref). HIF-1α modified is then recognised by von Hippel-Lindau protein (pVHL), part of an E3 ubiquitin-ligase complex and is tagged for ubiquitination and proteasomal degradation. This transcription factor is stabilised under

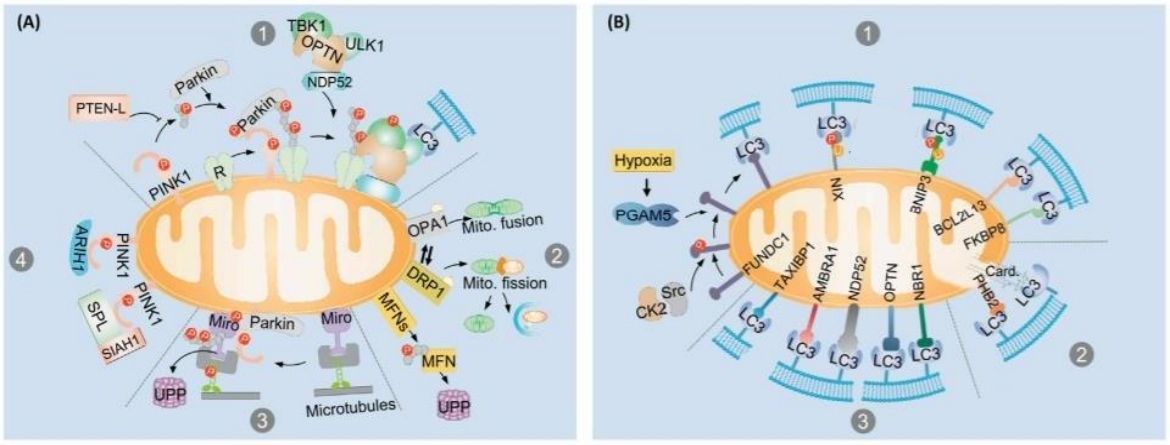

Figure 16: The mechanisms underlying mitophagy (Lou et al., 2020).
(A) Phosphatase and tensin homolog (PTEN)-induced putative kinase 1 (PINK1)-dependent and Parkin-(in)dependent pathways. (1) PINK1 is a mitochondrial protein with an MTS sequence that allows it to be translocated to the matrix by the TOM complex for cleavage. The translocation of PINK1 to the mitochondrial matrix is dependent on membrane potential. In the case of damaged mitochondria, the mitochondrial membrane potential can be disturbed and prevent PINK1 translocation to the matrix. PINK1 becomes localised to the OMM and instead interacts with the TOM. In this heterooligomeric complex, two molecules of PINK1 dimerize and cross-phosphorylate each other to become highly active. PINK1 is then able to phosphorylate both Parkin and ubiquitins. Phosphorylated Parkin will activate and in turn ubiquitinate mitochondrial proteins that are then recognised by the autophagosome. (2) Mitochondrial fragmentation can occur to facilitate the initiation of mitophagy. (3) Parkin and PINK1 can degrade proteins involved in mitochondrial motility such as Miro. (4) In PINK1-dependent Parkin-independent pathways other E3-ubiquitin ligases can take over such as Seven In Absentia Homolog 1 (SIAH1) and SPL to induce mitophagy.
(B) Receptor-mediated mitophagy pathways. (1) OMM proteins which has a direct interaction with LC3: including FUNDC1, NIX (BNIP3L), BNIP3, FKBP8, and BCL2L13 (the mammalian orthologue of the yeast Atg32). (2) Mitophagy receptor located at the IMM, including PHB2 and cardiolipin (Card.). (3) Autophagy receptors that are also involved in mitophagy, including AMBRA1, NDP52, TAXIBP1, NBR1, OPTN, and p62.

hypoxic conditions and will be able to bind to the hypoxic response element (HRE) found in the promoters of several genes encoding proteins such as BNIP and BNIP3L(Haase, 2010; Masoud & Li, 2015; Weidemann & Johnson, 2008). This induction of BNIP and BNIP3L expression leads to mitophagy, which decreases ROS production during hypoxic conditions (J. Zhang & Ney, 2009).

A depolarisation of the IMM can also lead to the recruitment of BNIP3L/NIX. This phenomenon has been observed in maturing reticulocytes (Schweers et al., 2007). During this process, a clearance of mitochondria is performed. The mechanism by which BNIP3L/NIX performs this clearance differs from hypoxic conditions. BNIP3L/NIX can open a mitochondrial permeability transition pore (mPTP). This change in the inner mitochondrial membrane permeability leads to a loss of membrane potential and thus depolarisation of the mitochondria. It would be the subsequent depolarisation of NIX activation that initiates mitophagy(J. Zhang & Ney, 2009).

FUNDC1 is also an OMM protein that is involved in hypoxia-induced mitophagy and can recruit LC3 family proteins by its LIR domain (L. Liu et al., 2012). This protein can induce mitophagy in an ATG5-dependent but Beclin-independent manner (**Figure 16**) (M. Chen et al., 2016). In normoxia, FUNDC1 is phosphorylated by Src, a Tyr kinase at Tyr18 and by casein kinase II (CKII) at Ser13. In this phosphorylated form, the protein is unable to bind LC3. In the absence of oxygen, Src kinase and CKII are not activated leaving FUNDC1 in a dephosphorylated form capable of binding LC3 and inducing mitophagy(Ding & Yin, 2012). In addition, FUNDC1 protein has also been identified as requited for the regulation of both OMM and IMM fission (M. Chen et al., 2016). FUNDC1 interacts with Drp-1 and OPA1 to facilitate fission and subsequently induce mitophagy. In the case of Drp-1, it is recruited by FUNDC1 to the membrane under conditions of cellular stress. Fission of IMM and OMM is then possible and thus facilitates the induction of mitophagy(M. Chen et al., 2016).

FKBP8 and BCL3L13 are adaptor proteins also able to bind to LC3 receptors by their LIR motif. These proteins are in the OMM and induced mitophagy Parkin-independent(Yoo & Jung, 2018b). FKBP8 has both similarities and differences to the BNIP and NIX proteins. Like these proteins, FKBP8 is a multiple adaptor that possesses anti-apoptotic activity and a LIR motif with a much higher affinity for the lipid form of LC3 than the BNIP and NIX proteins, facilitating the recruitment of LC3-II to damaged mitochondria(Shirane-Kitsuji & Nakayama, 2014; Xu et al., 2019; Yoo et al., 2020).

Hypoxia is able to induce FKBP8-dependent mitophagy (Yoo et al., 2020). The mechanism by which FKBP8 is activated is not yet well understood, but in response to stress conditions, the protein becomes localised to the budding sites of mitochondria undergoing mitophagy. Once the autophagophore membrane recruitment and elongation are initiated, FKBP8 can escape degradation by translocating to the ER membrane(Shirane-Kitsuji & Nakayama, 2014; Yoo et al., 2020). Another important feature of this protein is that FKBP8 is involved in Drp1-independent mitochondrial fragmentation. Indeed, ectopic overexpression of FKBP8 leads to the fragmentation of the mitochondrial network of MEF cell lines invalidated for the gene encoding Drp1. The fragmentation appears to be mediated by the LIR domain of FKBP8 which can interact with the OPA1 protein. The induction of this fragmentation was observed under hypoxic conditions but also in response to iron depletion(Yamashita et al., 2016; Yoo et al., 2020).

A.

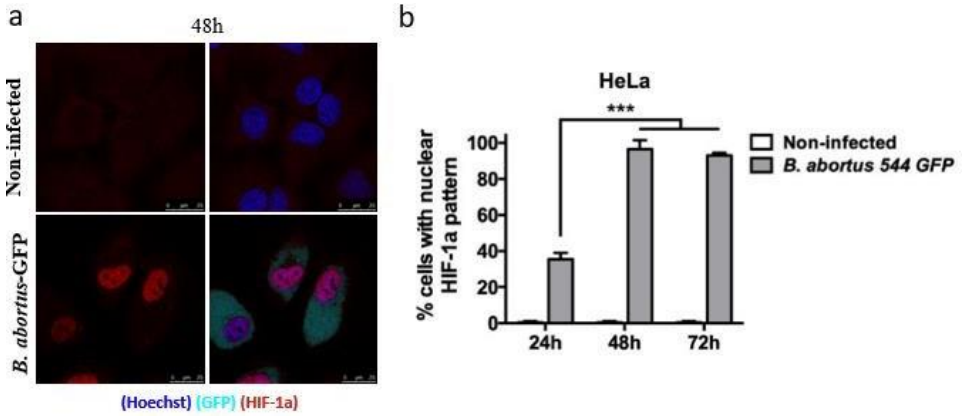

B.

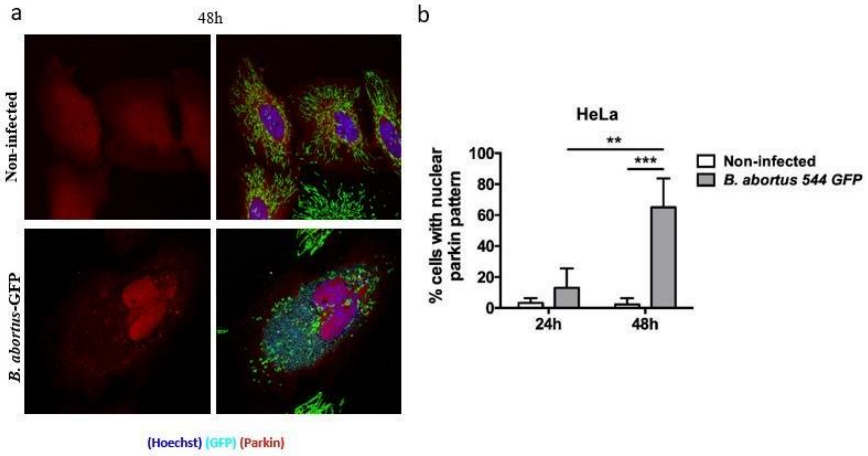

C.

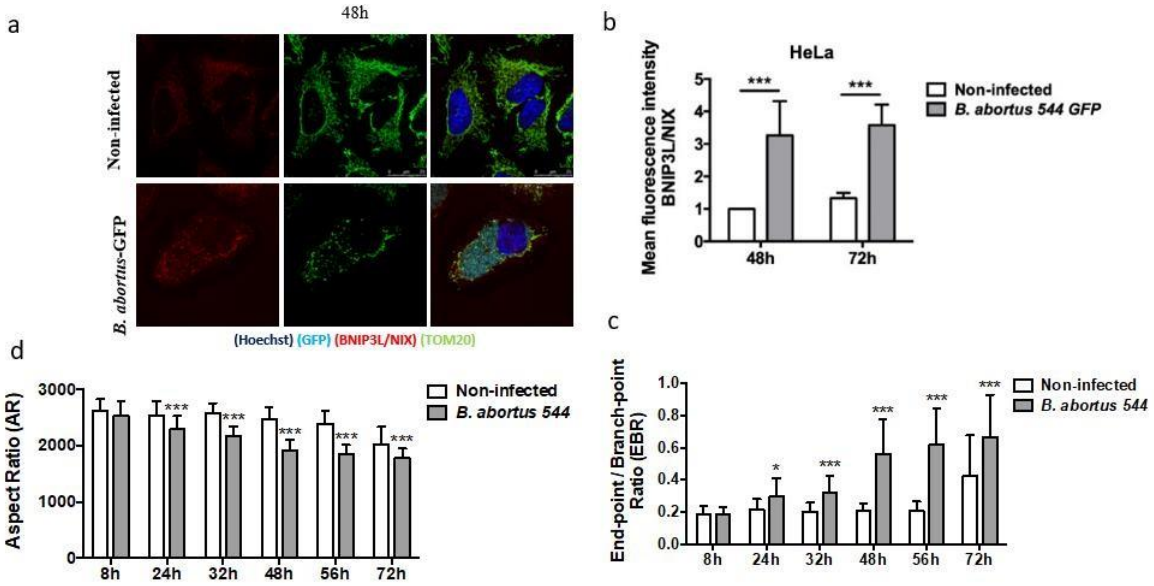

Figure 17: Overview of preliminary results (Jeremy Verbeke, PhD, unpublished data)
Legend on next page

D.

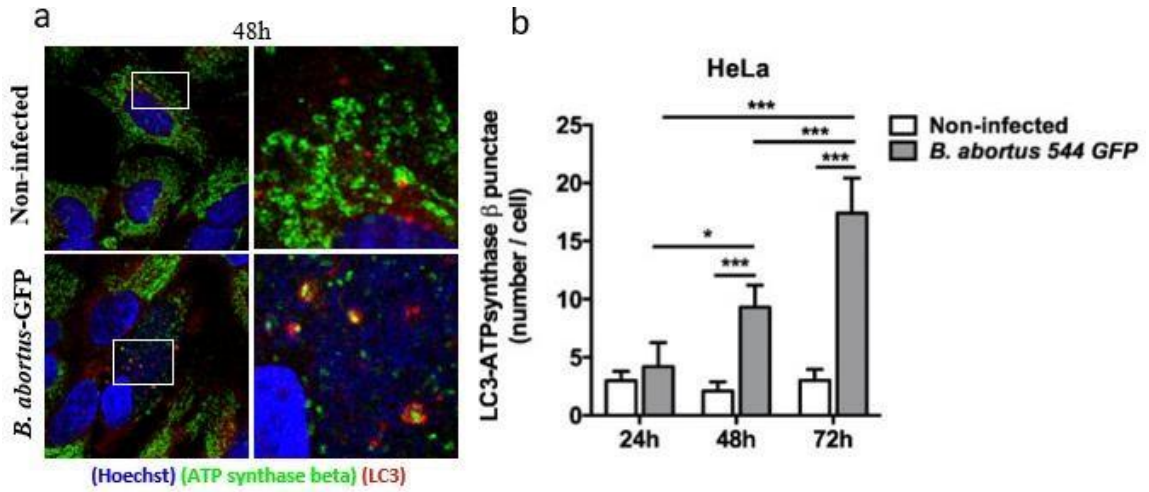

Figure 17: Overview of preliminary results (Jeremy Verbeke, PhD, unpublished data)
(A) Nuclear translocation of HIF-1α, a) Representative confocal micrographs of HeLa infected cells with *B. abortus* and stained for Hoechst (blue) as a nuclear counterstaining, or immuno-stained for HIF-1α (red) at 48 h p.i. b) Quantification (n = 3 independent experiments, 75 cells analysed/condition)
(B) Nuclear translocation of Parkin, a) Representative confocal micrographs of HeLa infected cells with *B. abortus* 544 GFP and immuno-stained for TOM 20 (green), Parkin (red), and stained with Hoechst (blue) as a nuclear counterstaining at 48 h p.i. Quantification (n = 3 independent experiments, 15 cells analysed/condition)
(C) BNIP3L/NIX expression and mitochondrial fragmentation, a) Representative confocal micrographs of HeLa infected cells with *B. abortus* 544 GFP and immuno-stained for TOM 20 (green), for BNIP3L/NIX (red), and stained with Hoechst (blue) as a nuclear counterstaining at 48 h p.i. b) Quantification of BNIP3L abundance by flow cytometry is shown in d (n = 4 independent experiments). Quantification of mitochondrial morphology is in c and d (n = 3 independent experiments, 75 cells analysed/condition).
(D) Mitophagy induction, a) Representative confocal micrographs of HeLa infected cells with *B. abortus* 544 GFP and immuno-stained for TOM 20 (green), LC3 (red) and stained with Hoechst (blue) as a nuclear counterstaining at 48 h p.i. b) Quantification of co-localisation events (n = 3 independent experiments, 75 cells analysed/condition).

PHB2 and cardiolipins are also important molecular actors of mitophagy (Youle & Narendra, 2011). These actors are, however, a bit more particular in view of both their localisation and their nature. Prohibitin 2 (PHB2) is localised at the level of the IMM. It is only when it is exposed by degradation of the OMM that this protein induces the recruitment of LC3 and contribute to the induction of mitophagy (Youle & Narendra, 2011). Cardiolipins, which are also found in the IMM, can be translocated to the OMM in response to a stress signal and allow the recruitment of proteins of the LC3 family(Yoo & Jung, 2018b).

In conclusion, a large diversity in mitophagy molecular actors have been identified so far, and its link with mitochondria fragmentation has been largely studied. In the last part of this introduction, what is known about the interactions between *Brucella* and mitochondria will be briefly reviewed.

1.2.4.5 Mitochondria and Brucella abortus infection

In view of the importance of the mitochondria and the close evolution relationship that *B. abortus* display with the organelle of the host cell, the question of the impact of this bacterium on the mitochondrial morphology was raised. As previously mentioned, mitochondria are often the target of intracellular bacteria, including *Brucella*, to promote their survival by triggering a decrease in bactericidal effects and/or an increase in energy supply(Tiku et al., 2020). One of the first effects on mitochondria that could be demonstrated was the Warburg-like effect induced by the bacteria in macrophages, characterized by a switch from OXPHOS to glycolysis, suggesting modifications/alterations in the bioenergetic functions of the organelle(Czyż et al., 2017). This metabolic modulation shows that *B. abortus* have also the ability to manipulate mitochondrial functions to their advantage. In addition, a previous study from the host lab by Elodie Lobet revealed close contacts between BCV and the mitochondria of the host cell, *in vitro*. In addition to this information, a strong fragmentation of the mitochondrial network was observed in HeLa cells at 48 h post-infection (**Figure 17**) (Lobet et al., 2018). In this study, it appears that fragmentation is Drp1 independent as the fragmentation was still observed in Drp1$^{-/-}$ mouse embryo fibroblast (MEF) infected by the bacteria. However, the consequences for the host cells or the benefits for the bacterium could not be demonstrated and were the basis of the PhD research of Jérémy Verbeke (PhD thesis, ongoing).

One of the first events that can be observed during a *Brucella abortus* infection is the **stabilisation and nuclear translocation of HIF-1α** at 24 h p.i. in HeLa and macrophages (**Figure 17**). This protein is known to be stabilised and activated in response to bacterial infection by a direct or indirect interaction. Direct activation occurs when virulence factors (siderophores, adhesins, LPS, toxins) produced by the bacterium interferes with the HIF-1α stabilisation pathway. In the case of siderophores, for example, iron deprivation prevents the activation of PDH and thus blocks the degradation of HIF-1α. Indirect activation of HIF-1α is generally due to a change in the cellular environment in response to infection. These changes may be due to host cell defence with production of ROS and NO, the establishment of an inflammatory response or excessive oxygen consumption, a condition that generates a local hypoxia(Devraj et al., 2017). Activation of HIF-1α in infected cells could be beneficial to both the host cell and the pathogen. Indeed, the stabilisation of HIF-1 can increase the bactericidal capabilities of phagocytes (Gomes et al., 2021). On the one hand, HIF-1α can, for example, initiate the secretion of pro-inflammatory cytokines or decrease bacterial internalisation (Knight & Stanley, 2019). On the other hand, HIF-1α can, under certain conditions, promote the survival and growth of bacteria(Devraj et al., 2017).

In response to *Brucella abortus*, the stabilisation of HIF-1α in macrophages appears to be mediated by STING. The entry of the bacterium into the cell will activate STING which will induce the production of ROS and thus facilitate the stabilisation of HIF-1. This stabilisation of HIF-1α would subsequently promote metabolic reprogramming within the macrophages(Gomes et al., 2021). However, there are still several open questions regarding the role of the transcription factor during infection. Indeed, the transcription factor controls the expression of hundred targets including mitophagy players such as BNIP3L that thus might have an impact on the fragmentation of the mitochondrial network that subsequently facilitate the removal of damaged mitochondria(Y. Zhang et al., 2019).

The induction of mitophagy is also a process that can be observed following a change in mitochondrial dynamics in *Brucella*-infected cells. **BNIP3L/NIX is stabilised** on mitochondria 48 h post-infection (**Figure 17**). As previously mentioned, BNIP3L expression is controlled by HIF-1α. This protein can also induce mitochondrial network fragmentation when overexpressed(da Silva Rosa et al., 2020; Simpson et al., 2021a). Indeed, it has been shown that NIX was able to induce Drp1-dependent mitochondrial fragmentation(Simpson et al., 2021a). However, in the study by Silva Rosa and collaborators, mitochondrial fragmentation appears to be induced by a release of calcium from the sarco-/endoplasmic reticulum (SR/ER) storage due to BNIP3L which leads to dephosphorylation of the GTPase and its activation(da Silva Rosa et al., 2020).

Eventually, in the search for mitophagy effectors, the **localisation of Parkin** in infected cells was studied. Contrary to what was expected, Parkin was found to be localised in the nucleus and cytosol of the infected-cell and not recruited at the mitochondria at 48 h p.i., as it would have been expected in case of a mitochondria uncoupling between the respiration and the phosphorylation of ADP in ATP in response to the trafficking of the bacteria (**Figure 17**). The nuclear translocation of Parkin is an event that has been identified recently (Shires et al., 2020). These authors showed in their study that ectopically overexpressed Parkin in HeLa cells, mouse embryonic fibroblasts (MEFs) and neonatal rat ventricular myocytes (NRVMs) targeted to the nucleus could work as a positive or a negative regulator of gene expression as the nuclear location could regulate gene expression by activating the Estrogen-Related Receptor α (ERRα), a transcription factor known to bind estrogen-related receptor response elements (ERREs) and regulate the expression of nuclear genes encoding mitochondrial proteins and Sirtuins(Shires et al., 2020). The stabilisation of Parkin and the activation of ERRα involved in the regulation of energy homeostasis by the regulation of mitochondrial biogenesis and oxidative phosphorylation(Heckler et al., 2014a). Furthermore, as previously mentioned, ERRα may be involved in the production of ROS during bacterial infection(West, Shadel, et al., 2011).

We thus decided to study whether the translocation of Parkin in the nucleus of *Brucella*-infected cells was robust or not.

1.2.5 Objectives of the thesis

In this master thesis, three main objectives have been defined:

1) to understand the role of nuclear translocation of HIF-1α and Parkin in the nuclei of the *B. abortus*-infected cells. The goal will be to determine whether this translocation is a defence of the cell and/or will benefit the growth and establishment of the replicative niche of the bacteria. We also tried to determine whether these events can induce the mitochondrial fragmentation and mitophagy that are observed in infected cells.
2) to determine whether BNIP3L/NIX is necessary for the induction of mitochondria fragmentation and mitophagy observed in infected cells. Indeed, it is interesting to better understand the role of this protein in the infection by *B. abortus* and thus to determine whether this molecular actor/effector plays a role in the intracellular cycle of the bacteria or not.
3) to better characterize the functional aspect of the fragmentation of the mitochondrial population infected cells. Indeed, the fragmentation of the organelle could be beneficial to either the host cell or the pathogen and could also facilitate a particular step in the infection cycle of the bacteria.

The output of this work should thus bring new information to better understand the interactions between *B. abortus* and mitochondria in infected cells.

Materials and Methods

Table 2: DNA and siRNA concentrations and transfection conditions

Plasmid	**Concentration**	**Supplier**	**Reference**
Parkin-mCherry	300 ng DNA/ml	Addgene	#23856
3xERRE-luciferase reporter construct	300 ng DNA/ml	Addgene	#37851
SiRNA	**Concentration**	**Supplier**	**Reference**
SiRNA-BNIP3L On-Target Plus Human BNIP3L- SMART pool	40 µM	Dharmacon	SO-2987917G
SiRNA-IRE1 ON-TARGET Plus Human ERN1- SMART pool	40 µM	Dharmacon	Catalog ID: L-004951-02-0005
Si-Non-Targeting ON-TARGET Plus Non-targeting Control Pool	40 µM	Dharmacon	Catalog ID: D-001810-10-05
Transfection agent	**Concentration**	**Supplier**	**Reference**
DharmaFECT 1 Transfection Reagent	25 µM	Dharmacon	Catalog ID: T-2001-01
X-tremeGENE™ 9 DNA Transfection Reagent	600 nl for 300 ng of DNA/well	Sigma	6365779001

2 MATERIALS AND METHODS

2.1 Cell cultures and cell treatments

HeLa cells (ATCC: American Tissue Cell Collection) were derived from a metastasis sample of a cervical cancer from an Afro-American patient, Henritta Lack (Lucey et al., 2009). These cells were cultured in Minimum Essential Medium (MEM, Gibco) supplemented with 1 % nonessential amino acids (Gibco), 1 mM pyruvate (Gibco) and 10 % foetal bovine serum (FBS, Gibco). HeLa cells were maintained in T25-culture flasks (25 cm²) or T75-culture flasks (75 cm²) (Corning-Costar, USA) in a humidified incubator at 37°C and 5 % CO_2. The cells were passed at confluence in 1 to 4 dilution for two days and 1 to 8 dilution for three days. For cell subcultures, cells were rinsed once with PBS (Phosphate Buffer Saline 1X: 10 mM phosphate buffer; pH 7.4, 150 mM NaCl), detached with 1 (25 cm²) or 2 (75 cm²) ml trypsin and ethylene diamine tetra-acetic acid (EDTA) (Gibco) during 5 min. Trypsine was inactivated by adding 5 times the volume of cell culture medium. Cells were then centrifuged and resuspended in fresh medium and seeded at the desired dilution.

RAW264.7 cells, a mouse macrophage cell line (ATCC, Manassas, VA, USA), were cultured in Dulbecco's Modified Eagle Medium High Glucose (4.5 g/L) and $NaHCO_3$ (1.5 g/L) (DHG-L1, Gibco-Life Technologies, Carlsbad, CA, USA), supplemented with 10 % heat-inactivated foetal bovine serum (FBS, Gibco). Macrophages were maintained in T25 cell culture flasks (25 cm²) or T75 cell culture flasks (75 cm²) (Corning-Costar,USA) in a humidified incubator at 37 °C containing 5 % CO_2. The cells were passed at confluence in 1 to 10 dilution for two days and 1 to 20 dilution for three days. Cells were detached with a scratcher and seeded at the desired concentration.

2.1.1 Transfection

In some experiments, cells were transfected 24 h after being seeded in a 24-well cell culture plate (Corning-Costar, USA) at a density of 20,000 cells/well in immunofluorescence and CFU experiment or in a 6-well cell culture plate (Corning-Costar, USA) at 100,000 cells/well in flow cytometry and western blot experiment. The mixture of transfection reagents consists of an optimal culture medium for transfection (Optimem 100 µl/well), the plasmid or the siRNA at the right concentration and the transfection agent (List in **Table 2**). The plasmids are used to study the translocation of Parkin into the nucleus of *B. abortus* infected cells. The Parkin-mCherry plasmid can be transfected alone or in combination with 3XERRE-luciferase reporter construct using X-treme GENE as transfection agent. The total DNA concentration should not exceed 300 ng/ml. The siRNAs were used to study the silencing of BNIP3L or IRE1 in HeLa cells infected with *B. abortus*. The silencing experiments had infected with *B. abortus* and uninfected conditions in which there were untransfected cells, cells transfected with the non-targeting siRNA used as a negative control and cells transfected with the siRNA of interest. The transfection agent used in these experiments was DharmaFECT.

Once all the components have been added, the mixture was incubated for 30 min at room temperature for the formation of the transfection complexes. Next, 100 µl per well of a 24-well plate and 200 µl per well of a 6-well plate of transfection mixture was added to the cultured medium of the cells requiring transfection and a 24 h-recovery period was preceded infection of the transfected cells.

2.1.2 Treatments for inducing a chemical hypoxia, UPR stress inductor or for uncoupling mitochondria

In some experiments, when indicated, cells were seeded for 6 h in a 24-well cell culture plate (Corning-Costar, USA) and then incubated with 100 µM $CoCl_2$ to induce a chemical hypoxia(Muñoz-Sánchez & Chánez-Cárdenas, 2019). In order to induce the erUPR stress, cells were treated with 5 µg/µL of tunicamycin 24h before the fixation. Finally, to induce the uncoupling of mitochondria, cells were treated with FCCP (20 µM) was added to the cells for 30 min before cell fixation (Blancke Soares et al., 2021). In some experiments, an HIF-1α inhibitor, PX-476, was used in HeLa cells at the concentration of 25 or 35 µM (Koh et al., 2008). The inhibitor was added to the cell culture medium 8 h after infection. A dimethyl sulfoxide control (DMSO; 0.1 %, the solubilising agent used for the inhibitor) has also been performed to assess the putative effect of the vehicle alone.

2.2 *Brucella* bacterial strain

The bacterial strain used in this study is the virulent GFP-expressing *B. abortus* strain 544. Bacteria were grown in Tryptic Soy Broth 5 % (TSB; 211825, BD Biosciences) and kept frozen at 80 °C in 15 % glycerol-TSB medium. For infection steps, 10 ml of TSB were inoculated with a double bacterial colony from a freshly streaked TSB (211825, BD Biosciences) agar (2145530, BD Biosciences) plate (639120, Greiner bio-one) and then grown at 37 °C in a shaker for 15 h (early stationary phase) up to an optical density (O.D.) ranging between 0.5 to 1 measured at 600 nm in a spectrophotometer (x-Mark, BIO RAD) to assess cell suspension density by turbidimetry(Detilleux et al., 1990).

2.3 Cell infection

When bacterial liquid cultures of 10 ml reached the optical density between 0.5 and 1, bacteria were pelleted by centrifugation (7000 g for 2'30") and rinsed twice with 10 ml of phosphate-buffered saline (PBS) at 22 °C, resuspended in 10 ml of eukaryotic cell culture media before adjusting the bacterial suspension density to the appropriate multiplicity of infection (MOI) (MOI for HeLa: 2000 and MOI for RAW264.7 : 200) in the corresponding eukaryotic cell culture media, MEM (Gibco) supplemented with 1 % nonessential amino acids (Gibco), 1 mM pyruvate (Gibco) and 10 % foetal bovine serum (FBS, Gibco) and DHG-L1 (Gibco-Life Technologies, Carlsbad, CA, USA), supplemented with 10 % heat-inactivated foetal bovine serum (FBS, Gibco), for HeLa and RAW264.7 cells, respectively. The infectious dose was monitored by plating bacteria on TSB agar plates and then counting Colony Forming Units (CFUs). For host cell infections, bacteria were sedimented onto cells by a centrifugation of 10 min at 500 g (20 °C) to promote the cell-bacteria contacts and then incubated for 1 h at 37 °C in an incubator containing a humidified atmosphere with 5 % CO_2. Cells were next incubated for 1 h with 50 µg/ml gentamycin (Invitrogen) of cell culture medium to eliminate the remaining extracellular bacteria. Cells were eventually incubated for different times post-infection (p.i.) with 10 µg/ml gentamycin of culture medium to avoid re-infection events.

2.4 CFU counts

Brucella replication in infected cells was assessed by CFU counting at several p.i time points (2, 6, 24, 48, or 72 h). Cells were rinsed once with 1 ml of PBS and lysed for 10 min with 0.5 ml of PBS containing 0.1% Triton X-100 (Sigma-Aldrich) at room temperature (RT). Viable bacteria were quantified by plating serial dilutions, depending on the p.i. time point, of this lysate on scare petri dish (639102, Greiner bio-one) containing TSB (211825, BD Biosciences) agar (214530, BD Biosciences).

Table 3: Antibodies used for immunofluorescence experiments

Primary antibody	Type	Dilution	Supplier	Reference
Anti-TOM 20	Mouse monoclonal antibody	1/200	ABCAM	ab186735
Anti-ATPsβ	Mouse / IgG1 Monoclonal antibody	1/300	Invitrogen	3D5AB1
Anti-HIF-1α	Mouse monoclonal antibody	1/100	ABCAM	Ab179483
Anti-Parkin	Recombinant Rabbit Monoclonal Antibody	1/100	Invitrogen	21H24L9
Anti-BNIP3L	Rabbit monoclonal antibody	1/100	Cell signalling	12396S
Anti-LC3	Rabbit Monoclonal Antibody	1/100	Abcam	Ab192890
Fluorescence staining of DNA and nuclei	**Type**	**Dilution**	**Supplier**	**Reference**
Hoechst	Cell-permeable DNA stain	1/500	Sigma	33258
Secondary antibody	**Type**	**Dilution**	**Supplier**	**Reference**
IgG Anti-mouse Alexa 633 nm Emission 650 nm	Goat Polyclonal Secondary Antibody	1/1000	Invitrogen	A21050
IgG Anti-rabbit Alexa 633 nm Emission 650 nm	Goat Polyclonal Secondary Antibody	1/1000	Invitrogen	A10225
IgG Anti-rabbit Alexa 514 nm Emission 543 nm	Goat Polyclonal Secondary Antibody	1/1000	Invitrogen	A1104
IgG Anti-mouse Alexa 514 nm Emission 543 nm	Goat Polyclonal Secondary Antibody	1/1000	Invitrogen	A11031

2.5 Bioscreen

When indicated, a bioscreen (consisting of the measurement of OD 600 nm in well containing *B. abortus* 544 GFP to monitor the multiplication rate of *B. abortus* overtime) was performed to assess the proliferation of bacteria in the presence of $CoCl_2$. Bacterial cultures of 10 ml were pelleted by centrifugation (7000 g, 2,3 min) and rinsed 3 times with 10 ml of PBS, resuspended 10 ml of TSB culture media before adjusting the culture O.D. at 0.05 by dilution in TSB culture media. The bacterial cultures were seeded in a 96-well plate (Greiner bio-One, Germany) 200 µl/well and incubated with different concentrations of $CoCl_2$ (0, 50, 100, or 500 nM) to determine the evolution of the bacteria proliferation as assessed by O.D. measurement every 30 min, in a Bioscreen spectrophotometer (ThermoFisher, ref.110001-536), over a period of 48 h.

2.6 Immunofluorescence

Cells were grown on coverslips in 24 or 6 well cell culture plates (Corning-Costar, USA) at a density of 20,000 cells/well for HeLa cells and 15,000 cells/well for RAW264.7 cells, and then infected by *B. abortus 544 GFP* for different incubation time points. After the indicated times p.i., cells were fixed with 4 % paraformaldehyde (PFA) for 30 min or 100 % methanol (-20 °C) for 15 min, rinsed 3 times with 1 ml of PBS at RT and then permeabilized for 10 min with 0.5 ml of 1 % Triton X-100 diluted in PBS. Methanol fixation was used for LC3 immunostaining. The fixed and permeabilized cells were rinsed 3 times (10 min each) with 0.5 ml of PBS-2 % Bovine Serum Albumin (BSA) prior to the addition of the primary antibody diluted in PBS-2 % BSA to a final volume of 30 µl per coverslip (antibodies used, dilutions and suppliers are listed in **Table 3**). Cells were incubated for 2 h (at RT) with the primary monoclonal antibody diluted in PBS containing 2 % BSA. At the end of the incubation period, cells were rinsed 3 times with 0,5 ml of PBS containing 2 % BSA (10 min each). Cells were next incubated for 1 h with the secondary antibody solution in a final volume of 30 µl per coverslip (antibodies used, dilutions and suppliers are listed in **Table 3**). At the end of the incubations, cells were rinsed 3 times with 0,5 ml of PBS containing 2 % BSA (10 min each), rinsed 3 times with PBS and then, eventually rinsed 3 rinses with distilled water before mounting the lenses with Mowiol. The observations were made by confocal microscopy using a confocal microscope (Leica) or a LSM980 confocal microscopy with Airyscan 2 (Zeiss).

2.7 Generating BNIP3L-KO HeLa cells lines by CRISPR-Cas9 genome engineering

To determine the putative effect of the BNIP3L protein in *Brucella*-infected cells, we decided to generate a HeLa cell line invalidated for BNIP3L. For that purpose, the CRISPR-Cas 9 system, RNA-guided nucleases that cleave specific foreign genetic elements, was used (Ann Ran et al., 2013). A complete view of the protocol is shown in **Figure 18**. A number of 3 single guide RNA (sgRNAs) was selected using CRISPRscan software (Giraldez Lab, Yale) that is based on several criteria for the selection of the most efficient sgRNA: chromatin accessibility, targeting essential exons, minimizing off-target complementarity, getting the GC-content right and ensuring the presence of a Protospacer Adjacent Motif (PAM) motif. The PAM sequence, NGG in this case, allows the binding of the Cas9 and allows the target cleavage 3-4 nucleotides upstream.

The 3 sgRNAs that emerged from this research are sgRNA1 (5'-CGGCGGCGGCTCGACTAGGTGGG-3'), sgRNA2 (5'-GGCCGTTTGGGCTCGCGGTCCGG-3') and sgRNA3 (5'-GTGCGGACTGGGTATCAGACTGG-3').

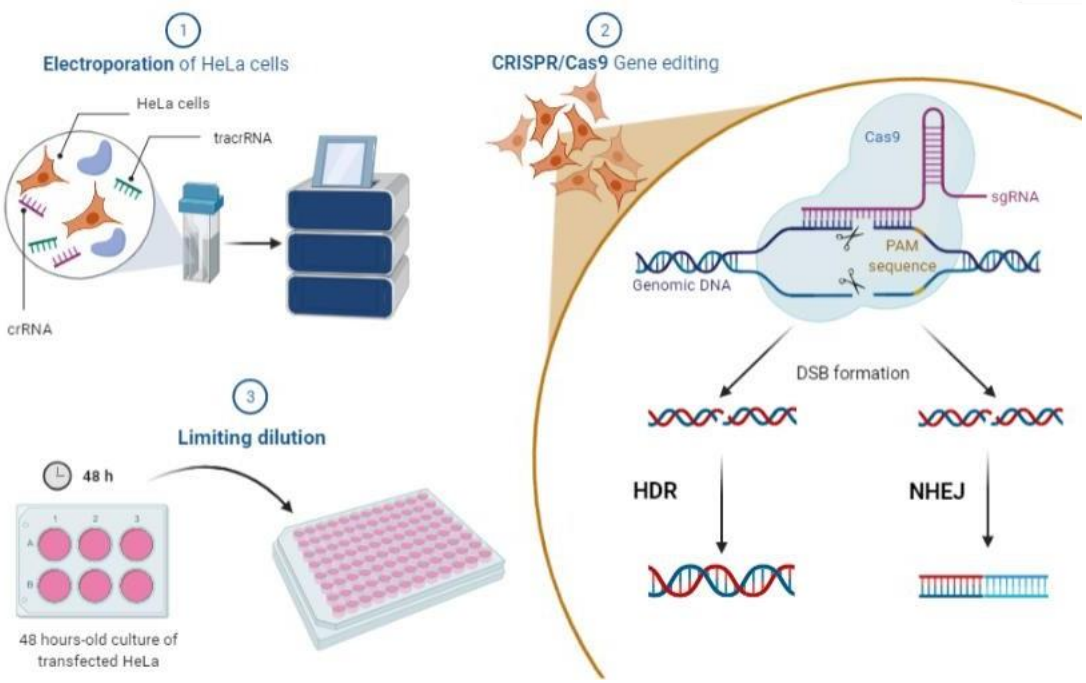

Figure 18: Overview of CRISPR/Cas9 gene editing of HeLa cells. About 1 million of HeLa cells per sgRNA are first electroporated in Amaxa nucleocuvette with the A-28 program and the CRISPR mixture (the Cas9 shown in blue, trackRNA and sgRNA). A double-strand break occurs 3-4 nucleotides above the PAM sequence. A repair of this double strand break is then implemented. Two repair mechanisms are thus possible: a Non-Homologous End Joining (NHEJ) or a Homology-Direct repair (HDR). The batch of electroporated cells was then allowed to recover for 48 h in a 6-well cell culture plate before undergoing a limiting dilution in a 96-well cell culture plate.

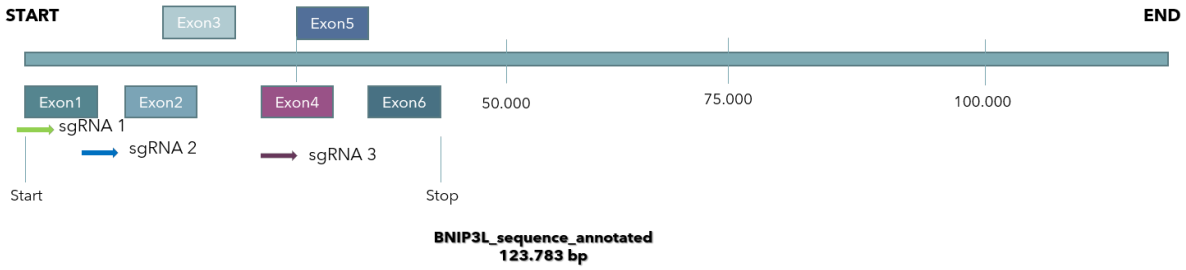

Figure 19: Localisation of sgRNA on BNIP3L sequence. Annotated sequence of the gene encoding BNIP3L containing the 6 exons represented by the different boxes, the beginning and the end of the coding and non-coding sequence, as well as the 3 sgRNAs (in green sgRNA1, in blue sgRNA2 and in purple sgRNA3).

Table 4: Sets of primers for PCR

#	Primers	Primer sequences	T° hybridation	% CG	Size amplicon (bp)
1	crRNA1-F	TCGCTTGTTGTGTTGTCATC	56,4	45	243
	crRNA1-R	AGAGACTGCTCATTTTCCTC	56,4	45	
2	crRNA2-F	AAGGCAGCTCATTGGCTC	56,3	56	447
	crRNA2-R	TGTGGCAACAAAGGAATGC	55	47	
3	crRNA3-F	TTCTGAGACACAACCTTATGA	55,4	38	367
	crRNA3-R	AGAACGTTTAGGGTGTCTG	55	47	

The double break made by Cas 9 will occur in either the first two sgRNAs in exon 1 and sgRNA3 in exon 4 (**Figure 19**). The double-strand break can be repaired by nonhomologous end joining (NHEJ), small insertions and deletions can be created and lead to early termination of the protein through frameshift introduction. Technically, HeLa cells were electroporated with Cell Line Nucleofector Kit R (Lonza) (protocol described in **Figure 18**).

The sgRNA (1.25 µl) and trackRNA (1.25 µl) (which allows the binding of Cas9 to the sgRNA) diluted in Nuclease-Free Duplex Buffer (7.5 µl) were placed in a PCR (Polymerase Chain Reaction) tube in a thermocycler (Eppendorf, Mastercycler) using a programme allowing cooling down from 95 to 30 °C at a rate of 5 °C per min. For the formation of the Ribo Nuclear Particule (RNP) complex, the Cas9 was added to the mixture for 10 min at RT. One million of HeLa cells were rinsed with X ml PBS and resuspended in 100 µl room-temperature Nucleofector® Solution per sample. The cells were electroporated in an "Amaxa nucleocuvette" using an optimized (A-28) program by Amaxa company. After that, cells recovered for 48 h in two 6-well cell culture plates per condition. A limiting dilution was performed after the 48 h in 96 well-plates to allow clonal selection. In addition, a volume of 2/3 of the cell population was kept frozen, and the rest (1/3 of the entire cell populations) was used for global DNA sequencing (see section 1.9). To reveal the efficiency of gene editing, DNA extraction and PCR were performed. Wells containing 1 and only 1 cell as determined by phase contrast microscopy observation were selected and monitored until cells reached 50 % confluency. Those clones were then seeded in 24, 12 and finally 6-well cell culture plates to maintain and expand cell populations. On these clones, a protein extraction (see section 1.10) was prepared for the analysis of BNIP3L abundance by western blot and selection of interesting BNIP3L-KO clone candidates.

2.8 DNA extraction

In order to perform DNA sequencing on the electroporated HeLa cell populations, DNA extraction was performed with the Wizard ® genomic purification kit (Promega). Cells were lysed in a volume of 600 µl of Nuclei Lysis Buffer and 3 µl of RNase solution were added to the nuclear cell lysates. Samples were incubated for 15-30 min at 37 °C. Proteins were next precipitated by adding 200 µl of Protein Precipitation Solution. Samples were vortexed vigorously and then centrifuged for 4 min at 16,000 g. The supernatant was collected and 600 µl of isopropanol (Merk, Germany) was added to precipitate the DNA. The samples were centrifuged for 1 min at 16,000 g and the DNA pellets were then resuspended in 600 µl of 70 % ethanol before a second centrifugation (1 min-16,000 g). Finally, the DNA was air dried and solubilised in 50 µl of ddH_20 overnight.

2.9 PCR

A final volume of 50 µl of the PCR mixture (composed of 10 µl 5X Q5 reaction buffer, 1 µl nucleotides mixture, 10 nM dNTPs, 2.5 µl 10 µM forward primer and reverse primer listed in **Table 4**, gDNA for 500 ng/µl, 0.5 µl Q5 High-Fidelity DNA Polymerase and the amount of water needed to reach the final volume) was prepared with the Q5 High-Fidelity DNA Polymerase (New England Biolabs). After preparing the mixture according to the manufacturer's instructions, DNA sequences were amplified with the PCR program (Q5) corresponding to an initial denaturation with 1 cycle at 98 °C for 30 sec, an amplification phase with 35 cycles (consisting of 3 successive steps of 98 °C for 10 sec, 64 °C for 30 sec and 72 °C for 30 sec) and finally the extension phase with 1 cycle at 72 °C for 2 min followed by cooling to 4 °C in a thermocycler (Eppendorf AG, Hamburg). PCR products (amplicons) were run on gel polymerize a 2% agarose gel and then cleaned with the Nucleospin gel and PCR clean-up

Table 5: Antibodies used for the western blot analysis

Antibodies	Dilution	Supplier	Reference
Anti-β Actine	1/10,000	Sigma- Aldrich	A5441
Anti-Bnip3L	1/1000	Cell Signalling	12396
Anti-IRE1α	1/1000	Abcam	EPR5253
Goat anti-Rabbit IgG 800 nm	1/10,000	Li-Cor Bioscience	926-32211
Goat anti-Rabbit IgG 680 nm Emission 704 nm	1/10,000	Li-Cor Bioscience	926-68071
Goat anti-Mouse IgG 800 nm	1/10,000	Li-Cor Bioscience	926-32210
Goat anti-Mouse IgG 680 nm Emission 704 nm	1/10,000	Li-Cor Bioscience	926-68070

(Macherey-Nagel). Cleaned PCR products were sequenced by the Sanger technique (Ref) (Genewiz).

2.10 Cell lysate preparation, protein assay and western blot analyses

HeLa clones were tested to determine their BNIP3L-KO/invalidation status and were incubated or not with 100 µM $CoCl_2$ for 16 h to induce the overexpression of BNIP3L. Cells were rinsed once in ice-cold PBS and then scraped in 3.75 µl/cm^2 of lysis buffer (20 mM Tris-HCl; pH 7.5, 150 mM NaCl, 15 % Glycerol, 1 % Triton X-100, 2 % Sodium Dodecyl Sulfate (SDS), 4 % Protease Inhibitor Cocktail (PIC) (Roche, Switzerland), and 4 % Phosphate Inhibitor Buffer (PIB) composed of: 25 mM Na_3VO_4 (Sigma, USA), 250 mM PNPP (4-nitrophenylphosphate) (Sigma, USA), 250 mM β-Glycerolphosphate (VWR, Belgium) and 125 mM NaF (Merck, Germany). The cell lysates were then collected and centrifuged (4 °C) for 15 min at 13,000rpm (Eppendorf Centrifuge 5414R, Germany). Sample proteins were frozen at -80°C until use.

Pierce 660 nm Protein Assay Reagent (ThermoFischer Scientific, 22660) was used to measure the protein concentration in supernatant according to the manufacturer's instructions. A calibration curve was performed with samples containing BSA (Thermofisher Scientific, USA) at different and known concentrations (from 0 to 10 µg/ml). The absorbance was measured at 660nm using the xMARK Microplate Absorbance Spectrophotometer (BioRad, USA).

An equivalent of 10 µg of proteins was diluted in distilled water and 5x loading buffer (0.143 M Tris-HCl; pH 8.0, 0.2 M SDS; 2 M β-mercaptoethanol; 25 % Glycerol; 0.75 mM Bromophenol Blue). Sample proteins were next heated for 5 min at 100 °C, centrifuged for 2 min at 13,000 rpm (Eppendorf, Minispin, Germany) and then loaded and resolved on 7.5-10 % homemade separation gel [composed of the separated gel made with 1,2 ml of separation buffer (1,5M Tris (Carl Roth, Belgium), 0,4% SDS (Carl Roth, Belgium) 1,2-1,7 ml of acrylamide (30/0,8%, PlusOne, Belgium) and 2,1-2,7 ml of H_2O and the staking gel made with 1,25 ml with the staking buffer (0,5M Tris (Carl Roth, Belgium) and 0,4% SDS (Carl Roth, Belgium)), 0,5 ml of acrylamide and 2,25 of distilled H_2O each polymerize by the addition of APS 10% (PlusOne, Belgium) and TEMED (PlusOne, Belgium)] with running buffer (composition: 2.5 mM Tris-HCl; pH 8.5, 19.2 mM Glycine, 0.01 % SDS). The determination of the molecular weight of the protein of interest is allowed by comparing the molecular weight to molecular weight maker (2 µl of Color Protein Standard Board Range (BioLabs, USA)). The migration was performed at 150V for 1 h. Proteins were then transferred on membrane Immobilon® to polyvinylidene difluoride (PVDF) (Merck, IPFL85R) previously activated by a one-min bath in 100 % methanol (Merck, Germany). The membrane was then assembled for a liquid transfer with 2 Whatman paper, 2 sponge, the PVDF membrane and a cassette. The transfer was done in a at 70 V for 2 h. The membrane was blocked with Odyssey Blocking Buffer (Licor, USA) for 1 h. Primary antibodies were incubated for 16 h at 4°C (antibodies used in experiments are listed in **Table 5**). Primary and secondary antibodies were diluted in Odyssey Blocking buffer containing 0.1 % Tween-20 (BioRad, USA), 0,2% SDS (Carl Roth, Belgium). Secondary antibodies were incubated for 1 h at room temperature. For the immunodetection of the β-actin used as a loading control, the primary and secondary antibody have been incubated 30 min at RT, with 3 rinses with PBS-0.1% Tween-20. Finally, the membrane was rinsed 3 times for 5 min in PBS containing 0.1% Tween-20 and twice in PBS. The quantification of the immunodetected fluorescence signal has been performed using Odyssey scanner (ODY-1896) (Licor, USA).

Table 6: Antibodies used for flow cytometry

Primary antibody	**Dilution**	**Supplier**	**Reference**
Anti-BNIP3L	1/100	Cell signaling	12396
Anti-P-IRE1	1/100	Abcam	EPR5253
Anti-XBP1	1/100	Abcam	Ab37152
Secondary antibody	**Dilution**	**Supplier**	**Reference**
IgG Anti-rabbit Alexa 633 nm Emission 650 nm	1/1000	Invitrogen	A102215

2.11 Flow cytometry

HeLa cells were seeded in 6-well culture plate (Corning-Costar, USA) at a density of 100,000 cells/well for flow cytometry analysis. Several technical controls were performed: non-infected cells without any immunostaining (to control cell autofluorescence), second, cells infected but without any immunostaining (to control the intensity of the GFP expressed by *B. abortus*), and non-infected cells stained with the secondary antibody alone (to control background fluorescence of the fluorophore). Cells were then infected with *B. abortus* 544 GFP for the indicated times p.i.. Cells were then rinsed in 1 ml PBS at RT before being detached with 160 µl of trypsin-EDTA per well at 37 °C. Trypsin was inactivated with 3 ml ice-cold PBS. The detached cells were transferred to a falcon before being centrifuged at 500 g for 5 min at 4 °C. Then, cells were rinsed twice in ice-cold FACS-Buffer (0.5 % BSA and 2 mM EDTA diluted in PBS) and centrifuged at 500 g for 5 min at 4°C (Eppendorf Centrifuge 5414R, Germany). Cells were next fixed with 200 µl of eBioscienceTM IC Fixation Buffer (Invitrogen, 00-8222-49) for 30 min at RT and centrifuged at 500 g for 5 min at RT (Eppendorf Centrifuge 5414R, Germany), permeabilized for 5 min with eBioscienceTM Permeabilisation Buffer (10X) (Invitrogen, 00-8333-56) diluted 10 times in ddH_2O and then centrifuged at 500 g, 5 min at RT. After removal the Permeabilisation Buffer, samples were incubated for 1 h (at RT and in the dark) with 100 µl of the appropriate primary antibody (**Table 6**) diluted 100 times in the Permeabilisation Buffer. Then, the primary antibody was removed by a centrifugation at 500 g for 5 min at RT, and cells were then rinsed once with 200 µl of the Permeabilisation Buffer. Thereafter, cells were incubated for 30 min at RT (in the dark) with 100 µl the secondary antibodies diluted 1000 times in the Permeabilisation Buffer. Cells were then rinsed once with 200 µl of Permeabilisation Buffer and then resuspended in 500 µl of flow cytometer buffer (500 ml PBS, 0,5% BSA (2,5g), 2 mM EDTA (3,72g)). At that step, samples can be stored at 4°C in the dark for a couple of days. Samples were then transferred into glass tubes for flow cytometry before analysis by flow cytometry (BD FACSVerseTM).

2.12 Statistical analyses

Results were usually expressed as means ± 1 S.D. for up to 3 independent replicates (unless indicated in the legends of the figure) and the statistical significance (p-value <0.05) of the differences between groups were determined by a two-way ANOVA test followed by a Turkey post-test. Statistical analyses were performed using GraphPad Prism 5 software.

Results

A.

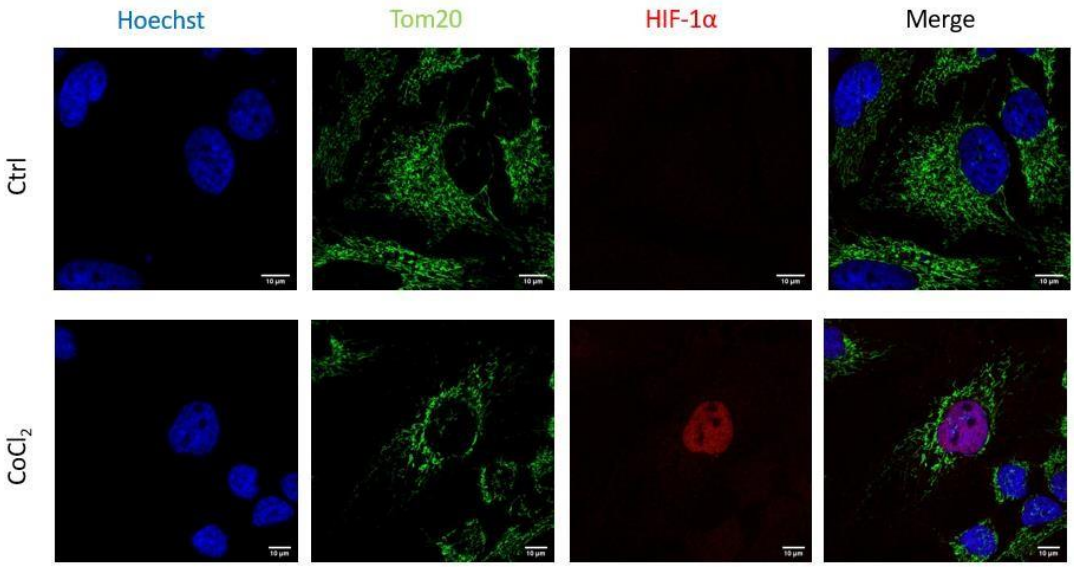
Hoechst
Tom20
HIF-1α
Merge
Ctrl
CoCl2

B.

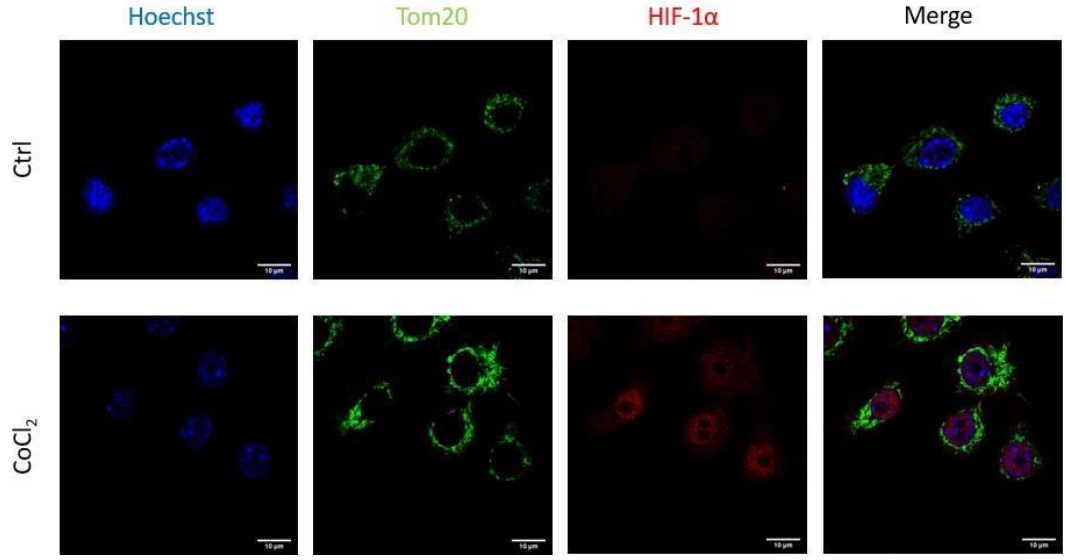
Hoechst
Tom20
HIF-1α
Merge
Ctrl
CoCl2

C.

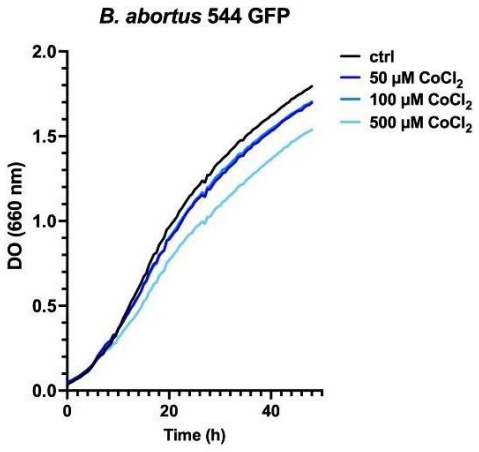
B. abortus 544 GFP
DO (660 nm)
Time (h)
ctrl
50 µM CoCl2
100 µM CoCl2
500 µM CoCl2

3 RESULTS :

3.1 Study of the role of HIF-1α in the infection of HeLa and RAW264.7 cells with *B. abortus*

Previous results at the beginning of this Master thesis showed that stabilisation of HIF-1α and its nuclear translocation was observed in both HeLa and RAW264.7 cells infected with *B. abortus* at 24 h p.i and 48 h p.i (**Figure 17**) (Jeremy Verbeke, PhD thesis, unpublished data). The first objective of this thesis was therefore to better understand the putative role of HIF-1α stabilisation at 24 h p.i for *B. abortus* and the potential link with the induced mitochondrial fragmentation observed in *Brucella*-infected cells(Lobet et al., 2018). To answer this research question, we first decided to modulate the accumulation of HIF-1α modulation (by two different strategies) on *B.abortus* proliferation and mitochondrial fragmentation in both HeLa and RAW264.7 cells.

First, we tested the effect of chloride cobalt ($CoCl_2$) to induce a chemical hypoxia and HIF-1α stabilisation before and during *B.abortus* infection in HeLa and RAW264.7 cells. Effectively, $CoCl_2$ is known to induce a strong stabilisation of HIF-1α and HIF-2α under normoxic conditions by (Muñoz-Sánchez and Chánez-Cárdenas, 2019). The molecular mechanism at the bottom line of the stabilisation of HIF-1α results from the inhibition of prolyl hydroxylases (PHDs) through displacement of Fe^{2+} by Co^{2+}.

In a second approach, we tested the effect of the inhibition of HIF-1α with PX-478, a HIF-1α inhibitor also used in anti-cancer treatments(Lee and Kim, 2011). PX-478 inhibits HIF-1α at multiple levels: it decreases HIF-1α mRNA levels; it blocks HIF-1α translation, and it inhibits HIF-1α deubiquitination, consequently leading to increased ubiquitination and enhanced degradation of the protein. However, the molecular mechanism underlying all these actions has not been studied to date.

3.1.1 Study of the effect of HIF-1α stabilisation by CoCl2 at different times prior to and/or following infection with B. abortus in HeLa and RAW264.7 cells

HIF-1α activation in bacterial infection was identified as a host response to infection by regulating the bactericidal capacities of phagocytic cells (Devraj et al., 2017). During infection, HIF-1α is important to induce NO production allowing the secretion of the pro-inflammatory cytokine TNF-α or to activate autophagy. However, activation of HIF-1α has also been shown to be beneficial to the growth and proliferation of the bacteria (Schaible et al., 2013). Indeed, this transcription factor increases the expression of the genes responsible for glucose uptake and thus energy intake during the early phase of the infection promoting the survival and proliferation of bacteria (Schaible et al., 2013). The dual roles of HIF-1α during intracellular bacterial infection led us to question its putative role during the infection of the host cells by Brucella. The stabilisation of this transcription factor before or during infection of HeLa or RAW264.7 cells by *B. abortus* will allow us to exacerbate the action of HIF-1α in our experimental model.

Firstly, we wanted to induce the stabilisation of HIF-1α prior to and following infection with *B. abortus* in HeLa and RAW264.7 cells to understand the putative effect of HIF-1α stabilisation on the proliferation/replication of *B. abortus* in host cells. In order to promote the accumulation of HIF-1α, cells were incubated with 100 µM of $CoCl_2$ to induce a chemical hypoxia. Stabilisation and nuclear translocation were confirmed in both HeLa (**Figure 20A**) and RAW264.7 cells (**Figure 20B**) incubated with the $CoCl_2$ for 48 h.

D.

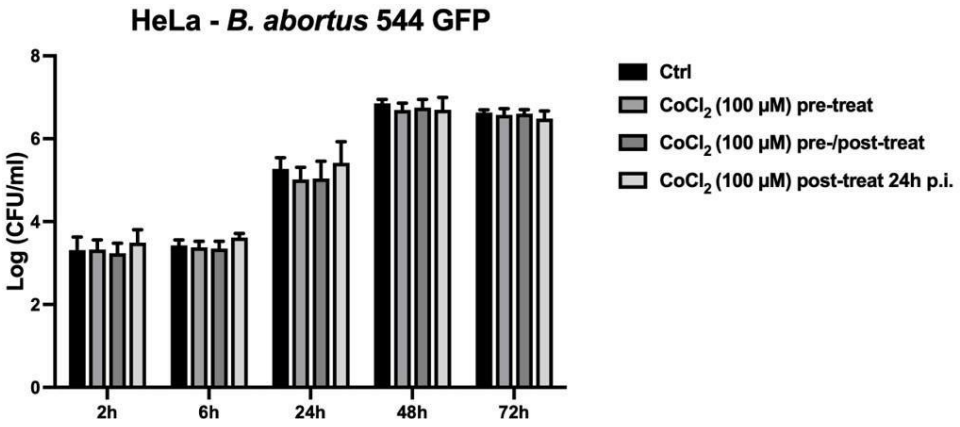

E.

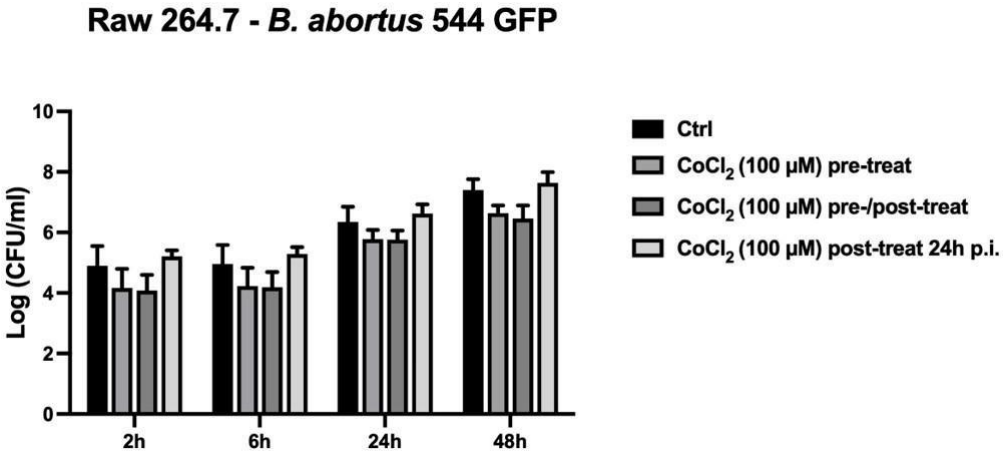

Figure 20: Effect of different $CoCl_2$ treatments on HIF-1α stabilisation, on the proliferation of *B. abortus* in *vitro* and on infection efficiency in HeLa and RAW264.7 cells.

(A) Representative confocal micrographs of HeLa cells incubated or not (Ctrl) with $CoCl_2$ for 16 h and immuno-stained for Tom 20 (green) or HIF-1α (red) and stained for Hoechst (blue). Cells were observed with a Leica confocal microscope. (Scale bars: 10 µm)

(B) Representative confocal micrographs of RAW264.7 cells incubated or not (Ctrl) with $CoCl_2$ for 16 h and immuno-stained for Tom 20 (green) or HIF-1α (red) and stained for Hoechst (blue). Cells were observed with a Leica confocal microscope. (Scale bars: 10 µm)

(C) Growth curves of *B. abortus* 544 GFP grown in TSB culture media with or without $CoCl_2$ (50, 100 or 500 µM) for 48 h. Growth curves represent mean values of culture media OD measured every 30 min during 48 h for three technical replicates. Inoculum had OD= 0.05 and incubation temperature was 37 °C.

(D) RAW264.7 cells or **(E)** and HeLa cells were incubated or not with 100 µM $CoCl_2$ according to several treatment protocols: control (no treatment), cells pre-treated for 16 h before the infection, cells pre-treated for 16 h with $CoCl_2$ before and directly after the infection, or cells only incubated with the molecule at 24 h post-infection. CFU assays were then performed at different post-infection time points (2, 6, 24, 48 or 72 h). Results are expressed as means ± 1 SD (n=3 for RAW264.7 and n=4 for HeLa cells). Statistical analysis performed (Two-way ANOVA using Tukey test).

Before testing the effect of $CoCl_2$ on the *Brucella* CFU counted after cell infection, it was necessary to verify whether $CoCl_2$ could exert any modulatory effect on the growth of *B. abortus in vitro* and by itself. We thus performed a "bioscreen assay" (Cooper et al., 2011). The growth and proliferation of the bacteria was assessed by measuring the OD of the bacterial liquid cultures, every 30 min for 48 h, when Brucella are incubated or not with different concentrations of $CoCl_2$ (50, 100 or 500 µM) (**Figure 20C**). For concentrations of 50 and 100 µM, no difference of proliferation was observed when compared to the control (untreated bacteria) (**Figure 20C**). A decrease in the OD of the bacterial culture over time is observed when the bacteria is exposed to 500 µM $CoCl_2$ when compared to the control, indicating an alteration in the growth/viability or proliferation of the bacteria (**Figure 20C**). In view of these results, a concentration of 100 µM was kept for the infection experiments.

To test the putative effect of HIF-1α accumulation induced by 100 µM $CoCl_2$ on the proliferation of *B. abortus* in host cells (RAW264.7 or HeLa), cells were either pre-treated (or not (control cells) for 16 h with the molecule before the infection, pre-treated before and during the infection or only treated with the molecule at 24 h post-infection. Infected cells were lysed after 2, 6, 24, 48 and 72 h p.i to perform colony-forming unit assays (CFUs) (**Figure 20**).

For HeLa cells, no change in CFUs was observed no matter what the condition considered (**Figure 20D**). The activation of HIF-1α in HeLa cells does not seem to have any effect on the intracellular growth/proliferation and viability of *Brucella* abortus (**Figure 20E**). However, for RAW264.7 macrophages, a decrease in the number of CFUs (0.5 log) was observed when cells were pre-incubated with $CoCl_2$ before infection or before and post-infection but not when post-treated at 24 h p.i. (**Figure 20E**). The decrease is observed very rapidly and already at 2 h p.i. suggesting that the invasion/entry of the bacteria might be affected by $CoCl_2$ and thus the accumulation of HIF-1a in the nuclei of infected cells.

Several interesting observations can be made based on these initial data. Phagocytic cells have a response to the stabilisation of HIF-1α as opposed to the epithelial cells (HeLa cells). This stabilisation is manifested by a decrease in CFU numbers when this occurs prior to or during the early phase of infection. These observations suggest that the entry or survival of the bacteria may be disrupted. This hypothesis can be supported by the fact that phagocytic cells will, upon activation of HIF-1, promote glycolytic metabolism which induces polarisation into pro-inflammatory M1 macrophages(T. Wang et al., 2017a). These M1 macrophages might then be more apt to fight a bacterial infection by limiting the survival of bacteria.

3.1.2 Study of the role of HIF-1α inhibition on the infection of HeLa cells by B. abortus

We next wanted to test the possibility of inhibiting HIF-1α observed in response to Brucella infection and test the effect of the inhibition on the CFUs. Based on the literature, we found an inhibitor, PX-478 (S-2-amino-3-[4-N,N,-bis(2-chloroethyl)amino] phenyl propionic acid N-oxide dihydrochloride), a molecule described to decrease the expression of the HIF-1α protein expression and to increase its degradation in both normoxic and hypoxic conditions in cancer cells (Koh et al., 2008). PX-478 is used in anti-cancer treatments and has been shown to be a specific inhibitor for HIF-1α protein by a mechanism that is not dependent on pVHL activity and allows a decrease in the expression of HIF-1α target genes such as the genes encoding Vascular Epithelium Growth Factor (VEGF), erythropoietin (EPO) and glucose transporter 1 (GLUT1)(Koh et al., 2008; Lee and Kim, 2011).

To test the effect of PX-478 on the inhibition of HIF-1α in *B. abortus* infected HeLa cells (48 h), HeLa cells were treated with 25 or 35 µM of this inhibitor 16 h (= at 32 h p.i.) before

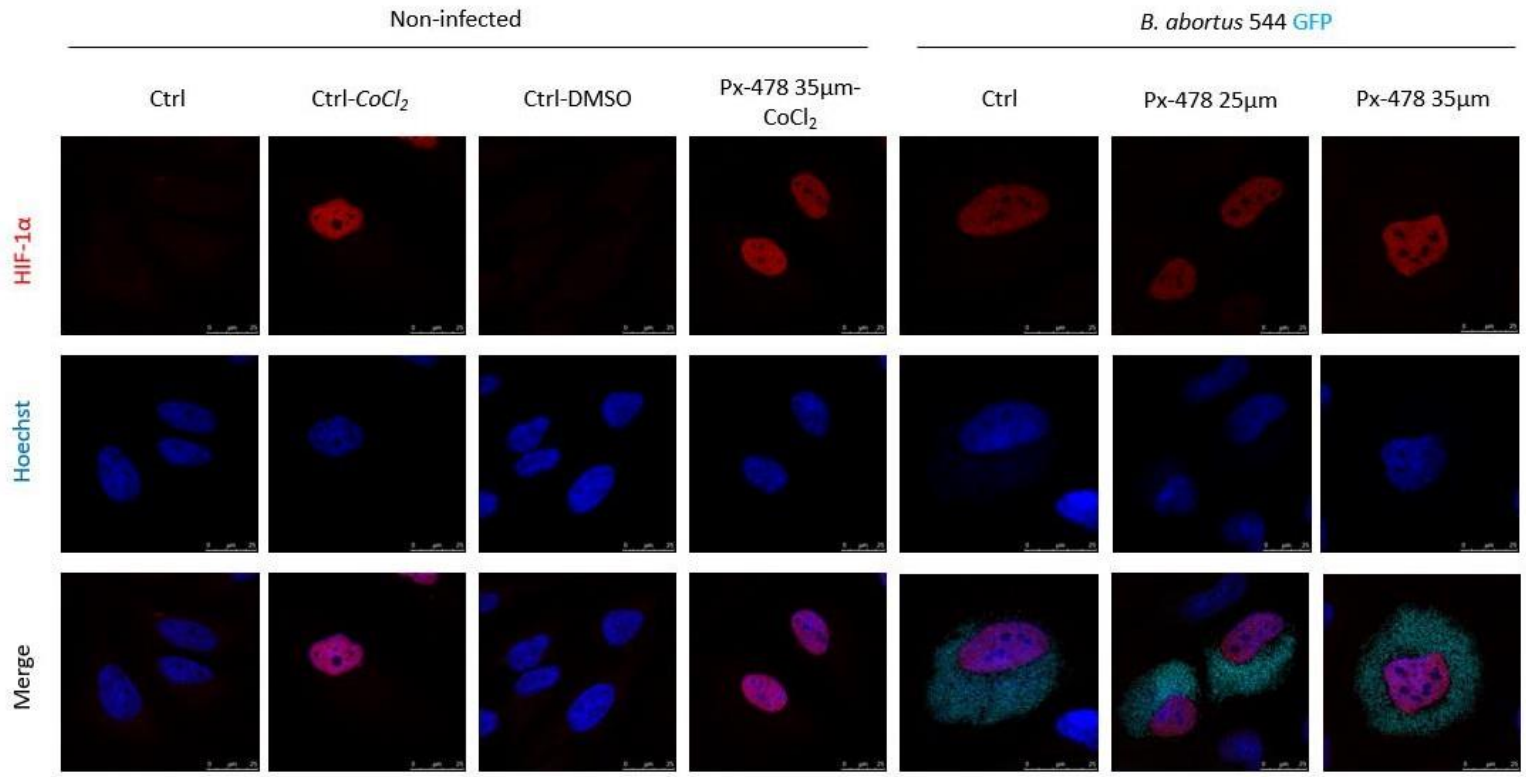

Figure 21: Effect of the inhibitor PX-478 on the stabilisation of HIF-1α induced by *B. abortus* in HeLa cells at 48 h p.i.
Representative confocal micrographs of HeLa cells incubated or not (Ctrl) with 100 µM $CoCl_2$ and the inhibitor PX-478, 8 h after infection at 2 different concentrations (25 µM and 35 µM). Cells were fixed at 48 h p.i and immuno-stained for HIF-1α (red) and using Hoechst (blue) as a nuclear counterstaining for nuclei. Cells were observed with the Leica confocal microscope. Scale bar: 25 µm
Scale bars: 25 mm

A.

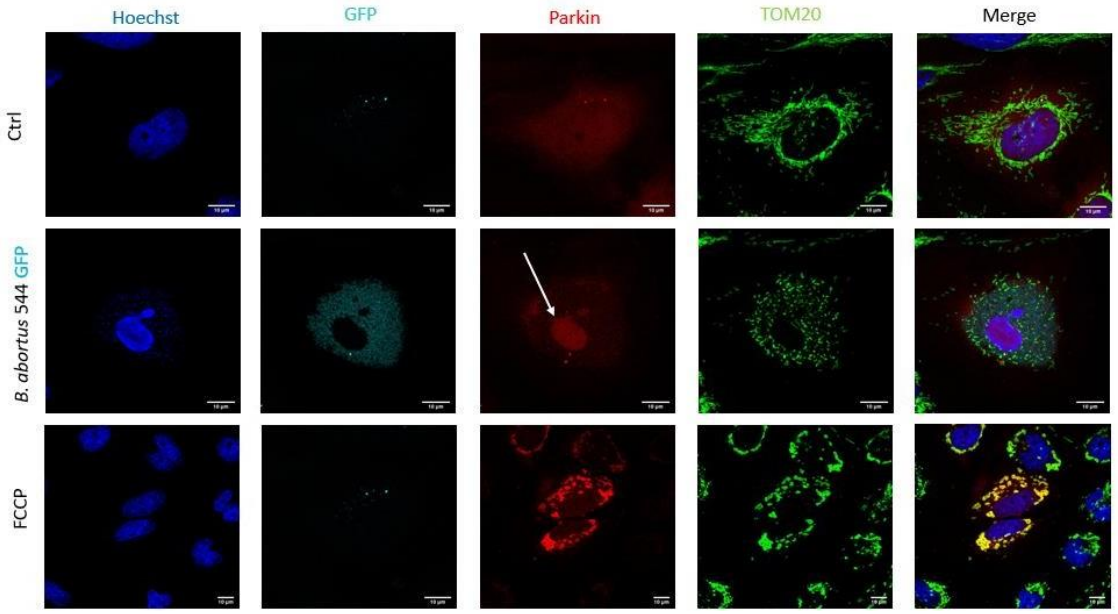

Figure 22: Effect of a FCCP on the mitochondrial recruitment of mCherry-Parkin and localisation of the protein in *B. abortus* 544 GFP infected HeLa cells at 48 h p.i.
Representative confocal micrographs of HeLa cells transfected with a plasmid encoding mCherry-Parkin (red) 24 h before the infection or not (Ctrl) with *B. abortus* 544 GFP (cyan). For the positive control, cells were incubated with 20 µM FCCP for 30 min to induce an inner mitochondrial membrane uncoupling. Cells were then immuno-stained for TOM 20 (green) and stained with Hoechst (blue) for nuclei localisation at 48 h p.i. Cells were observed with a Leica confocal microscope. Scale bar: 25 µm

the fixation of the cells. This incubation time was chosen based on the reference paper(Koh et al., 2008). Indeed, these authors demonstrated that an incubation period of 16 h is necessary to achieve complete inhibition (**Figure 21**). In these conditions, no inhibition could be observed on the stabilisation of HIF-1a in Brucella-infected HeLa cells.

Wee next tested the inhibitor at 35 mM on the stabilisation of HIF-1α when the protein induced by chemical hypoxia (100 µM of $CoCl_2$ added at the same time as the inhibitor). As shown in Figure 21, no inhibition on HIF-1α stabilisation could be observed under these experimental conditions since the cells still display a nuclear accumulation of HIF-1α in cells in the presence of PX-478.

As we could not show any inhibitory effect of the molecule PX-478 on HIF-1α stabilisation, the inhibitor is therefore not suitable to analyse the effect of HIF-1 inhibition on the proliferation and viability of the bacteria in *Brucella*-infected cells. In future experiments, the use of siRNA against HIF-1α should be considered.

3.2 Study of the nuclear translocation of Parkin in HeLa cells infected with B. abortus

Preliminary data of the host lab revealed a possible translocation of Parkin in the nucleus of HeLa cells infected with *B. abortus* (Jérémy Verbeke, ongoing PhD thesis, unpublished data). Sarah Shires' study showed that a nuclear translocation of Parkin was observable in cells subjected to hypoxic conditions. This nuclear translocation of Parkin overexpresses in HeLa cells or Parkin-NLS has been identified as contributing to both increased and decreased transcription of genes involved in regulating multiple metabolic pathways. It was notably observed that Parkin could bind the transcription factor Estrogen-Related Receptor alpha (ERRα) and induce its ubiquitination. However, Parkin has been identified as a co-activator of ERRα(Shires et al., 2020).

However, this intriguing observation needed to be validated. We first tried to confirm the observation of the ectopically overexpressed mCherry-Parkin nuclear translocation by confocal microscopy in the infected HeLa cells. We next tried to determine the putative role of nuclear Parkin as a co-activator of ERRa by using a reporter system. This reporter system consists of a promoter with 3 copies of an ERRE (Estrogen-Responsive Receptor Element) followed by of the luciferase encoding gene (Addgene, 37852) (Heckler et al., 2014b). The putative activation of ERRa by Parkin allows binding to the ERRE sequence and thus allows the expression of luciferase detected by immunofluorescence and visualised by confocal microscopy (Leica). Due to the class of bacteria (BL3), a most sensitive luciferase assay biochemical assay could not be envisaged.

3.2.1 Observation of Parkin nuclear translocation induced by B. abortus at 48 h p.i

To assess the nuclear translocation of Parkin in *B. abortus*-infected HeLa cells, cells were first transfected with a plasmid encoding mCherry-Parkin and then infected with *B. abortus* 544 GFP for 48 h. To visualise the expected behaviour of Parkin in cells that display a depolarisation of mitochondrial membrane, a positive control was generated by incubating some cells for 30 min with 20 mM carbonyl cyanide 4-(trifluoromethoxy) phenylhydrazone (FCCP), a molecule able to depolarize mitochondria leading to the stabilisation of PINK1 which, in turn, induces translocation of Parkin to the mitochondrial membrane (Narendra et al., 2008). Cells were then immuno-stained for TOM20 to visualise mitochondrial population and counterstained with Hoechst to localise the nuclei. Cells were next observed by confocal microscopy to detect TOM20, Parkin, the nuclei and GFP-*Brucella* (**Figure 22**).

A.

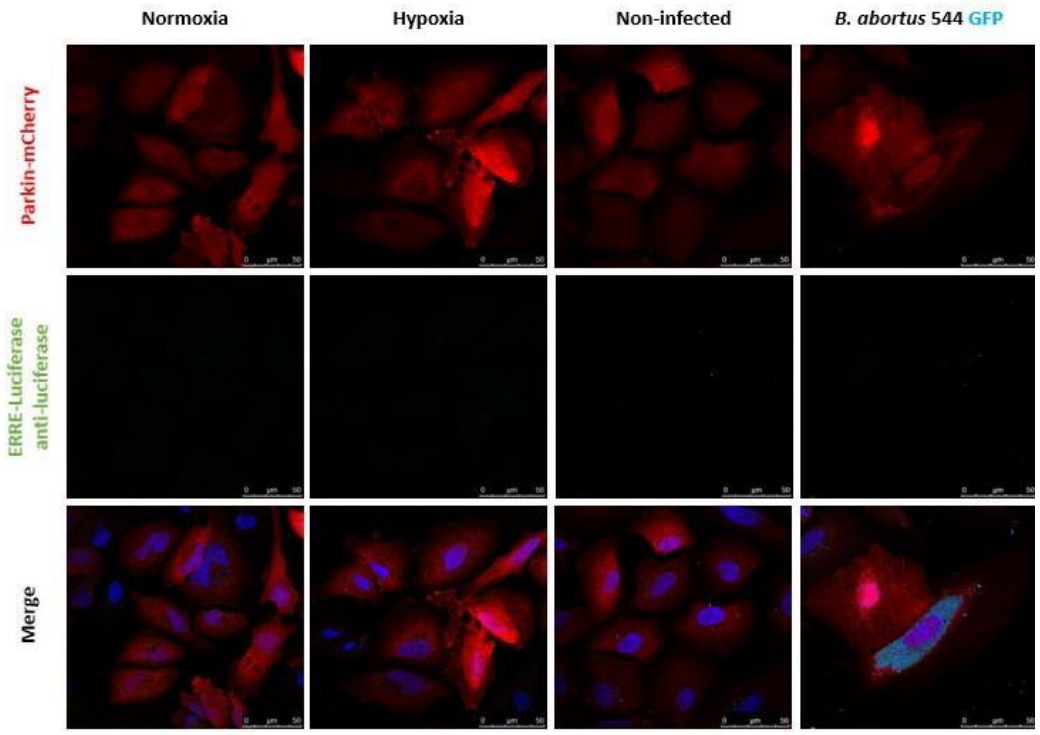

Figure 23: Effect of *B. abortus* 544 GFP on the nuclear localisation of Parkin and its role as positive regulator of ERR*α* at 48h p.i.

Representative confocal micrographs of HeLa cells transfected with a plasmid encoding mCherry-Parkin (red) and a plasmid encoding ERRE follow by the luciferase sequence 24 h before the infection or not (Ctrl) with *B. abortus* 544 GFP (cyan). For the positive control, cells were incubated in a hypoxic incubator for 24h. Cells were then stained with Hoechst (blue) for nuclei localisation at 48 h p.i. Cells were observed with a Leica confocal microscope. Scale bar 25 µm

As expected, Parkin is recruited to the mitochondria in cells exposed to FCCP that display a mitochondrial membrane depolarisation, but this was not observed in the Brucella-infected cells (**Figure 22**). What is most intriguing is that Parkin appears to accumulate in the nucleus of the *B. abortus*-infected HeLa cells at 48 h p.i.

3.2.2 Analysis of the potential effects of B. abortus-induced Parkin nuclear translocation

To investigate the putative role of Parkin nuclear translocation in *Brucella*-infected cells, we tested whether nuclear Parkin could increase ERRα expression and act as a co-activator of the transcription factor as described previously (see section 1.2.4.5 in the introduction) (Shires et al., 2020). The increase in ERRα activity leads to an increase in the expression of target genes that display an ERRE-binding sequence in their promoter. Based on these data, we wanted to determine whether an increase in the expression of luciferase driven by an ERRα-sensitive promoter (using a reporter construct) could be observed in *Brucella*-infected HeLa cells in response to the Parkin nuclear translocation. The luciferase produced should, in theory, be detected by immunofluorescence and confocal microscopy. Unfortunately, as observed in **Figure 23**, no luciferase expression could be detected regardless of the experimental conditions.

The hypoxic condition initially described as a condition for mCherry-Parkin nuclear translocation is only seen in a very small number of cells. In addition, no fluorescence signal for the luciferase could be observed under this condition. Moreover, a mCherry-Parkin nuclear translocation can also be observed in some of the non-infected cells which therefore appears to be non-specific and random event. This hypothesis is also supported by the fact that the cytoplasm found at the outer end of the cell without bacteria has a similar intensity to that found in the nucleus.

It is also important to consider several elements. The first is that in the 2020 paper by Shires and collaborators, the increase in ERRα transcript level is only observed for a construct encoding a Parkin protein that contains a NLS (Nuclear Localisation Signal) sequence (Shores et al., 2020). This is not the case in our experimental conditions. Secondly, there is no condition that allows us to confirm the functionality of the reporter system used. The use of an endogenous activator of ERRα would have been necessary, such as cholesterol (D. Li et al., 2019). However, the use of cholesterol is hardly compatible with the microscopy imaging techniques used to analyse *Brucella*-infected cells. Finally, as Parkin is not endogenously expressed by HeLa cells (Naeem et al., 2020), the different phenotypes such as mitochondria fragmentation or HIF-1a accumulation in the nucleus observed in *Brucella*-infected cells must be Parkin-independent.

Parkin was initially observed to see whether it was involved in *B. abortus*-induced mitophagy. However, in view of the results, it was necessary to reconsider other players in mitophagy. It was therefore necessary to put into perspective the stabilisation of HIF-1α induced by *B. abortus* in host cells (HeLa and RAW264.7). We were next interested to study the role of HIF-1α transcription factor in the fragmentation of mitochondria and subsequent activation of mitophagy, especially because the gene encoding BNIP3L/NIX is regulated by this transcription factor.

A.

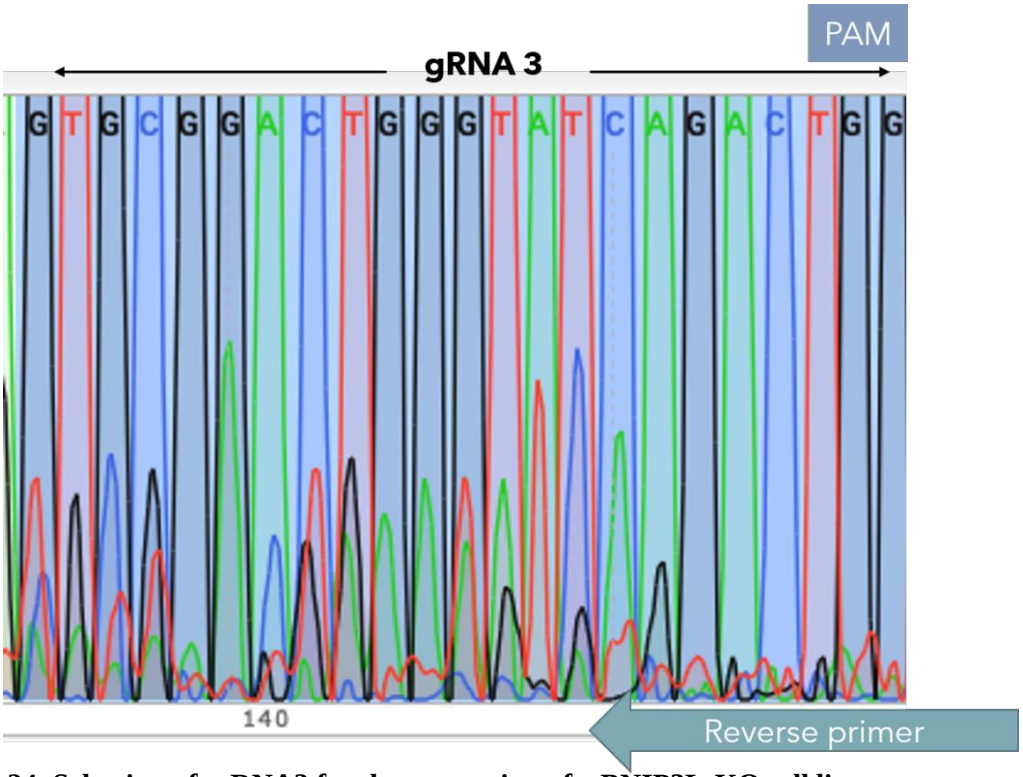

Figure 24: Selection of sgRNA3 for the generation of a BNIP3L-KO cell line.
Sequence fragment of the HeLa cell population electroporated with the third guide RNA (GTGCGGACTGGGTATCAGAACTGG). The PAM sequence, corresponding to the 3 nucleotides "TGG", allows a cleavage 3-4 nucleotides upstream leading to Non-Homology End Joining (NHEJ) repair. A sequence superposition is thus obtained at this particular sequence location. The superposition of the peaks corresponds to the different nucleotides obtained at the location during the sequencing.

A.

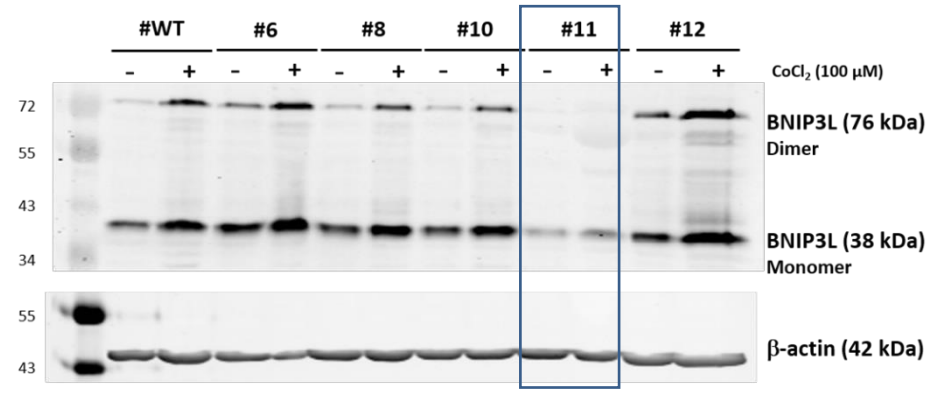

B.

C.

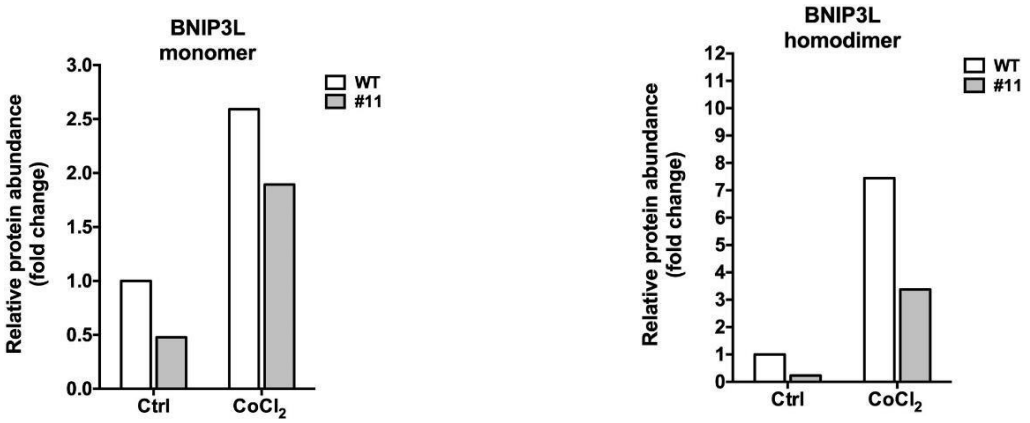

D.

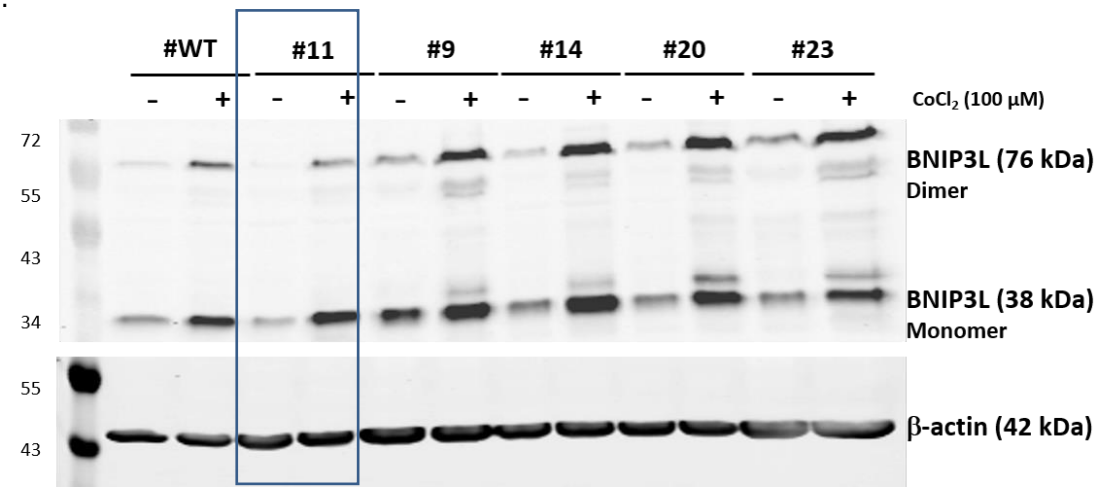

Figure 25: Identification of putative BNIP3L knockdown clone after CRISPR/Cas9 editing.
Legend and western blot on the next page

3.3 Study of the role of BNIP3L/NIX in the B. abortus-induced mitochondrial fragmentation and/or mitophagy

As mentioned in the section 1.2.4.5 of the introduction, *B. abortus* induce an increase in the expression of BNIP3L/NIX and mitochondria fragmentation at 48 h p.i in both HeLa and RAW264.7 cells. To test whether BNIP3L/NIX is required for *B. abortus*-induced mitophagy and/or mitochondrial fragmentation or not, we wanted to test the effect of invalidation or silencing approaches of BNIP3L expression in host cells (HeLa cells) in order to observe the putative effect of the absence or reduced expression, respectively, on the morphology of the mitochondrial population.

3.3.1 Generation of a BNIP3L-KO HeLa cell lines by CRISPR-Cas9 engineering

In order to invalidate the expression of BNIP3L, the use of CRISPR-Cas9 technology was tested to generate a BNIP3L-KO cell line on HeLa cells.

Identification of the most efficient single guide RNA by DNA sequencing performed on the cell population

Initially, 3 sgRNAs were selected to identify the sgRNA that induces the most efficient gene editing in the cell population. Cells were electroporated with one of the different sgRNA (each batch of 1 million HeLa cells electroporated with 1,5 µL of 120 µM crRNA and 1,5 µL of 120 µM tracrRNA (sgRNA)). An aliquot of the electroporated cells corresponding to one third of the initial cell population was then collected to perform DNA extraction and sequencing.

The sequencing of the DNA edited with the third sgRNA (sgRNA3) from a cell population was the only one that gave us enough efficiency (**Figure 24**). Indeed, several overlapping sequences were observed 3 nucleotides upstream of the PAM. However, these overlapping sequences (sequence superposition on top of the green box of **Figure 24**) are less high and therefore less represented in the population when compared to the major sequence observed in the sample which correspond to the cells without edited sequences. This data suggests, as expected, that there are several sequences after the break. The main peaks show that DNA repair may not affect the entire cell population.

However, it is still impossible to determine whether these sequences are coming from few amounts of different editing cells, or if they are generated from many edited cells that harbour several copies of the gene, therefore making the editing less efficient.

Identification of putative BNIP3L knockdown clones after CRISPR/Cas 9 editing

To generate clonal populations of the edited cells, the electroporated cells with sgRNA3 were seeded respecting a limiting dilution in a 96-well cell culture plate in order to obtain, at the most, one cell per well. The aim was to expend the cells that harbour the edited DNA and to avoid working with a heterogeneous cell population. After cell expansion of several clones, when enough cell biomass was obtained, protein extraction and analysis of BNIP3L abundance by western blot were performed (**Figure 25**). In addition, as the goal was to identify a good clone for which cells do not express BNIP3L in response to a stimulation, some cells were incubated with $CoCl_2$ (**Figure 25**). As already mentioned, $CoCl_2$ induces the stabilisation of HIF-1α which, in turn, increase the expression of target genes such as BNIP3L/NIX (Muñoz-Sánchez and Chánez-Cárdenas, 2019).

BNIP3L has a molecular weight of 38 kDa for the monomeric form and 76 kDa for the homodimeric form which was maintained under detergent conditions (**Figure 25A**). Although

E.

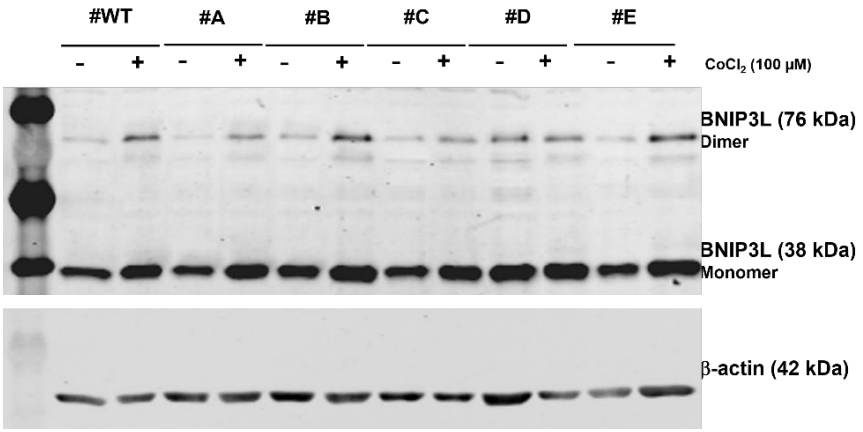

Figure 25: Identification of putative BNIP3L knockdown clones after CRISPR/Cas9 editing. CRIPSR/Cas9 technology was used in HeLa cells to try to reduce BNIP3L expression using the third sgRNA (**see Figure 19**). After clonal expansion, clones were incubated or not with 100 µM $CoCl_2$ for 16 h before cell lysate preparations.

(A) Western blot analysis in fluorescence of the abundance of BNIP3L at 16h p.t in cell lysates prepared from electroporated HeLa cells treated or not with 100 µM $CoCl_2$ using an anti-BNIP3L antibody.

(B-C) Quantification of the abundance of BNIP3L monomer and homodimer (38 and 76 kDa, respectively) normalized for the abundance of β-actin (42 kDa) used as loading control. The results are expressed in fold change between the normalized BNIP3L monomer (B) and BNIP3L homodimer (C) abundance in control cells (incubated or not CoCl2) and the normalized abundance of the protein detected in clone #11 (incubated or not with $CoCl_2$) was calculated.

(D) Analysis of the abundance of Clone#11 cells treated or not with $CoCl_2$ of BNIP3L at 16h p.t by fluorescence western blot using anti-BNIP3L antibody.

(E) Western blot analysis in fluorescence of the abundance of BNIP3L at 16h p.t in cell lysates prepared from electroporated HeLa cells treated or not with 100 µM $CoCl_2$ using an anti-BNIP3L antibody.

it may seem strange, the homodimeric form of BNIP3L is maintained under denaturing conditions. BNIP3L will associate with itself via its transmembrane domain associated with a GXXXG motif. An identification of specific residues, that are critical for BNIP3 TM self-association in membranes, are also important for dimerization in SDS micelles, suggesting that homodimer observed in membranes is preserved in detergent (Sulistijo et al., 2003b). In the first set of forty clones, BNIP3L expression is induced in cells exposed to 100 mM $CoCl_2$ treatment for 16 h. Interestingly, for clone #11, a lower BNIP3L protein abundance is observed both in control cells as well as in cells exposed to $CoCl_2$ (**Figure 25A**). These observations were confirmed by the quantification of the BNIP3L signals when the abundance was normalised for the β-actin, used as a loading control (**Figure 25B, C**).

These results indicate that cells from clone #11 display a strong decrease in the abundance of BNIP3L protein not only in the constitutive expression but also in response to a stimulus such as $CoCl_2$-treatment. Clone #11 therefore appeared, at first, to be a good knock down clone (**Figure 25A**). However, during the expansion of this clone for routine use, an increase in growth rate was observed. A second western blot analysis to check the abundance of BNIP3L in this clone was performed (**Figure 25D**). Unfortunately, the abundance of BNIP3L of this clone recovered a comparable abundance observed in control cells (**Figure 25D**).

Unfortunately, we could thus not use the clone #11 in our future studies aiming to assess the potential role of BNIP3L in *B. abortus*-induced mitochondrial fragmentation and/or mitophagy. It is important to note that multiple copies of the same chromosome, multiple gene duplications, insertions and/or deletions can be observed within the genome of HeLa cells (Landry et al., 2013). Some genes can therefore be found in multiple copies in the genome, making it less likely that all copies could be affected by the CRISPR/Cas9 engineering technique(Landry et al., 2013). The hypothesis is that a transcriptional adaptation can take place to prevent or reduce the effect of a detrimental phenotype (Sztal and Stainier, 2020). This transcriptional adaptation could manifest itself in our case by overexpressing the remaining non-mutated copies of BNIP3L to reach an expression level comparable to the one found in control cells. It would thus therefore necessary to identify a knock-out clone to avoid this compensation phenomenon overtime when cells are maintained in culture.

The manipulation was repeated by increasing the concentration of transfected ribonucleoprotein complexes within HeLa cells by 2 and 3. The aim was to increase our chances of affecting all copies of BNIP3L genes present in HeLa cells. The protocol used is identical to that used previously. Forty clones were again isolated and used for analysis of BNIP3L protein abundance. Unfortunately, out of the forty clones isolated, no good candidates could be identified (**Figure 25E**).

The isolation of a knockout line for BNIP3L being laborious and complex, we next decided to redirect ourselves to a simpler and faster technique based on the silencing of gene expression using siRNA.

3.3.2 Effect of BNIP3L expression silencing on the B. abortus-induced mitochondrial fragmentation in HeLa cells

To further investigate the putative role of BNIP3L in *B. abortus*-infected cells, we decided to move towards the use of small interfering RNA (siRNA) to silence and reduce its expression. A siRNA smart pool containing 4 siRNA sequences targeting several regions of BNIP3L mRNA was used to maximise the silencing of the BNIP3L protein.

A.

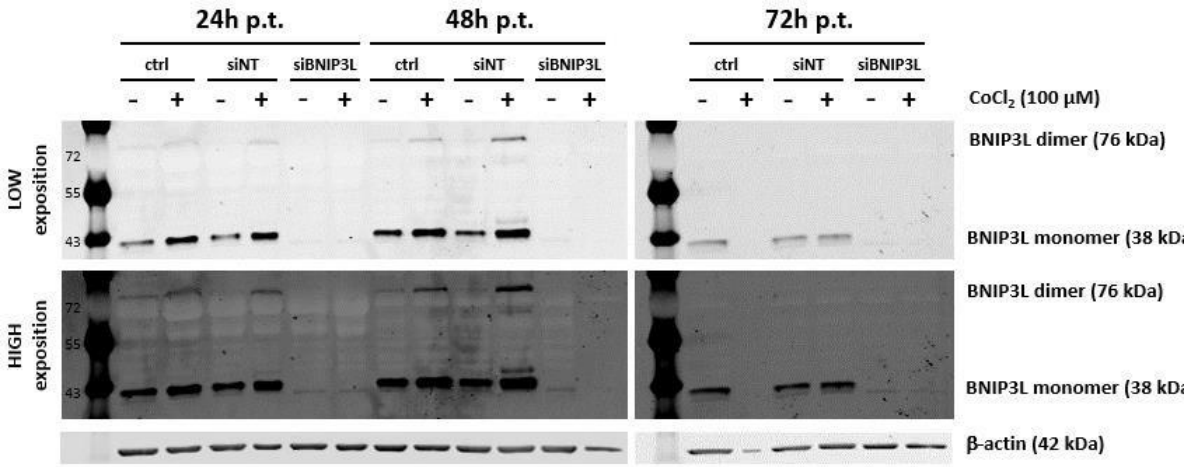

B.

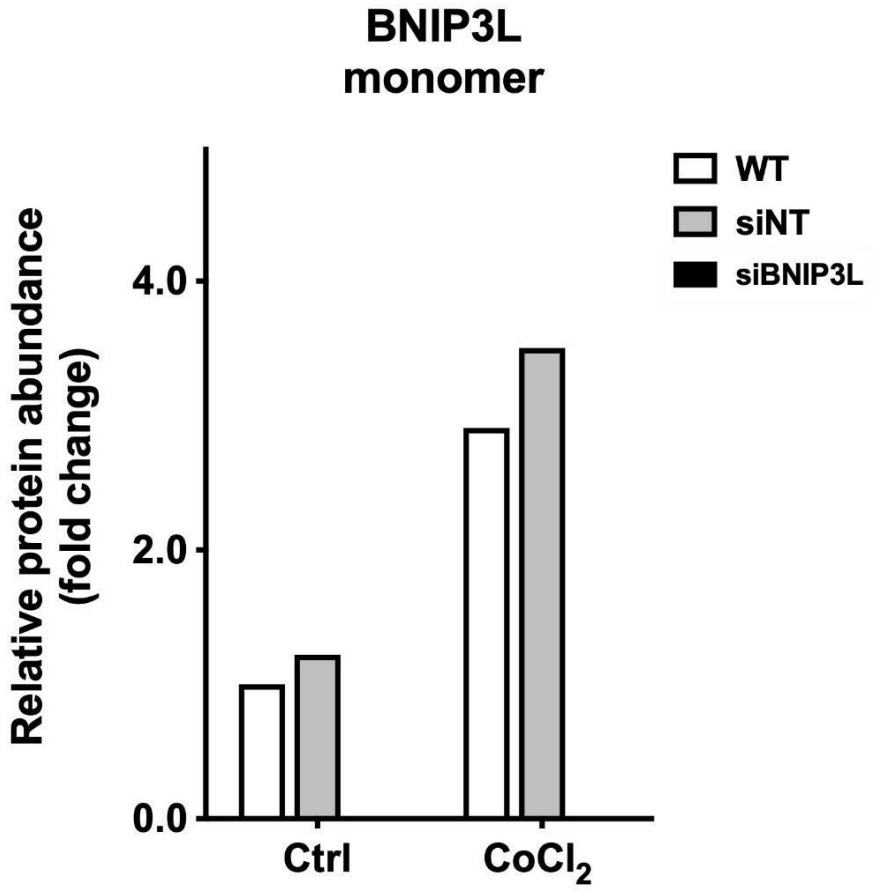

Figure 26: Efficiency of the silencing of BNIP3L with a smart pool siRNA in HeLa cells at 24, 48 and 72h p.t.

Legend and flow cytometry on the next page

C.

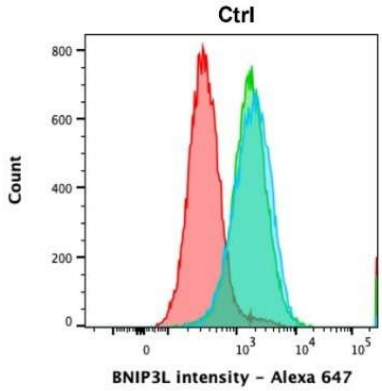

	Sample Name	Subset Name	Count	Median : Alexa 647-A
	HeLa_empty_ctrl.fcs	Live cells	27482	1793
	HeLa_siNT_ctrl.fcs	Live cells	26504	1603
	HeLa_siBNIP3L_ctrl.fcs	Live cells	26847	337

D.

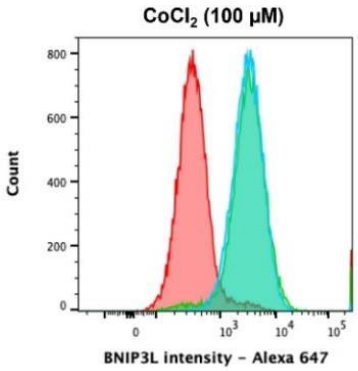

	Sample Name	Subset Name	Count	Median : Alexa 647-A
	HeLa_empty_CoCl2.fcs	Live cells	27954	2976
	HeLa_siNT_CoCl2.fcs	Live cells	26558	3119
	HeLa_siBNIP3L_CoCl2.fcs	Live cells	26414	368

Figure 26: Effect of the silencing of BNIP3L with a SMARTpool siRNA in HeLa cells at 24, 48 and 72h p.t.

HeLa cells were transfected or not with either 40 µM of siRNA Non-Targeting (siNT) or siRNA directed against the BNIP3L mRNA (siBNIP3L) and then treated or not with 100 µM $CoCl_2$ for 24 h before cell lysate preparation and western blot analysis (A) or 48 h before fixation for flow cytometry (C-D).

(A) Western blot analysis in fluorescence of the abundance of BNIP3L in cell lysates prepared from HeLa cells transfected or not (ctrl) for 24 h with siNT or siBNIP3L and then treated or not with $CoCl_2$ for 24 h. Cells were immuno-stained for BNIP3L.

(B) Quantification of the abundance of BNIP3L monomer (38 kDa) normalized for the abundance of immuno-detected β-actin (42 kDa) used as a loading control. The results are expressed in fold change between BNIP3L monomer abundance in control cells (incubated or not with 100 µM of $CoCl_2$) and the normalized abundance of the protein recovered in cells transfected with the smart pool of siRNA against BNIP3L at 24 post transfection (p.tr).

(C) Flow cytometry analysis of BNIP3L abundance performed on HeLa cells transfected or not (control (red)) for 48 h with 40 µM siRNA Non-Targeting (green) or with 40 µM of siBNIP3L (blue). Cells were immuno-stained for BNIP3L.

(D) Flow cytometry analysis of BNIP3L abundance performed on HeLa cells transfected or not (control (red)) for 48 h with 40 µM siRNA Non-Targeting (green) or with 40 µM of siBNIP3L (blue) and then incubated with 100 µM $CoCl_2$ for 48. Cells were immuno-stained for BNIP3L.

3.3.2.1 Analysis of the efficiency of the siRNA smart pool directed against BNIP3L

3.3.2.1.1 Analysis of the efficiency of the siRNA smart pool directed against BNIP3Lby western blot

It was first necessary to test the efficiency of the smart pool of siRNA directed against BNIP3L. HeLa cells were transfected for 24 h after seeding with 40 µM of the BNIP3L siRNA or with a non-targeting siRNA (siNT) which served as a control. For each condition, cells were treated or not with 100 µM $CoCl_2$ to induce chemical hypoxia, stabilisation of HIF-1α and thus expression of BNIP3L. Clear cell lysates were then performed for the different conditions at 24, 48 and 72 h post-transfection (p.tr.). Protein abundance was then analysed by western blot in fluorescence on an equivalent of 10 µg of proteins.

As observed in the **Figure 26A**, a very strong decrease in the abundance of BNIP3L is observed in cells transfected with siRNA directed against the transcript of the gene encoding BNIP3L when compared to cells transfected with non-target siRNA (controls) no matter what the cells were treated with $CoCl_2$ or not. These observations were confirmed by the quantification of the fluorescence signals when the abundance is normalised for the β-actin, used as a loading control (**Figure 26B**).

However, the information obtained from the western blot analysis does only allow to analyse the global abundance at the level of the cell population, showing only the "mass effect". The flow cytometry analysis has next been used to get information on the siRNA efficiency at a single-cell level.

3.3.2.1.2 Analysis of the efficiency of the BNIP3L smart pool siRNA by flow cytometry

The samples and conditions for flow cytometry were prepared as the samples prepared for the western blot analysis. At 48 p.t., the cells were fixed, permeabilised and immuno-stained with a specific BNIP3L antibody. The intensities of the fluorescence signals were measured at 48 h p.t. on cells transfected with a non-target siRNA (control) or siRNA pool directed against the BNIP3L mRNA incubated or not (**Figure 26C**) with 100 mM CoCl2 to induve the expression of the gene (**Figure 26 D**).

An almost complete leftward shift is observed in the fluorescence intensity for the cells transfected with the pool of siRNA directed against the BNIP3L mRNA in both, the cells treated with $CoCl_2$-treated or control cells. No reduction of BNIP3L expression is observed in the cells transfected with the non-target siRNA. In conclusion, on the basis of these different observations, we now have an efficient tool to silence and reduce the expression of the gene encoding BNIP3L.

3.3.2.2 Analysis of the effect of BNIP3L silencing on B. abortus-induced mitochondrial fragmentation by confocal microscopy

In order to better understand the role of BNIP3L induced during *B. abortus* infection in HeLa cells, the smart pool of siRNA directed against the BNIP3L mRNA was used in HeLa cells infected with *B. abortus*. In the micrographs shown in **Figure 27A**, several observations can be made. First of all, as expected the induction of BNIP3L was almost completely decreased in cells transfected with the siRNA directed against BNIP3L mRNA. More interestingly, when the expression of BNIP3L is silenced in *B. abortus*-infected cells, a decrease in the fragmentation of the mitochondrial population is observed when compared to morphology of the control cells transfected with the non-target siRNA (**Figure 27A**). This observation is encouraging and gives us a first argument supporting the fact that BNIP3L plays a role in the *B. abortus*-induced mitochondrial fragmentation.

A.

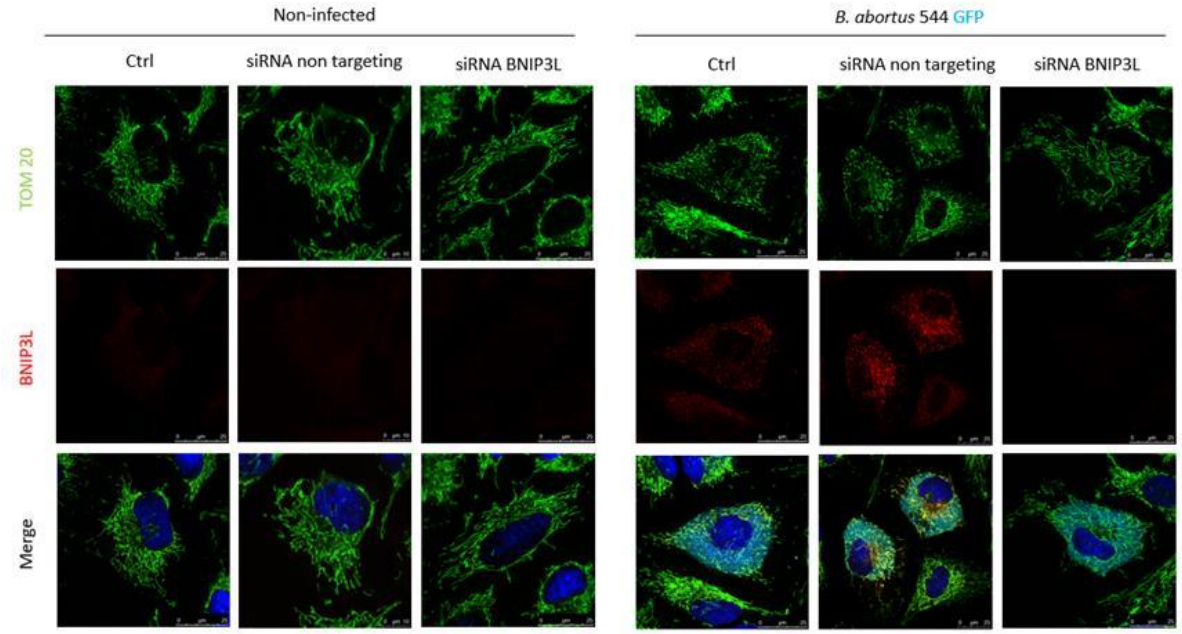

B.

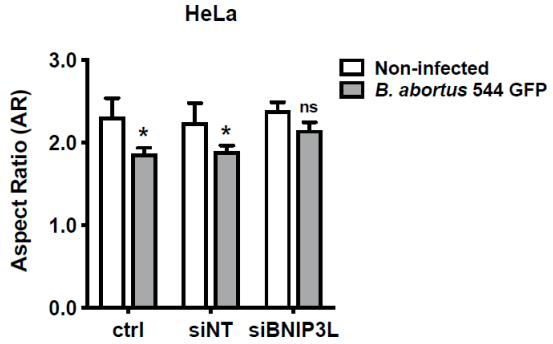

C.

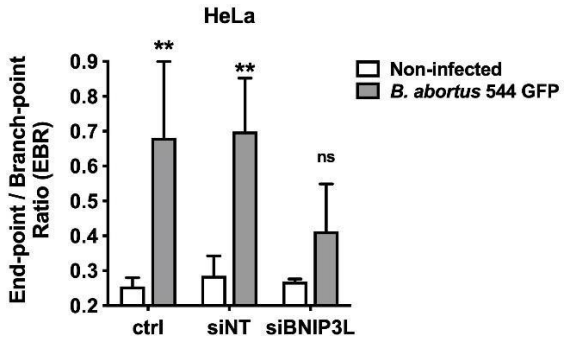

Figure 27: Effect of BNIP3L silencing on the *B. abortus* 544 GFP-induced mitochondrial fragmentation in HeLa cells.

(A) Representative confocal micrographs of HeLa infected cells transfected or not (Ctrl) with 40 µM of siNT or siBNIP3L and then infected or not (non-infected) by *B. abortus* 544 GFP. Cells were immuno-stained for TOM20 (green), BNIP3L (red) and stained with Hoechst (blue) for nuclei localisation. Cells were observed with a LSM 980 with Airyscan 2 (Zeiss). Scale bar 25 µm

(B) Quantification of the aspect ratio of the mitochondrial network for the different conditions. Results are expressed as means ± 1 SD for 3 independent replicates for an average of 35 cells per condition for each replicate. Statistical analysis performed on over 100 cells (Two-way ANOVA using Tukey test: **: $p<0.05$, ns: $p>0.05$)

(C) Quantification of the end point branch point of the mitochondrial network for the different conditions. Results are expressed as means ± 1 SD for 3 independent replicates for an average of 35 cells per condition for each replicate. Statistical analysis performed on over 100 cells (Two-way ANOVA using Tukey test. **: $p<0.05$, ns: $p>0.05$).

A.

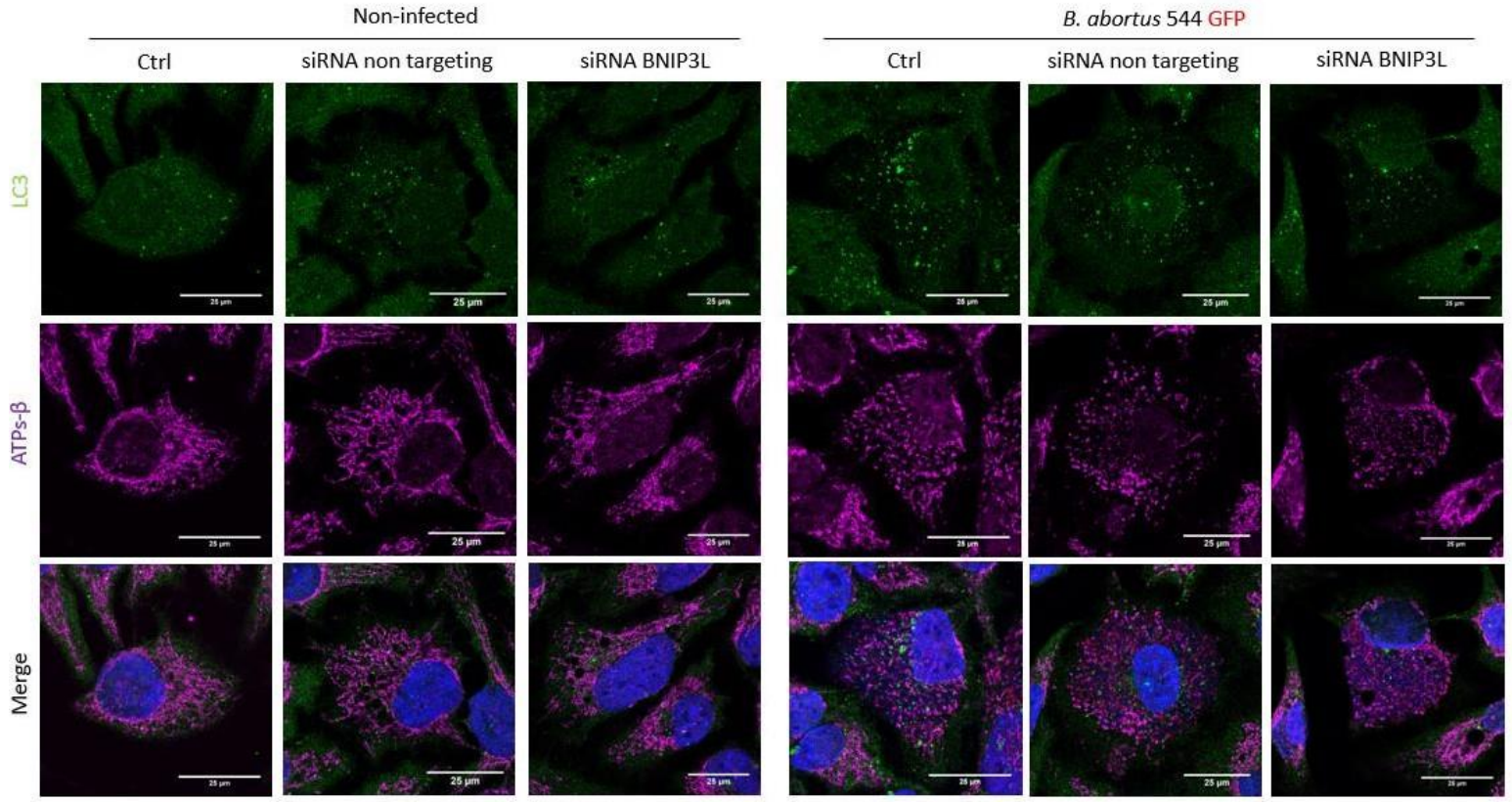

Figure 28: Effect of BNIP3L silencing on the *B. abortus 544 GFP*-induced mitophagy in HeLa cells – 48h p.i.
Representative confocal micrographs of HeLa *B. abortus* 544 GFP (red) infected cells transfected with or without 40µM siRNA Non-Targeting or siBNIP3L 24 h before the infection and fixed at 48 h post-infection. Cells were then immunostained for LC3 (green), TOM20 (magenta) and Hoechst (blue) as a nuclear counterstained. Observed with the Airyscan. Scale bar 25 µm

This observation is also confirmed by the quantification of the mitochondrial population morphologies performed on the micrographs acquired with a confocal microscope. The morphology (fragmentation or elongation/branching status) analysis was performed by determining the aspect ratio (AR) and the endpoint/branch-point ratio (EBR) (**Figure 27B, C**). The AR of a mitochondrial network is defined as the ratio of the centre line to the mean width, in other words the ratio of the length of the different fragments to their width(Luz et al., 2015). The EBR is a measure of mitochondrial network connectivity with the ratio between the sum of the number of ends and the sum of the number of branches/connection points. The AR calculated for the infected-cells is significantly reduced when compared to non-infected cells or non-infected cells previously transfected with non-target siRNA. Interestingly, the AR calculated for the infected-cells that have previously been transfected with the siRNA directed against BNIP3LmRNA is only slightly reduced and significantly higher that the AR calculated for infected cells transfected with the non-target siRNA (controls) (**Figure 27B**).

These observations were corroborated by the quantifications of EBR (**Figure 27C**). For this parameter, the silencing of BNIP3L expression seems to almost completely prevent the increase in EBR observed in *B.abortus*-infected cells, suggesting a more elongated and branched network of the mitochondrial population in these conditions.

In conclusion, these observations allow us to suggest that in the absence of BNIP3L, the mitochondrial fragmentation observed in *Brucella*-infected cells is, at least, partially reduced. On the one hand, the partial, but significant, recovery can be explained by the silencing that might not be complete even if relatively efficient as demonstrated by either western blot or flow cytometry analyses. The residual expression of BNIP3L may thus be sufficient to maintain a certain level of mitochondrial fragmentation. On the other hand, BNIP3L may not be the only molecular actor involved in the fragmentation of the network. This observation is encouraging and gives us a first argument to support a role for BNIP3L in the *B. abortus*-inducedmitochondrial fragmentation.

As explained in section 1.2.4.3, fragmentation is usually a process that precedes mitophagy (Wai & Langer, 2016a). Therefore, the effect of BNIP3L silencing on *B. abortus*-induced mitophagy in HeLa cells was investigated.

3.3.3 Effect of BNIP3L silencing on the B. abortus-induced mitophagy in HeLa cells

We next wanted to focus on mitophagy. Initially, BNIP3L is known to induce mitophagy, especially under hypoxic conditions, by a direct and physical interaction mediated by its LIR (LC3 Interacting Region) motif with the LC3 protein found on autophagosome membranes(Ney, 2015).

The analysis of the putative effects of BNIP3L silencing on *B.abortus*-induced mitophagy was done by assessing the number of the co-localisation events between LC3B protein and a beta-subunit of the ATP synthase using immunofluorescence and confocal microscopy.

3.3.3.1 Effect of BNIP3L silencing on the B. abortus induced colocalization between LC3 and the mitochondria in HeLa cells.

In order to study the role of BNIP3L in the colocalization between LC3 and the mitochondria, HeLa cells were transfected or not with 40 µM siNT or siBNIP3L 24 hours after seeding. The day after transfection, HeLa cells were infected and maintained in culture for 48h. The cells are fixed and immunostained for LC3 and the mitochondrial network via ATP synthas-β (**Figure 28**).

A.

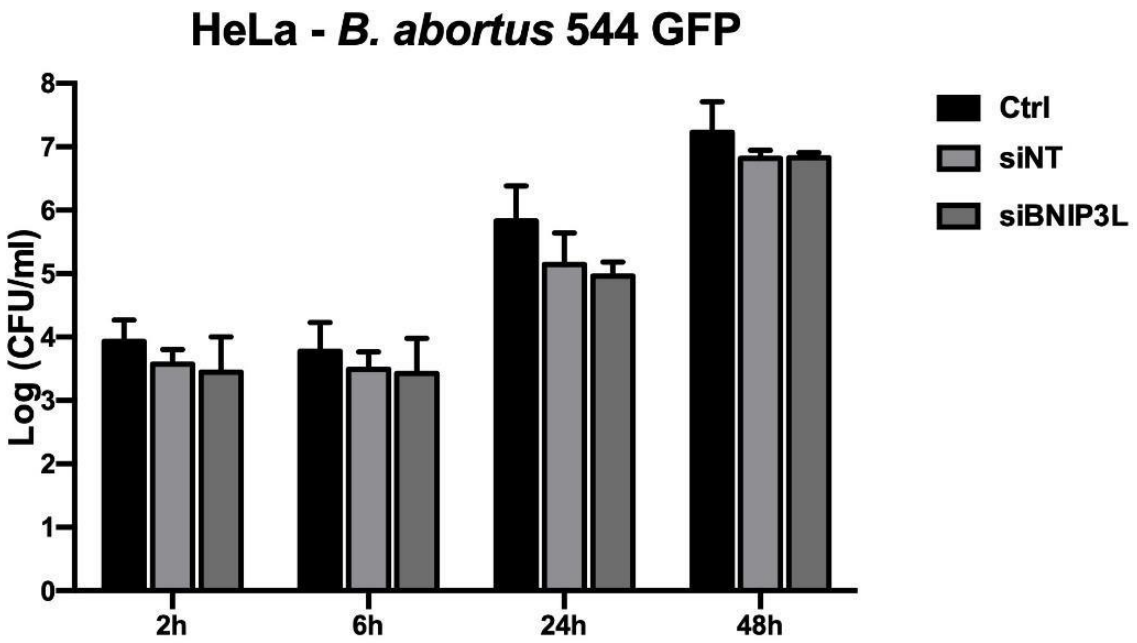

Figure 29: Effect of BNIP3L silencing on the *B. abortus* 544 GFP-proliferation in HeLa cells. HeLa cells were transfected 24 h before the infection with or without 40 µM of siRNA Non-Targeting or siBNIP3L CFU assays were then performed at different post-infection time point (2, 6, 24 or 48 h) on 3 replicate. Results are expressed as means +/- 1 SD for n=3. Statistical analysis performed (Two-way ANOVA using Turkey test)

The results obtained by confocal microscopy allow us to hypothesise that a decrease in mitophagy can be observed in the conditions transfected with siBNIP3L and that this is even more marked in the infected conditions. Moreover, it can be noted that fusion of the mitochondrial network is also associated with a decrease and/or inhibition of mitophagy (Yoo and Jung, 2018), so these first results corroborate those observed in the literature.

It is important to note that the methanol fixation required for LC3 labelling will force us to use the ATPs-β labelling and not TOM20 (which does not work upon methanol fixation) as in the vast majority of our experiments. However, methanol fixation leads to an alteration in mitochondrial labelling providing this fragmented appearance, making this mitochondrial marker in those fixation conditions inappropriate network morphology quantification (Donna R., et al, 2015).

In conclusion, there seems to be a decrease of the colocalization between LC3 and ATPs-β in siBNIP3L conditions suggesting that BNIP3L would be implicated in *B. abortus* induced mitophagy.

3.3.4 Effect of BNIP3L silencing on B. abortus proliferation in the host cells

In view of the interesting effects, with the partial prevention of mitochondrial fragmentation and mitophagy observed in *Brucella*-infected host cells previously transfected with siBNIP3L, we wondered whether this change in the host cell phenotype could affect the proliferation of *B.abortus*.

As in previous experiments using siRNA, cells were seeded and transfected the next day before starting the infection, 24 h later. The study of bacterial proliferation has been done by counting the CFU obtained 2, 6, 24 or 48 h p.i. times for control non-transfected cells, or cells transfected with either siNT or siBNIP3L (**Figure 29**).

A slight and transient effect of transfection seems to be observed on short infection times with a decrease in the number of CFU/ml observed at 2 and 6 h p.i. times. But based on 3 independent replicates, no significant difference could be observed in *Brucella* CFU in cells that display a silencing of BNIP3L expression. Under the experimental conditions, one can thus conclude that the silencing of BNIP3L does not have any effect on the proliferation of the bacteria.

3.4 Analysis of the effect of B. abortus-induced UPR activation on BNIP3L expression, mitochondrial network fragmentation and B. abortus proliferation

During the research carried out by our team, several data questioned the link between HIF-1α and BNIP3L in cells infected by *Brucella*. Indeed, experiments carried out by Youri Fayt (Master thesis, 2022) showed an absence (or very low signs) of hypoxia in the infected-cells. This observation indicated that the stabilisation of HIF-1α induced by *B. abortus* was not dependent on oxygen. He then became interested in the stabilisation of HIF-1α induced during iron deprivation by certain pathogenic microorganisms. This new research hypothesis led to an iron supplementation experiment on HeLa cells infected with *B. abortus*. Interestingly, under these conditions, while HIF-1α was no longer stabilised and translocated in the nucleus, a fragmentation of the mitochondrial network was still observed in *Brucella*-infected cells. Based on these data, as we have described above, we decided to study other inducers of autophagy and in particular the mitophagy actor BNIP3L.

Our attention was thus next focused on the erUPR (Endoplamic Reticulum Unfolded Protein Response) pathway. Indeed, during the intracellular trafficking of the bacteria in a *B.*

A.

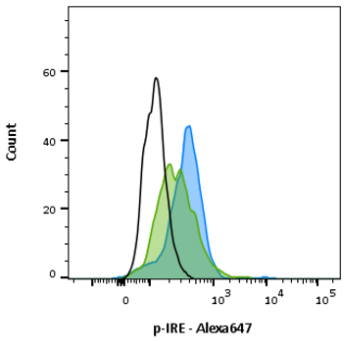

	Sample Name	Subset Name	Count	Median : Alexa 647-A
☐	pIRE_24h_ctrl.fcs	DownsampleDP	1472	120
☐	pIRE_24h_544GFP.fcs	GFP-positive	1472	246
☐	pIRE_24h_Tn.fcs	DownsampleDP	1472	362

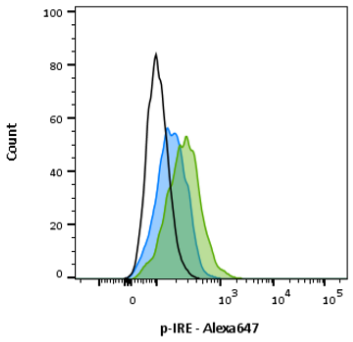

	Sample Name	Subset Name	Count	Median : Alexa 647-A
☐	pIRE_48h_ctrl.fcs	DownsampleDP	2090	101
☐	pIRE_48h_544GFP.fcs	GFP-positive	2090	262
☐	pIRE_48h_Tn.fcs	DownsampleDP	2090	170

B.

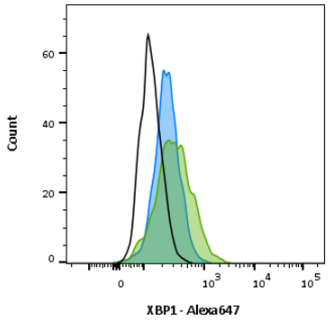

	Sample Name	Subset Name	Count	Median : Alexa 647-A
☐	XBP1_24h_ctrl.fcs	DownsampleDP	1642	129
☐	XBP1_24h_544GFP.fcs	GFP-positive	1642	305
☐	XBP1_24h_Tn.fcs	DownsampleDP	1642	237

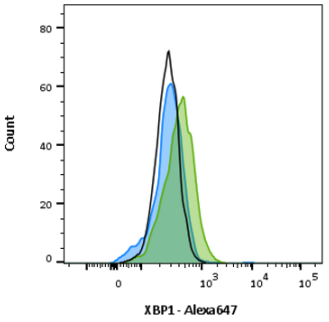

	Sample Name	Subset Name	Count	Median : Alexa 647-A
☐	XBP1_48h_ctrl.fcs	DownsampleDP	1968	266
☐	XBP1_48h_544GFP.fcs	GFP-positive	1968	414
☐	XBP1_48h_Tn.fcs	DownsampleDP	1968	287

C.

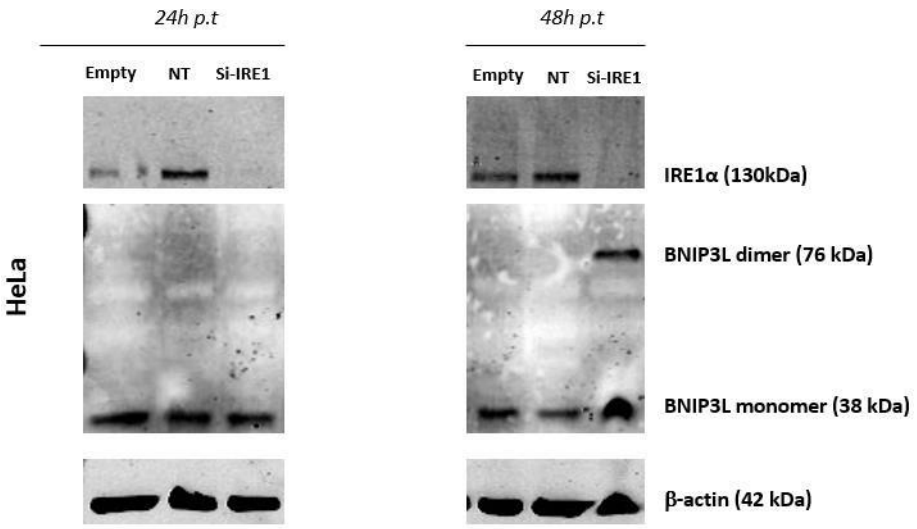

Figure 30: Activation of UPR at 24h and 48h p.i. by *B. abortus* 544 GFP and validation of the siRNA approach in HeLa cells.
Legend and quantification of the protein abundance of the western blot on next page

D.

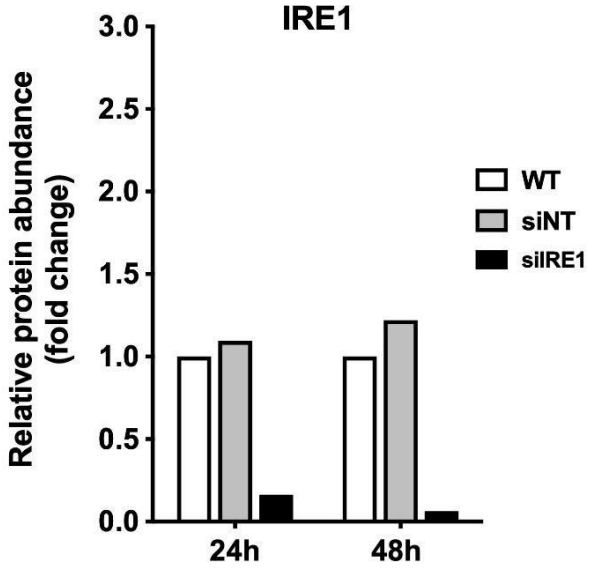

E.

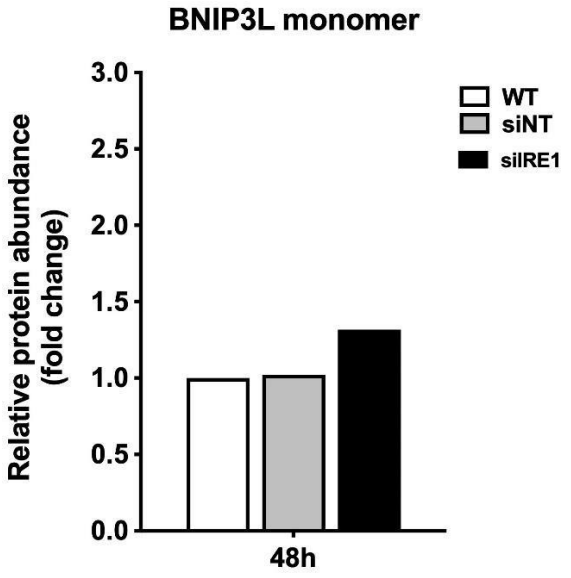

Figure 30: Activation of UPR at 24h and 48h p.i. by *B. abortus* 544 GFP and validation of the siRNA approach in HeLa cells.

HeLa cells were transfected or not with 40 µM of si Non targeting or siIRE1 and then infected by *B. abortus* 544 GFP 24 h after the transfection, some cells were also treated with 5 µg/ml of tunicamycin

(A) Measurement of fluorescence intensity of p-IRE1 at 24h and 48h by flow cytometry on a population of HeLa cells infected with *B. abortus* 544 GFP (green), HeLa cells treated with 5 µg/ml of tunicamycin as positive control (blue) and HeLa cells that have not received any treatment as control (white). Cells were stained for P-IRE.

(B) Measurement of fluorescence intensity of XBP1 at 24 h and 48h post infection by flow cytometry on a population of HeLa cells infected with *B. abortus* 544 GFP (green), HeLa cells treated with 5 µg/ml of tunicamycin as positive control (blue) and HeLa cells that have not received any treatment as control (white). Cells were stained for P-IRE.

(C) Analysis of the abundance in lysate collected from HeLa transfected/Ctrl cells of IRE1 at 24 and 48 h p.t by fluorescence western blot using anti-BNIP3L antibody.

(D) Quantification of the abundance of IRE1 (130 kDa) normalized against the abundance of β-actin (42 kDa) used as loading control. The results are expressed in fold change between IRE1 abundance in control cells or transfected cells with 40 µM of siRNA Non-Targeting or siIRE1 and the normalized abundance of the protein in the presence SiRNA against IRE1 at 24 and 48h p.t.

(E) Quantification of the abundance of BNIP3L monomer (38 kDa) normalized against the abundance of β-actin (42 kDa) used as loading control. The results are expressed in fold change between IRE1 abundance in control cells or transfected cells with 40 µM of si Non targeting or siIRE1 and the normalized abundance of the protein in the presence SiRNA against IRE1 at 48h p.t.

abortus infection, the activation of the erUPR can be observed at 8 and 24 h p.i, especially the IRE1 pathway(Y et al., 2015), also known to regulate autophagy (Deegan et al., 2015; Domínguez-Martín et al., 2018). Based on this information, we hypothesised that *B. abortus*-induced activation of the UPR could lead to the upregulation of autophagy genes (Atg) but also of molecular actors involved in mitophagy such as BNIP3L.

In order to answer this research question, we first tried to confirm the activation of the erUPR pathway in *Brucella*-infected cells as reported in the literature but also an activation of this pathway observable at longer infection times such as 48 h p.i. We then use siRNA against IRE1 to determine its putative effect on the proliferation of *B.abortus* and the role of IRE1 in the expression of BNIP3L.

3.4.1 Analysis of the activation of the IRE1 pathway induced by B. abortus at 24 and 48 h post-infection

HeLa cells were seeded in 6-well cell culture plates at a density of 100,000 cells/well. The next day, cells were then incubated or not with 5 µg/ml tunicamycin known to induce the activation of the erUPR pathway(S. H. Kim et al., 2018) or infected with *B. abortus*. Tunicamycin is a compound which blocked the N-linked glycosylation by inhibiting the transfer of UDP-N-acetylglucosamine (GlcNAc) to dolichol phosphate in the ER of eukaryotic cells(Wu et al., 2018). At the end of the incubation times, the cells were fixed and immuno-stained for the phosphorylated and activated form of IRE1 (p IRE1), and XBP1 which is a downstream activated transcription factor of this pathway. The fluorescence intensity was then measured by flow cytometry (**Figure 30A** and **B**, respectively).

We can observe that the fluorescence intensities in the cells either incubated with tunicamycin or infected with *B. abortus* are shifted to the right, indicating an increase in the abundance of both IRE1 and XBP-1 in these conditions.

These results suggest that the IRE1 branch of the erUPR pathway is activated in HeLa cells infected with *B. abortus* at both 24 and 48 h p.i.

3.4.2 Effect of IRE1 silencing on the B. abortus-induced mitochondrial fragmentation in HeLa cells

To further investigate the role of IRE1 in *B. abortus* infected cells, we decided to move towards the use of small interfering RNA (siRNA) to reduce the expression of the targeted gene. A smart pool was used to maximise the silencing of the IRE1 protein.

3.4.2.1 Analysis of the efficiency of the IRE1 smart pool siRNA and its impact on BNIP3L protein abundance by western blot

In order to analyse the efficiency of siIRE1, we decided to study the protein abundance obtained following siRNA transfection in HeLa cells by western blot. The abundance of the BNIP3L protein is also analysed under these conditions. HeLa cells will be seeded in 6-well culture plates at a density of 100 000 cells per well. Protein abundance analysis was measured at 24 and 48 hours p.t. in 3 conditions: a control condition with cells receiving no treatment, cells transfected with siNT used as negative control and cells transfected with siIRE1. Protein abundance was measured on the basis of 10 µg of protein extracted from the cell lysate.

These results shown a significant protein decrease of IRE1 under siIRE1 conditions whatever the time post treatment (**Figure 30C**). These results are also supported by the quantifications performed based on this blot. One of the first conclusions that can be drawn from this graph is that siIRE1 is effective in silencing this protein.

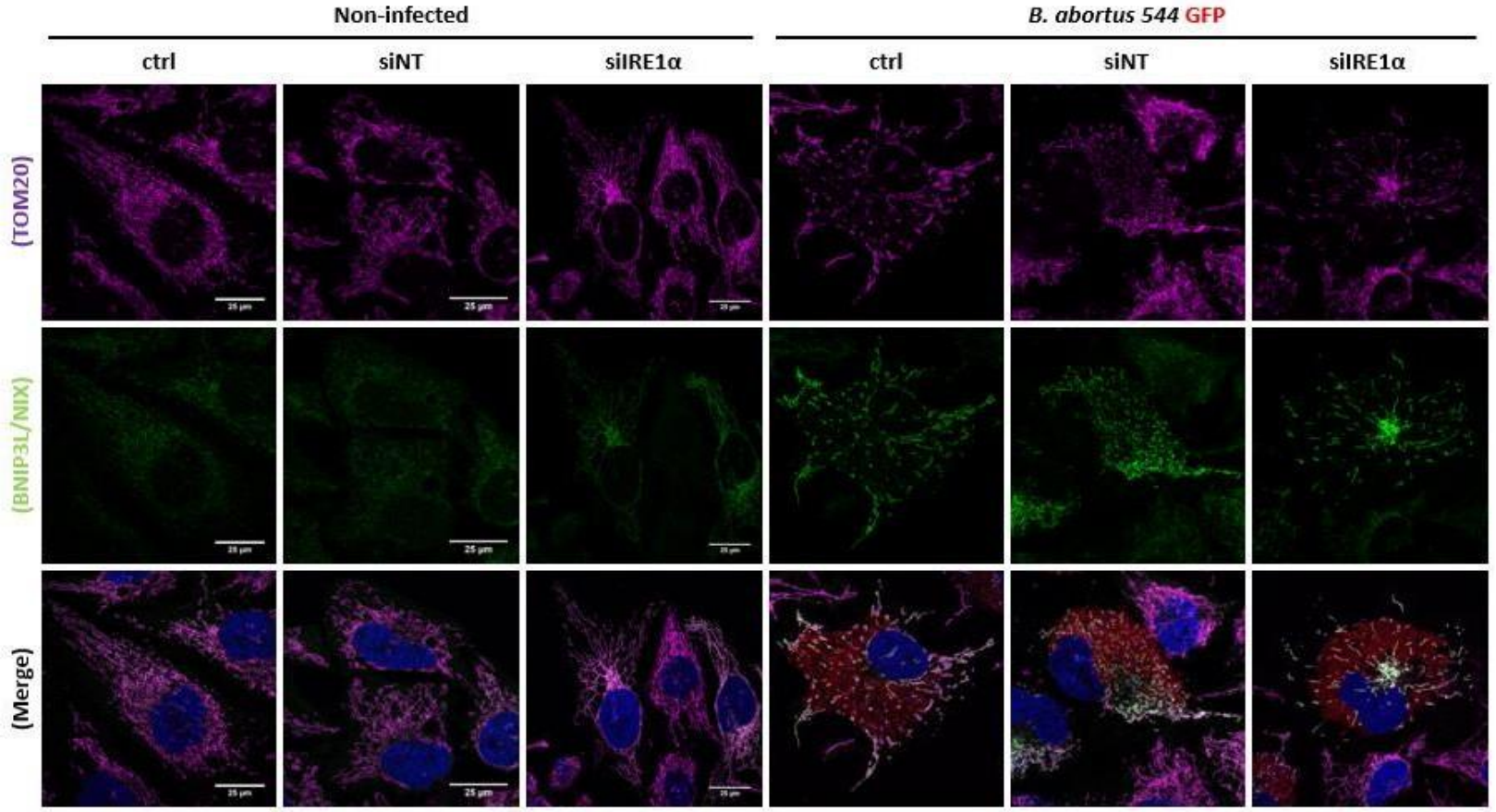

Figure 31: Effect of IRE1 silencing on the *B.abortus* 544 GFP-induced mitochondrial fragmentation in HeLa cells- 48h p.i.
Representative confocal micrographs of HeLa infected or not with *B. abortus* 544 GFP (red) transfected with or without 40 µM of siIRE1 24 h previous to the infection. Cells were then fixed at 48 h p.i and immunostained for BNIP3L (green), TOM20 (magenta) and Hoechst (blue) as a nuclear counterstain. Observed with Airyscan. Scale bar: 25 µm

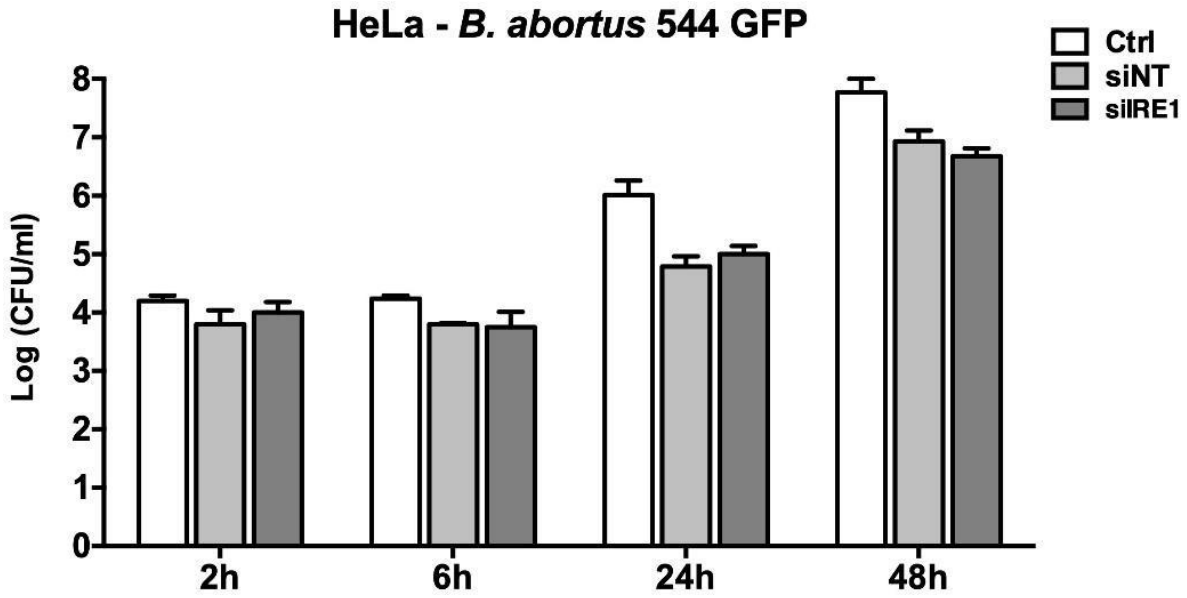

Figure 32: Effect of IRE1 silencing on the *B. abortus*-proliferation in HeLa cells.
HeLa cells were transfected 24 h before the infection with or without 40 µM of siRNA Non Targeting or siIRE1. CFU assays were then performed at different post-infection time point (2, 6, 24 or 48 h). Results are expressed as means +/- 1 SD for n=1

Then, we wanted to study the impact of siIRE1 on the expression of BNIP3L and the result obtained was not the expected one. An increase in the abundance of BNIP3L is observed under IRE1 silencing conditions. The active dimeric form is even present at time 48 p.t.

This first observation does not follow our initial hypothesis. Investigation of this phenomenon in the literature has shown that silencing of IRE1 or underlying players such as XBP1 leads to an induction of autophagy. This over-activation is explained by the fact that the IRE1 pathway may play a role in the over-activation of autophagy induced by the PERK pathway by inhibiting the expression of autophagy factors(Kroemer et al., 2010). Silencing of IRE1 therefore leads to overexpression of autophagy factors. However, contradictory information is also observed. PERK- and IRE-regulated upregulation can be observed on autophagy players such as BNIP3L. Inhibition of IRE1 leads to a significant reduction in BNIP3L expression. We therefore decided to verify this quantitative information by a confocal microscopy analysis in order to visualise the impact of IRE1 silencing on the expression of BNIP3L in each cell.

3.4.2.2 Analysis of the impact of IRE1 silencing on the BNIP3L expression and mitochondrial fragmentation under B. abortus infection

In order to obtain more qualitative information, we decided to study the impact of IRE1 silencing on both the induction of BNIP3L and the fragmentation of the mitochondrial network induced by *B. abortus* infection via confocal microscopy (**Figure 31A**).

HeLa cells were seeded in 3 conditions: control cells receiving no treatment, negative control cells transfected with siNT and cells transfected with siIRE1. Transfection was performed 24 hours after seeding the cells in a 24-well culture plate at a rate of 20,000 cells per well. Infection of the cells with *B. abortus* 544 GFP is performed 24 hours after transfection for infected conditions. At the end of the 48 h p.i., the cells were fixed and immunostained for TOM20 and BNIP3L.

Several observations can be made based on these micrographs. Firstly, in terms of BNIP3L induction, the fluorescence intensity is higher in the infected conditions. Secondly, at the level of the mitochondrial network, a fragmentation remains observable in the infected conditions regardless of the conditions observed.

Based on these results, we were able to observe that an induction of BNIP3L was still observable under IRE1 silencing conditions. This presence of BNIP3L does not counteract the mitochondrial fragmentation induced by *B. abortus*. Activation of the UPR pathway does not appear at first sight to be involved in the induction of BNIP3L in the infection model used by our team (HeLa cells infected by *B. abortus*). The presence of BNIP3L therefore leads to a fragmentation of the mitochondrial network that cannot be resolved by silencing the IRE1 pathway of the UPR.

3.4.3 Effect of IRE1 expression silencing on B. abortus proliferation

HeLa cells were either transfected (or not) with a non-target siRNA (siNT) or smart pool of siRNA directed against the IRE1 mRNA (siIRE1). Transfection was performed using the same protocol as the one followed for siBNIP3L (see section 3.2.3). At the end of the incubations, infected cells were lysed to calculate the number of colony-forming units (CFUs) obtained after 2, 6, 24, 48 or 72 h post-infection (**Figure 32**).

An effect of transfection seems to be observed. It is important to note that for the transfected cells, a certain proportion of cell death among the infected cells is observed in

comparison to the control non-transfected cells leading, most likely, to a small decrease in the number of CFU (0.5 log) observed for the *Brucella*-transfected cells. But based on these results, no significant difference could be observed for *Brucella* proliferation rate between transfected and non-transfected HeLa cells.

These observations are intriguing as they are not consistent with data observed in the literature (Y et al., 2015) . Indeed, IRE1 has been identified as being necessary for the establishment of a mature replicative niche for *B. abortus*. When IRE1 is inhibited, replication is disrupted because the formation of rBCVs with the sequestration of bacteria within the reticulum-derived membranes is no longer possible. *B. abortus* therefore becomes trapped in the endo-lysosomal compartment. However, our data does not seem to corroborate these observations as proliferation remains possible. One hypothesis is that silencing of IRE1 leaves a low expression of IRE1 that is sufficient to allow rBCV formation. There is also no evidence to completely exclude that another UPR pathway cannot take over to allow rBCV formation. The use of siRNAs directed against all UPR pathways could therefore be used.

Discussion, perspectives and Conclusion

4 DISCUSSION AND PERSPECTIVES

The main goal of this master thesis was to study the mechanisms of mitophagy induced by *Brucella abortus* in HeLa and RAW264.7 cells. Based on the preliminary results obtained and showing a nuclear translocation of HIF-1α at 24 h p.i in HeLa and RAW264.7 infected by *B. abortus*, a nuclear translocation of Parkin at 48 h p.i in HeLa infected cells by *B. abortus*, an overexpression of BNIP3L with *B. abortus*-induced fragmentation and mitophagy at 48 h p.i in HeLa cells (**Figure 17**) (Jérémy Verbeke, ongoing PhD thesis, data unpublished), three lines of research were defined: 1) to study the role of HIF-1α in the infection of HeLa and RAW264.7 cells with *B. abortus*, 2) to study the nuclear translocation of Parkin in HeLa cells infected with *B. abortus* and 3) to study of the role of BNIP3L/NIX in the *B. abortus*-induced mitochondrial fragmentation and/or mitophagy in infected HeLa cells.

4.1 Study of the role of HIF-1α in the infection of HeLa and RAW264.7 cells with B. abortus

The first line of research concerns the stabilisation of HIF-1α and its nuclear translocation observed in HeLa and RAW264.7 cells infected with *B. abortus* at 24 and 48 h p.i. The aim of this first axis was to better understand the putative role of HIF-1α stabilisation for *B. abortus* and the potential link with the mitochondrial fragmentation observed in *B. abortus*-infected-cells.

First, we thought to induce HIF-1α accumulation in order study its putative role on the proliferation and the replication of *B. abortus* in host cells. $CoCl_2$-mediated HIF-1α stabilisation before and during *B. abortus* infection in HeLa and RAW264.7 cells was analysed by CFU count obtained after infection. In the case of HeLa cells, no difference in bacterial viability/proliferation could be observed in cells treated with the chemical used to induce a chemical hypoxia before or during the infection when compared to infected cells. In RAW264.7 macrophages, a decrease in the number of CFUs (0.5 log) was observed when cells were pre-incubated with $CoCl_2$ before infection or before and immediately post-infection but not when post-treated at 24 h p.i.

One hypothesis to explain this observation is that HIF-1α would allow macrophages to initiate an inflammatory response at the early stage of the infection and thus allow a better elimination of intracellular bacteria directly after their entry. Indeed, HIF-1α induces a switch to aerobic glycolysis and polarisation into M1 macrophages (T. Wang et al., 2017). This metabolic switch increases the expression of glycolytic genes (PdK1, PgK1, Glut1, GcK, PkM2) and increased levels of pentose phosphate pathway metabolic intermediates necessary for the growth and the proliferation of macrophages (T. Wang et al., 2017b). This metabolism modulation is also needed for the expression of pro-inflammatory chemokines and cytokines (TNF-α, IL1-β, IL-6, IL-12, and IL-23), as well as inducible nitric oxide synthase (iNOS) and antimicrobial peptides (cathelicidin or signal transducer and activator of transcription 1 (STAT1)) (Knight and Stanley, 2019). In addition, to enhance the bactericidal properties of macrophages through inflammatory cytokine expression and ROS production, HIF-1α has also been shown to upregulate the expression of autophagy-related genes. A study on the activation of HIF-1α on the enhancement of bactericidal effects induced by macrophages (U937) in the context of *M. tuberculosis* infection showed that activation of HIF-1α induces the expression of LC3B (structural protein of autophagosomal membranes), sequestome-1 (SQSTM1) (a protein involved in the transport of substrate in the autophagosome)(Li et al., 2021). This HIF-1α-mediated induction of autophagy can also be bacterial-specific and is called xenophagy. In one study, HIF-1α was shown to be required for the initiation of xenophagy to allow the

degradation of adherent and invasive *E. coli* (AIEC) in human colon carcinoma cell line T84 (Mimouna et al., 2014). Upon infection with AIEC, HIF-1α upregulates Carcinoembryonic antigen-related (CEA) Cell Adhesion Molecule 6 (CEACAM6), which activates TLR5 to initiate phosphorylation of ULK1. Activated ULK1, then allows the specific recruitment of the autophagy machinery to AIEC-containing vesicles(Mimouna et al., 2014). Based on these observations and the information found in the literature, we can hypothesise that early activation of HIF-1α in macrophages would initiate defence mechanisms and could improve the specific clearance of *B. abortus*.

In a second step, we tried inhibiting HIF-1α in order to test the impact of its inhibition in the fragmentation of the mitochondrial network on HeLa cells infected with *B. abortus*. For this analysis, we used the inhibitor PX-478, a molecule described to decrease the expression of the HIF-1α protein and to increase its degradation in both normoxic and hypoxic conditions (Koh et al., 2008). HIF-1α inhibition was analysed both in HeLa cells treated with 100 µM $CoCl_2$ (used as a positive control for HIF-1α stabilisation) and in *B. abortus*-infected cells. No efficient effect of the inhibitor PX-478 could be observed in HeLa cells infected with *B. abortus* nor in cells treated with $CoCl_2$. PX-478 could thus not be used to analyse the inhibition of HIF-1α on the proliferation and viability of *B. abortus* in infected cells. This lack of effect in our model could be explained by the fact that, in the original paper, the inhibitor PX-478 was tested under conditions of reduced oxygen pressure (real hypoxia) and not $CoCl_2$-induced chemical hypoxia (Koh et al., 2008). Variable efficiency on the inhibition of HIF-1α for the same inhibitor concentration is also observed between the different cancer cell lines used (K. Lee & Kim, 2011). Finally, we tested higher concentrations of the inhibitor on HeLa cells but significant cell death was observed following treatment (data not shown).

In order to analyse the effect of HIF-1α inhibition in *B. abortus*-infected cells, it would be interesting to use a siRNA-mediated approach against HIF-1α. The use of siRNA could first be used to test the putative effect of HIF-1α silencing on the viability and proliferation of *B. abortus* in infected cells. It will also allow us to determine whether HIF-1α is indeed involved in the increase in BNIP3L expression, mitophagy and mitochondrial fragmentation observed at 48 h p.i. in *B. abortus*-infected HeLa cells.

4.2 Study of the nuclear translocation of Parkin in HeLa cells infected with B. abortus

The second line of research was based on preliminary results which seemed to indicate a nuclear translocation of Parkin in HeLa infected cells with *B. abortus* at 48 h p.i.. The aim of this second part was firstly to try to validate the nuclear translocation of Parkin during infection of HeLa cells by *B. abortus*. Then, the second step was to determine the role of that nuclear Parkin and more precisely its role as a co-activator of the transcription factor ERRα as it has been described in the literature(Shires et al., 2020).

We therefore first transfected HeLa cells with a Parkin-mCherry plasmid and then infected them with *B. abortus* 544 GFP for 48 h. We observed that a nuclear translocation of Parkin seemed to take place in HeLa cells infected with the bacteria.

We next aimed to investigate the putative role of Parkin nuclear translocation in *Brucella*-infected cells. We tested whether nuclear Parkin could increase ERRα activity as a transcriptional co-activator using a reporter system in which a luciferase reporter gene is driven by an ERRα-sensitive promoter. The luciferase produced could then be detected by immunofluorescence. For this experiment, HeLa cells were co-transfected with both plasmids (Parkin-mCherry and 3X ERRE-luciferase) before being infected or not with *B. abortus*. A

hypoxia condition was also used to induce the nuclear translocation of Parkin as reported by Shires and collaborators(Shires et al., 2020). However, none of the conditions could reveal luciferase expression. This result does not allow us to determine whether our reporter system is functional neither give us any indication of the co-activator role of Parkin. In addition, as the Parkin translocation was also observed in non-infected cells, it is very likely that the response is non-specific.

In view of these observations, it is important to consider several elements. The first is that in the 2020 paper by Shires and collaborators, the increase in ERRα transcript level is only observed for a construct encoding a Parkin protein that contains a NLS (Nuclear Localisation Signal) sequence used to force the nuclear localisation of Parkin (Shires et al., 2020). This is not the case in our experimental conditions. Secondly, as mentioned above, there is no condition that allows us to confirm the functionality of the reporter system used. The use of an endogenous activator of ERRα would have been necessary. Only one endogenous activator such as cholesterol has been identified so far in the literature (Li et al., 2019) . Cholesterol will be able to form a stable complex with ERRα facilitating the interaction with its co-activator PGC-1β and thus induce its transcriptional activity. However, the use of cholesterol is hardly compatible with the microscopy imaging techniques used to analyse *Brucella*-infected cells. Furthermore, we could observe that this nuclear translocation was not specific to infected cells and therefore certainly not specific to *B. abortus* infection. It is also important to mention that during his Master thesis, Youri Fayt was able to demonstrate that infection with *B. abortus* does not induce a hypoxic environment within the infected cells (Youri Fayt, Master thesis, 2022). Finally, as we found later that Parkin is not endogenously expressed by HeLa cells(Denison et al., 2003), the different phenotypes such as mitochondria fragmentation or HIF-1α accumulation in the nucleus observed in *Brucella*-infected HeLa cells must be Parkin-independent. For these reasons, we did not follow up the investigation for this second objective of the master thesis.

4.3 Study of the role of BNIP3L/NIX in the B. abortus-induced mitochondrial fragmentation and/or mitophagy

The third objective concerned the role of the increase in BNIP3L expression observed in HeLa and RAW264.7 cells infected with *B. abortus* at 48 h p.i. We were particularly interested in the role of BNIP3L, a mitophagy receptor, in the fragmentation of the mitochondrial network and mitophagy phenotypes induced by *B. abortus*.

In order to study the effect of the invalidation of BNIP3L on the mitochondrial fragmentation and mitophagy induced by *B. abortus,* we first attempted to generate a BNIP3L knock-out (KO) HeLa cell line by using CRISPR/Cas9 engineering. HeLa cells were electroporated with the ribonucleoprotein complex consisting of the third guide RNA selected and the Cas9 protein. Following a limit dilution and expansion of about 80 clones, one knock down (KD) clone was first identified based on the abundance of the protein analysed by western blot in cells incubated or not with $CoCl_2$. However, when this clone was routinely expanded, an acceleration in growth rate prompted us to reanalyse the protein abundance of BNIP3L protein. We observed that this clone had recovered a BNIP3L protein abundance comparable to the one found in wild type cells. One of the explanations is that HeLa cells could have multiple copies of the BNIP3L gene making HeLa cells prone to transcriptional adaptation. A study carried out on the genome of HeLa cells shows that these cells can carry from 3 to 8 copies of the same gene (Landry et al., 2013). It is therefore very likely that Cas9 did not

succeed in affecting all the copies of the gene if we assume that the HeLa cells used for these experiments have several copies of BNIP3L.

Techniques are now available to achieve simultaneously multiple knockouts (L. Wang et al., 2018). Whole genome sequencing of HeLa cells can be performed to determine the number of copies of the BNIP3L gene present within the genome of these cells. Once all copies of the gene have been identified, guide RNAs can be designed for each of these copies and combined into a single vector. HeLa cells can then be transfected with the vector containing the guide RNAs and a plasmid containing Cas9. NHEJ-mediated gene disruption is then expected in the copy set targeted by the transfection mix. Clone isolation and western blot analysis can be performed to identify a good and true KO clone for BNIP3L. This editing method has been developed and tested, at least in yeast (Wang et al., 2018). Theoretically, this method could be applied to our model in order to target all putative BNIP3L gene copies more efficiently. This technique would have required a huge amount of work and time, so we decided to pursue our work with the use of small interfering RNA.

Our aim was to observe the impact of a BNIP3L silencing on mitochondrial fragmentation and mitophagy induced by *B. abortus* in HeLa cells. The efficiency of siRNA SMARTpool against BNIP3L (siBNIP3L) was first tested on HeLa transfected cells or controlled cells treated or not with 100 µM of $CoCl_2$ by western blot analysis at 24, 48 and 72 h post transfection, in order to have a semi-quantitative view of the protein abundance in the global cell population. The analysis was also carried out in the same conditions by flow cytometry at 48 h post-transfection in order to have a view of the siRNA efficiency at a single-cell level. The results showed a decrease in BNIP3L abundance in western blot at 24, 48 and 72 h post transfection in cells treated or not with $CoCl_2$. Flow cytometry data supported the first observation with a decrease in fluorescence intensity at 48 h post-treatment in HeLa cells transfected with the siBNIP3L. These different observations allowed us to demonstrate the efficiency of the siBNIP3L SMARTpool on HeLa cells up to 72 h post-transfection, which could therefore be used in further experiments.

Firstly, we tested the impact of BNIP3L silencing on *B. abortus*-induced mitochondrial fragmentation in HeLa cells at 48 h p.i.. HeLa cells were transfected or not with a non-target siRNA or siBNIP3L before being infected with *B. abortus* for 48 h. Analysis of the effect of BNIP3L silencing on *B. abortus*-induced mitochondrial fragmentation revealed by immunofluorescence of TOM20 and confocal microscopy that the siBNIP3L prevents the fragmentation of the mitochondrial network. The reduction of the fragmented mitochondria phenotype could be confirmed by the quantification of the aspect ratio and the end point- branch point. Based on this analysis, we observed that no significant difference could be observed between cells transfected with siBNIP3L and non-infected cells. These sets of data confirm that a decrease in mitochondrial fragmentation is observed in cells transfected with siBNIP3L that display a mitochondrial network comparable to the one observed in non-infected cells. We can thus conclude here that BNIP3L is involved in *B. abortus*-induced fragmentation.

As mentioned in section 1.2.4.3, a close relationship does exist between mitochondrial dynamics and mitophagy. We were therefore interested in the putative effect of BNIP3L silencing on *B. abortus*-induced mitophagy in HeLa cells at 48 h p.i.. Our immunofluorescence and confocal microscopy obseervations seem to indicate a decrease in the LC3 abundance at the mitochondria in cells transfected with siBNIP3L. Although these results are open to interpretation and need quantification to draw clear conclusions, they seem to indicate that BNIP3L is also involved in *B. abortus*-induced mitophagy in HeLa cells.

While a decrease in mitochondrial network fragmentation was observed as well as a putative decrease in mitophagy, none of these observations allowed us to really understand the effect of BNIP3L silencing on *B. abortus*. We were therefore interested in the effect of the siBNIP3L on the proliferation of *B. abortus* in transfected HeLa cells. The analysis of colony-forming units (CFUs) obtained under siRNA transfection or not after 2, 6, 24 and 48 h post-infection does not support any alteration in the proliferation of *B. abortus* in cells that display a reduced abundance of BNIP3L.

Several questions now arise from these observations. One of the first questions is to identify the mechanism by which BNIP3L induces mitochondrial fragmentation. In the literature, the phenomenon of induction of mitochondrial network fragmentation is known, but the mechanisms underlying these observations are still unclear. A first clue was given by Simpson and collaborators. Indeed, these authors were able to observe that an induction of mitochondrial fragmentation mediated by the recruitment of FIS1 via BNIP3L to the mitochondrial membrane of Normal Human Epidermal Keratinocytes (NHEKs) cells. The recruitment of FIS1 and its stabilisation at the membrane initiates, in turn, the recruitment of the DRP1 protein which initiates mitochondrial fragmentation(Simpson et al., 2021b). However, using infection in DRP1 invalidated cells, the involvement of DRP1 was rule out by Elodie Lobet's studies. But there is evidence to question whether FIS1 is involved in DRP1-induced fission. Indeed, FIS1 has no effect on the hydrolysis of DRP1 required for fission initiation(Koirala et al., 2013a). Furthermore, the minimal combination of FIS and DRP1 of human origin does not induce mitochondrial fragmentation in yeast lacking all the fission proteins(Koirala et al., 2013b). In addition to these observations, some studies suggest that FIS may induce mitochondrial fragmentation through the inhibition of fusion mechanisms (Yu et al., 2019), this hypothesis being more in line with the results obtained by Elodie Lobet (Lobet et al., 2018). Based on this hypothesis, it could be interesting to use siRNA directed against FIS1 to test whether FIS1 silencing can have an impact on the fragmentation induced by *B. abortus*.

Another question arises as to the role of mitophagy in infected cells. Indeed, the use of a siBNIP3L does not allow us to visualise an effect on the proliferation or the survival of *B. abortus* on the basis of the micrographs and CFU assays.

One of the first hypotheses that can be put forward is that mitophagy will be able to play a role in the continuation of the intracellular cycle of the bacteria and in particular at the level of the egress. Mitophagy may contribute to the membrane supply for aBCV biogenesis. Jean Celli was also able to highlight the involvement of certain autophagy players in the biogenesis of aBCVs such as ULK1, Beclin1 and ATG14(Celli, 2019). BNIP3L could therefore be an additional actor in this process. In order to answer this question, we will analyse the effect of BNIP3L silencing on the bacterial egression. The bacterial exit can be monitored by confocal microscopy by counting the number of reinfection events observed around an infected cell.

The second hypothesis that can be put forward is that *B. abortus* could be able to modulate mitophagy mechanisms to provide a favourable environment for its survival. One study showed that BNIP3L was involved in the polarisation of macrophages into M1 macrophages. Indeed, the expression of the glycolysis pathway gene (LDHA, ENO1, PFKFB3, GADPH) is decreased in a BNIP3L silencing model of *M. tuberculosis* infected peripheral blood mononuclear cells (PBMCs). This decrease is also accompanied by and correlated with a decrease in the polarisation of macrophages into M1 with a decrease in the expression of pro-inflammatory cytokines (Mahla et al., 2021). It may therefore be of interest to characterise

macrophage polarisation in our infection model to determine whether BNIP3L silencing modulates macrophage polarisation into M1 macrophages based on pro-inflammatory cytokine expression (Alves-Silva et al., 2017).

Still in the context of host-induced defences, a link can also be observed between the inflammasome and BNIP3L-induced mitophagy. Indeed, a study showed that a decrease in the activation of inflammasome allows the upregulation of HIF-1α and BNIP3L during contrast-induced acute kidney injury and reduce apoptosis (Lin et al., 2020). It may therefore be of interest to investigate the activation of the inflammasome in HeLa cells infected with *B. abortus*. In order to monitor the activation of the inflammasome, imaging techniques can be used such as fluorescent antibodies directed against the component of the inflammasome such as NLRP3 or Apoptosis-associated speck-like protein containing a CARD (ASC) (Nandi et al., 2021). In addition to analysis by confocal microscopy, analysis of the abundance of cytokines such as IL-1β and IL-18 can be performed by ELISA or flow cytometry in the presence of inhibitor of secretory pathway such as monensin or brefeldin A (Schuerwegh et al., 2001). This activation could also be analysed in the presence of siBNIP3L in infected HeLa cells.

Finally, it is interesting to note that mitophagy can use redundant pathways. In a study of mitophagy induced during hypoxia, a double KO of Nix and BNIP3 prevented less than half of the mitophagy events induced by $CoCl_2$ (Sulkshane et al., 2021). Furthermore, the use of siRNA shows that the recovery of the fused mitochondrial network remains partial when compared to non-infected cells. Although the use of siBNIP3L does not result in an absence of BNIP3L expression, it can be hypothesised that other mitophagy actors may be involved in our infection model. It could therefore be interesting to analyse the expression of several mitophagy actors such as FUNDC1 and FKBP8 by confocal microscopy or flow cytometry. FKBP8 is an interesting target because it is involved in the initiation of mitophagy during iron deprivation. Yourit Fayt was able to demonstrate that iron deprivation induced by *Brucella abortus* could induce HIF-1α stabilisation and BNIP3L expression in host cells (HeLa and RAW264.7). The addition of iron to the culture medium prevents HIF-1α stabilisation and BNIP3L expression but has no impact on the fragmentation of the mitochondrial network. Preliminary results (Youri Fayt, Master thesis 2022) have shown that the mammalian siderophore 2,5-DHBA, which resembles the bacterial siderophore (Z. Liu et al., 2014), may be involved in this fragmentation process. The hypothesis is that *B. abortus* is able to divert this siderophore 2,5-DHBA. The addition of iron and siderophore seems to prevent mitochondrial fragmentation.

4.4 Analysis of the impact of B. abortus-induced UPR activation on BNIP3L expression, mitochondrial network fragmentation and B. abortus proliferation

Finally, based on preliminary data obtained in our laboratory, the possible link between HIF-1 and the mitochondrial fragmentation was questioned. We therefore thought to identify other inducers of autophagy and more specifically of the mitophagy actor BNIP3L in *B. abortus*-infected HeLa cells. The UPR was recently identified as a pathway able to induce the expression of autophagy-related actors among which BNIP3L (Domínguez-Martín et al., 2018).

First, we confirmed that the erUPR was activated in *Brucella*-infected HeLa cells and more specifically the IRE1 pathway, identified as the pathway mainly activated during *B. abortus* infection (Y et al., 2015). Our flow cytometry data revealed an increase in the abundance of p-IRE1 and XBP1 in *B. abortus*-infected HeLa cells at time 24 and 48 h p.i., confirming the activation of the IRE1 by *B. abortus* in infected cells. Next, in order to determine whether the IRE1 pathway was involved in the induction of BNIP3L expression, we used a

siRNA SMARTpool directed against IRE1. The efficiency of siIRE1 was analysed by western blot. The results show that a strong decrease in the protein abundance of IRE1 is observed in cells transfected with siIRE1. Under the same conditions, we tried to analyse the effect of siIRE1 on the protein abundance of BNIP3 and we were able to observe an increase in the protein abundance of BNIP3L in cells transfected with siIRE.

However, based on western blot analysis, it is not possible to determine whether this increased in the abundance of BNIP3L comes from a few cells that overexpress BNIP3L or whether this increase in the abundance of the protein is observed in the entire cell population. We therefore continued to study the effect of siIRE1 on the fragmentation of the mitochondrial network. The observations obtained by confocal imaging show that, in terms of BNIP3L induction, the fluorescence intensity seems to be higher in the infected cells. Moreover, at the level of the mitochondrial population, a mitochondria fragmentation remains observable in the infected cells regardless of the conditions observed.

In view of these results, there is no indication that the IRE1 pathway is involved in the regulation of BNIP3L expression nor that it can modulate mitochondrial fragmentation. But there is certainly no question of ruling out a possible link between the UPR and mitophagy. It is important to come back to the different observations obtained and those observed in the literature. Indeed, we did not observe any effect of the IRE1silencing on bacterial proliferation. However, several studies indicate that IRE1 is essential for rBCV biogenesis(Guimarães et al., 2019; Y et al., 2015). The first possibility is that another branch of the UPR pathway compensates for the silencing of IRE1. Although the activation of other UPR pathways is controversial, some recent studies indicate that PERK and ATF6 can also be activated in response to *B. abortus* infection and are necessary for the establishment of the replicative niche of the bacterium(Byndloss et al., 2019; Zhou et al., 2018a).

In addition, the UPR has also been identified in the modulation of mitochondrial network fragmentation. The PERK pathway of the UPR regulates mitochondrial dynamics by phosphorylation-dependent translational attenuation of eIF2α, which leads to activation of the stress-induced mitochondrial hyperfusion (SIMH) protein(Lebeau et al., 2018). The IRE1 pathway has also been identified to modulate mitochondrial dynamics through reduced expression of fusion proteins such as Mfn2 (Delmotte and Sieck, 2020).

It may therefore be interesting to target the entire UPR pathway by using siRNAs in order to test the effect of simultaneous inhibition of multiple erUPR signalling pathways on *B. abortus* proliferation or mitochondrial population fragmentation.

5 CONCLUSION

In the course of this master thesis, we were able to investigate several avenues of research on the three main actors identified on the basis of preliminary research by Jeremy Verbeke. Several conclusions can be drawn from the different results obtained in this thesis.

The first objective was to determine the role of HIF-1α in the infection of HeLa and RAW264.7 cells with *B. abortus*. In order to answer this question, we decided to modulate the stabilisation of HIF-1α by enhancing or inhibiting its activation. The results obtained on the reduction of bacterial proliferation in macrophages, in which stabilisation of HIF-1α had been previously induced, gave us some indications. HIF-1a might play a role in the modulation of the inflammatory response and the clearance of bacteria in phagocytic cells.

The second objective was to study the nuclear translocation of Parkin in HeLa cells infected with *B. abortus*. The results obtained allowed us to reposition ourselves in the face of the first observations. Indeed, the nuclear translocation of Parkin seems to be random and not specific to infected cells. Moreover, HeLa cells do not endogenously express Parkin and thus it is unlikely/impossible that Parkin plays any role in mitochondria fragmentation and/or mitophagy in *Brucella*-infected HeLa cells. The situation in other, more relevant, cell types that express Parkin, should be investigated.

Finally, the third and major objective of this work was to better delineate the role of BNIP3L/NIX in the *B. abortus*-induced mitochondrial fragmentation and/or mitophagy. Although the CRISPR/Cas9 technique did not allow us to isolate a HeLa KO clone for BNIP3L, we were able to use small interfering RNAs which gave interesting results. We observed that the siRNA SMARTpool directed against BNIP3L partly prevents the *B. abortus*-induced mitochondrial fragmentation in HeLa cells. The BNIP3L silencing also seems to prevent *B. abortus*-induced mitophagy in HeLa cells with a possible reduction in the number of LC3B foci localised with the mitochondrial network. These first data suggests that BNIP3L is an actor responsible at least in part for *B. abortus*-induced mitochondrial fragmentation and mitophagy.

Although some answers have been found, many questions remain unanswered and a more detailed understanding of the mechanisms and the link between each of the actors is still needed. However, these first data are encouraging and prompt us to continue our research. Indeed, these studies allow a better understanding of the interactions between *Brucella* and its host in order to target potential host cell actors and interfere with the trafficking of *Brucella abortus* in the long term. In the future, the output of our research could bring a better understanding of the crosstalk between the bacteria and mitochondria and their putative importance in the symptoms associated with *Brucella* infection.

References

6 BIBLIOGRAPHY

Ackermann, M. R., Cheville, N. F., & Deyoe, B. L. (1988). Bovine Ileal Dome Lymphoepithelial Cells: Endocytosis and Transport of Brucella abortus Strain 19. *Veterinary Pathology*, *25*(1), 28–35. https://doi.org/10.1177/030098588802500104

Adachi, Y., Kato, T., Yamada, T., Murata, D., Arai, K., Stahelin, R. v., Chan, D. C., Iijima, M., & Sesaki, H. (2020). Drp1 Tubulates the ER in a GTPase-Independent Manner. *Molecular Cell*, *80*(4), 621-632.e6. https://doi.org/10.1016/J.MOLCEL.2020.10.013

Alves-Silva, J., Tavares, I. P., Guimarães, E. S., Costa Franco, M. M., Figueiredo, B. C., Marques, J. T., Splitter, G., & Oliveira, S. C. (2017). Modulation of microtubule dynamics affects Brucella abortus intracellular survival, pathogen-containing vacuole maturation, and pro-inflammatory cytokine production in infected macrophages. *Frontiers in Microbiology*, *8*(NOV). https://doi.org/10.3389/FMICB.2017.02217/FULL

Amjadi, O., Rafiei, A., Mardani, M., Zafari, P., & Zarifian, A. (2019). A review of the immunopathogenesis of Brucellosis. *Https://Doi.Org/10.1080/23744235.2019.1568545*, *51*(5), 321–333. https://doi.org/10.1080/23744235.2019.1568545

Atluri, V. L., Xavier, M. N., Jong, M. F. de, Hartigh, A. B. den, & Tsolis, R. M. (2011). Interactions of the Human Pathogenic Brucella Species with Their Hosts. *Http://Dx.Doi.Org/10.1146/Annurev-Micro-090110-102905*, *65*, 523–541. https://doi.org/10.1146/ANNUREV-MICRO-090110-102905

Barquero-Calvo, E., Mora-Cartín, R., Arce-Gorvel, V., de Diego, J. L., Chacón-Díaz, C., Chaves-Olarte, E., Guzmán-Verri, C., Buret, A. G., Gorvel, J. P., & Moreno, E. (2015). Brucella abortus Induces the Premature Death of Human Neutrophils through the Action of Its Lipopolysaccharide. *PLOS Pathogens*, *11*(5), e1004853. https://doi.org/10.1371/JOURNAL.PPAT.1004853

Barrionuevo, P., Delpino, M. V., Velásquez, L. N., García Samartino, C., Coria, L. M., Ibañez, A. E., Rodríguez, M. E., Cassataro, J., & Giambartolomei, G. H. (2011). Brucella abortus inhibits IFN-γ-induced FcγRI expression and FcγRI-restricted phagocytosis via toll-like receptor 2 on human monocytes/macrophages. *Microbes and Infection*, *13*(3), 239–250. https://doi.org/10.1016/J.MICINF.2010.10.020

Basu, U., Bostwick, A. M., Das, K., Dittenhafer-Reed, K. E., & Patel, S. S. (2020). Structure, mechanism, and regulation of mitochondrial DNA transcription initiation. *The Journal of Biological Chemistry*, *295*(52), 18406–18425. https://doi.org/10.1074/JBC.REV120.011202

Biasizzo, M., & Kopitar-Jerala, N. (2020). Interplay Between NLRP3 Inflammasome and Autophagy. *Frontiers in Immunology*, *0*, 2470. https://doi.org/10.3389/FIMMU.2020.591803

Blancke Soares, A., Meier, R., Liebsch, G., Schwenk-Zieger, S., Kirmaier, M. E., Theurich, S., Widmann, M., Canis, M., Gires, O., & Haubner, F. (2021). High-resolution spatiotemporal pH e and pO 2 imaging in head and neck and oesophageal carcinoma cells. *Cancer & Metabolism*, *9*(1). https://doi.org/10.1186/S40170-021-00257-6

Boschiroli, M. L., Ouahrani-Bettache, S., Foulongne, V., Michaux-Charachon, S., Bourg, G., Allardet-Servent, A., Cazevieille, C., Liautard, J. P., Ramuz, M., & O'Callaghan, D. (2002). The Brucella suis virB operon is induced intracellularly in macrophages. *Proceedings of the National Academy of Sciences of the United States of America*, *99*(3), 1544–1549. https://doi.org/10.1073/pnas.032514299

Byndloss, M. X., Tsai, A. Y., Walker, G. T., Miller, C. N., Young, B. M., English, B. C., Seyffert, N., Kerrinnes, T., de Jong, M. F., Atluri, V. L., Winter, M. G., Celli, J., & Tsolis, R. M. (2019).

Brucella abortus infection of placental trophoblasts triggers endoplasmic reticulum stress-mediated cell death and fetal loss via type iv secretion system-dependent activation of CHOP. *MBio*, *10*(4). https://doi.org/10.1128/MBIO.01538-19/SUPPL_FILE/MBIO.01538-19-ST003.PDF

C, C., A, W., M, Y., S, D., S, S., H, F., D, S., N, W., N, R., H, W., C, S., & T, M. (2008). Subversion of Toll-like receptor signaling by a unique family of bacterial Toll/interleukin-1 receptor domain-containing proteins. *Nature Medicine*, *14*(4), 399–406. https://doi.org/10.1038/NM1734

Campos, P. C., Gomes, M. T. R., Marinho, F. A. V., Guimarães, E. S., de Moura Lodi Cruz, M. G. F., & Oliveira, S. C. (2019). Brucella abortus nitric oxide metabolite regulates inflammasome activation and IL-1β secretion in murine macrophages. *European Journal of Immunology*, *49*(7), 1023–1037. https://doi.org/10.1002/EJI.201848016

Cardoso, P. G., Macedo, G. C., Azevedo, V., & Oliveira, S. C. (2006). Brucella spp noncanonical LPS: structure, biosynthesis, and interaction with host immune system. *Microbial Cell Factories*, *5*, 13. https://doi.org/10.1186/1475-2859-5-13

Celli, J. (2006). Surviving inside a macrophage: The many ways of Brucella. In *Research in Microbiology* (Vol. 157, Issue 2, pp. 93–98). Res Microbiol. https://doi.org/10.1016/j.resmic.2005.10.002

Celli, J. (2015). The changing nature of the Brucella-containing vacuole. *Cellular Microbiology*, *17*(7), 951–958. https://doi.org/10.1111/cmi.12452

Celli, J. (2019). The Intracellular Life Cycle of Brucella spp . *Microbiology Spectrum*, *7*(2). https://doi.org/10.1128/MICROBIOLSPEC.BAI-0006-2019

Celli, J., de Chastellier, C., Franchini, D. M., Pizarro-Cerda, J., Moreno, E., & Gorvel, J. P. (2003). Brucella evades macrophage killing via VirB-dependent sustained interactions with the endoplasmic reticulum. *Journal of Experimental Medicine*, *198*(4), 545–556. https://doi.org/10.1084/jem.20030088

Celli, J., & Gorvel, J. P. (2004). Organelle robbery: Brucella interactions with the endoplasmic reticulum. In *Current Opinion in Microbiology* (Vol. 7, Issue 1, pp. 93–97). Elsevier Ltd. https://doi.org/10.1016/j.mib.2003.11.001

Chan, D. C. (2020). Mitochondrial Dynamics and Its Involvement in Disease. *Https://Doi.Org/10.1146/Annurev-Pathmechdis-012419-032711*, *15*, 235–259. https://doi.org/10.1146/ANNUREV-PATHMECHDIS-012419-032711

Checchetto, V., & Szabo, I. (2018). Novel Channels of the Outer Membrane of Mitochondria: Recent Discoveries Change Our View. *BioEssays*, *40*(6), 1700232. https://doi.org/10.1002/BIES.201700232

Chen, M., Chen, Z., Wang, Y., Tan, Z., Zhu, C., Li, Y., Han, Z., Chen, L., Gao, R., Liu, L., & Chen, Q. (2016). Mitophagy receptor FUNDC1 regulates mitochondrial dynamics and mitophagy. *Autophagy*, *12*(4), 689–702. https://doi.org/10.1080/15548627.2016.1151580/SUPPL_FILE/KAUP_A_1151580_SM2634.ZIP

Chen, Y., & Dorn, G. W. (2013). PINK1-phosphorylated mitofusin 2 is a parkin receptor for culling damaged mitochondria. *Science*, *340*(6131), 471–475. https://doi.org/10.1126/science.1231031

CN, M., EP, S., JA, C., LA, K., J, B. B., V, L., & J, C. (2017). A Brucella Type IV Effector Targets the COG Tethering Complex to Remodel Host Secretory Traffic and Promote Intracellular

Replication. *Cell Host & Microbe*, *22*(3), 317-329.e7. https://doi.org/10.1016/J.CHOM.2017.07.017

Cooper, C. J., Denyer, S. P., & Maillard, J. Y. (2011). Rapid and quantitative automated measurement of bacteriophage activity against cystic fibrosis isolates of Pseudomonas aeruginosa. *Journal of Applied Microbiology*, *110*(3), 631–640. https://doi.org/10.1111/J.1365-2672.2010.04928.X

Coronas-Serna, J. M., Louche, A., Rodríguez-Escudero, M., Roussin, M., Imbert, P. R. C., Rodríguez-Escudero, I., Terradot, L., Molina, M., Gorvel, J. P., Cid, V. J., & Salcedo, S. P. (2020). The TIR-domain containing effectors BtpA and BtpB from Brucella abortus impact NAD metabolism. *PLoS Pathogens*, *16*(4). https://doi.org/10.1371/JOURNAL.PPAT.1007979

Costa Franco, M. M., Marim, F., Guimarães, E. S., Assis, N. R. G., Cerqueira, D. M., Alves-Silva, J., Harms, J., Splitter, G., Smith, J., Kanneganti, T.-D., de Queiroz, N. M. G. P., Gutman, D., Barber, G. N., & Oliveira, S. C. (2018). Brucella abortus Triggers a cGAS-Independent STING Pathway To Induce Host Protection That Involves Guanylate-Binding Proteins and Inflammasome Activation . *The Journal of Immunology*, *200*(2), 607–622. https://doi.org/10.4049/JIMMUNOL.1700725/-/DCSUPPLEMENTAL

Czyż, D. M., Willett, J. W., & Crosson, S. (2017). Brucella abortus Induces a Warburg Shift in Host Metabolism That Is Linked to Enhanced Intracellular Survival of the Pathogen. *Journal of Bacteriology*, *199*(15). https://doi.org/10.1128/JB.00227-17

D, S., & ZA, R. (2015). UPR, autophagy, and mitochondria crosstalk underlies the ER stress response. *Trends in Biochemical Sciences*, *40*(3), 141–148. https://doi.org/10.1016/J.TIBS.2015.01.002

da Silva Rosa, S. C., Martens, M. D., Field, J. T., Nguyen, L., Kereliuk, S. M., Hai, Y., Chapman, D., Diehl-Jones, W., Aliani, M., West, A. R., Thliveris, J., Ghavami, S., Rampitsch, C., Dolinsky, V. W., & Gordon, J. W. (2020). BNIP3L/Nix-induced mitochondrial fission, mitophagy, and impaired myocyte glucose uptake are abrogated by PRKA/PKA phosphorylation. *Autophagy*, *00*(00), 1–16. https://doi.org/10.1080/15548627.2020.1821548

de Figueiredo, P., Ficht, T. A., Rice-Ficht, A., Rossetti, C. A., & Adams, L. G. (2015). Pathogenesis and Immunobiology of Brucellosis: Review of Brucella–Host Interactions. *The American Journal of Pathology*, *185*(6), 1505–1517. https://doi.org/10.1016/J.AJPATH.2015.03.003

de Jong, M. F., Starr, T., Winter, M. G., den Hartigh, A. B., Child, R., Knodler, L. A., van Dijl, J. M., Celli, J., & Tsolis, R. M. (2013). Sensing of bacterial type IV secretion via the unfolded protein response. *MBio*, *4*(1). https://doi.org/10.1128/MBIO.00418-12/SUPPL_FILE/MBO001131441ST2.PDF

Deegan, S., Koryga, I., Glynn, S. A., Gupta, S., Gorman, A. M., & Samali, A. (2015). A close connection between the PERK and IRE arms of the UPR and the transcriptional regulation of autophagy. *Biochemical and Biophysical Research Communications*, *456*(1), 305–311. https://doi.org/10.1016/j.bbrc.2014.11.076

Deghelt, M., Mullier, C., Sternon, J.-F., Francis, N., Laloux, G., Dotreppe, D., van der Henst, C., Jacobs-Wagner, C., Letesson, J.-J., & de Bolle, X. (2014). G1-arrested newborn cells are the predominant infectious form of the pathogen Brucella abortus. *Nature Communications 2014 5:1*, *5*(1), 1–12. https://doi.org/10.1038/ncomms5366

Delmotte, P., & Sieck, G. C. (2020). Endoplasmic Reticulum Stress and Mitochondrial Function in Airway Smooth Muscle. *Frontiers in Cell and Developmental Biology*, *7*. https://doi.org/10.3389/FCELL.2019.00374

Denison, S. R., Wang, F., Becker, N. A., Schüle, B., Kock, N., Phillips, L. A., Klein, C., & Smith, D. I. (2003). Alterations in the common fragile site gene Parkin in ovarian and other cancers. *Oncogene 2003 22:51*, *22*(51), 8370–8378. https://doi.org/10.1038/sj.onc.1207072

Detilleux, P. G., Deyoe, B. L., & Cheville, N. F. (1990). Penetration and intracellular growth of Brucella abortus in nonphagocytic cells in vitro. *Infection and Immunity*, *58*(7), 2320–2328. https://doi.org/10.1128/IAI.58.7.2320-2328.1990

Devraj, G., Beerlage, C., Brüne, B., & Kempf, V. A. J. (2017). Hypoxia and HIF-1 activation in bacterial infections. *Microbes and Infection*, *19*(3), 144–156. https://doi.org/10.1016/j.micinf.2016.11.003

DÍAZ APARICIO, D. (2013). Epidemiology of brucellosis in domestic animals caused by Brucella melitensis, Brucella suis and Brucella abortus. *Revue Scientifique et Technique de l'OIE*, *32*(1), 53–60. https://doi.org/10.20506/RST.32.1.2187

Diebold, L., & Chandel, N. S. (2016). Mitochondrial ROS regulation of proliferating cells. *Free Radical Biology and Medicine*, *100*, 86–93. https://doi.org/10.1016/J.FREERADBIOMED.2016.04.198

Ding, W. X., & Yin, X. M. (2012). Mitophagy: mechanisms, pathophysiological roles, and analysis. *Biological Chemistry*, *393*(7), 547–564. https://doi.org/10.1515/HSZ-2012-0119

Domínguez-Martín, E., Ongay-Larios, L., Kawasaki, L., Vincent, O., Coello, G., Coria, R., & Escalante, R. (2018). IreA controls endoplasmic reticulum stress-induced autophagy and survival through homeostasis recovery. *Molecular and Cellular Biology*, *38*(13), MCB.00054-18. https://doi.org/10.1128/mcb.00054-18

Eiyama, A., & Okamoto, K. (2015). PINK1/Parkin-mediated mitophagy in mammalian cells. *Current Opinion in Cell Biology*, *33*, 95–101. https://doi.org/10.1016/J.CEB.2015.01.002

Foulongne, V., Michaux-Charachon, S., O'Callaghan, D., & Ramuz, M. (2002). Syst??mes de s??cr??tion des prot??ines de type IV et virulence bact??rienne. *Medecine/Sciences*, *18*(4), 439–447.

Franco, M. P., Mulder, M., Gilman, R. H., & Smits, H. L. (2007). Human brucellosis. In *Lancet Infectious Diseases* (Vol. 7, Issue 12, pp. 775–786). https://doi.org/10.1016/S1473-3099(07)70286-4

Fugier, E., Salcedo, S. P., Chastellier, C. de, Pophillat, M., Muller, A., Arce-Gorvel, V., Fourquet, P., & Gorvel, J.-P. (2009). The Glyceraldehyde-3-Phosphate Dehydrogenase and the Small GTPase Rab 2 Are Crucial for Brucella Replication. *PLOS Pathogens*, *5*(6), e1000487. https://doi.org/10.1371/JOURNAL.PPAT.1000487

G, P., P, P., N, A., L, C., & EV, T. (2006). The new global map of human brucellosis. *The Lancet. Infectious Diseases*, *6*(2), 91–99. https://doi.org/10.1016/S1473-3099(06)70382-6

Garin-Bastuji, B., Mick, V., le Carrou, G., Allix, S., Perrett, L. L., Dawson, C. E., Groussaud, P., Stubberfield, E. J., Koylass, M., & Whatmore, A. M. (2014). Examination of taxonomic uncertainties surrounding Brucella abortus bv. 7 by phenotypic and molecular approaches. *Applied and Environmental Microbiology*, *80*(5), 1570–1579. https://doi.org/10.1128/AEM.03755-13

Giacomello, M., Pyakurel, A., Glytsou, C., & Scorrano, L. (2020). The cell biology of mitochondrial membrane dynamics. *Nature Reviews Molecular Cell Biology 2020 21:4*, *21*(4), 204–224. https://doi.org/10.1038/s41580-020-0210-7

Gilkerson, R., de La Torre, P., & st. Vallier, S. (2021). Mitochondrial OMA1 and OPA1 as Gatekeepers of Organellar Structure/Function and Cellular Stress Response. *Frontiers in Cell and Developmental Biology*, *9*, 527. https://doi.org/10.3389/FCELL.2021.626117/BIBTEX

GŁOWACKA, P., ŻAKOWSKA, D., NAYLOR, K., NIEMCEWICZ, M., & BIELAWSKA-DRÓZD, A. (2018). Brucella – Virulence Factors, Pathogenesis and Treatment. *Polish Journal of Microbiology*, *67*(2), 151. https://doi.org/10.21307/PJM-2018-029

Godfroid, J., Scholz, H. C., Barbier, T., Nicolas, C., Wattiau, P., Fretin, D., Whatmore, A. M., Cloeckaert, A., Blasco, J. M., Moriyon, I., Saegerman, C., Muma, J. B., al Dahouk, S., Neubauer, H., & Letesson, J. J. (2011). Brucellosis at the animal/ecosystem/human interface at the beginning of the 21st century. *Preventive Veterinary Medicine*, *102*(2), 118–131. https://doi.org/10.1016/J.PREVETMED.2011.04.007

Gomes, M. T. R., Campos, P. C., Oliveira, F. S., Corsetti, P. P., Bortoluci, K. R., Cunha, L. D., Zamboni, D. S., & Oliveira, S. C. (2013). Critical role of ASC inflammasomes and bacterial type IV secretion system in caspase-1 activation and host innate resistance to Brucella abortus infection. *Journal of Immunology (Baltimore, Md. : 1950)*, *190*(7), 3629–3638. https://doi.org/10.4049/JIMMUNOL.1202817

Gomes, M. T. R., Guimarães, E. S., Marinho, F. v., Macedo, I., Aguiar, E. R. G. R., Barber, G. N., Moraes-Vieira, P. M. M., Alves-Filho, J. C., & Oliveira, S. C. (2021). STING regulates metabolic reprogramming in macrophages via HIF-1α during Brucella infection. *PLOS Pathogens*, *17*(5), e1009597. https://doi.org/10.1371/journal.ppat.1009597

González-Espinoza, G., Arce-Gorvel, V., Mémet, S., & Gorvel, J. P. (2021). Brucella: Reservoirs and niches in animals and humans. In *Pathogens* (Vol. 10, Issue 2, pp. 1–21). MDPI AG. https://doi.org/10.3390/pathogens10020186

Gray, M. W. (2013). Mitochondria. *Brenner's Encyclopedia of Genetics: Second Edition*, 430–432. https://doi.org/10.1016/B978-0-12-374984-0.00957-8

Guimarães, E. S., Gomes, M. T. R., Campos, P. C., Mansur, D. S., dos Santos, A. A., Harms, J., Splitter, G., Smith, J. A., Barber, G. N., & Oliveira, S. C. (2019). Brucella abortus Cyclic Dinucleotides Trigger STING-Dependent Unfolded Protein Response That Favors Bacterial Replication . *The Journal of Immunology*, *202*(9), 2671–2681. https://doi.org/10.4049/JIMMUNOL.1801233/-/DCSUPPLEMENTAL

Haase, V. H. (2010). The sweet side of HIF. In *Kidney International* (Vol. 78, Issue 1, pp. 10–13). Nature Publishing Group. https://doi.org/10.1038/ki.2010.112

Heckler, M. M., Thakor, H., Schafer, C. C., & Riggins, R. B. (2014a). ERK/MAPK regulates ERRγ expression, transcriptional activity and receptor-mediated tamoxifen resistance in ER+ breast cancer. *FEBS Journal*, *281*(10), 2431–2442. https://doi.org/10.1111/febs.12797

Heckler, M. M., Thakor, H., Schafer, C. C., & Riggins, R. B. (2014b). ERK/MAPK regulates ERRγ expression, transcriptional activity and receptor-mediated tamoxifen resistance in ER+ breast cancer. *The FEBS Journal*, *281*(10), 2431–2442. https://doi.org/10.1111/FEBS.12797

Horvath, S. E., & Daum, G. (2013). Lipids of mitochondria. *Progress in Lipid Research*, *52*(4), 590–614. https://doi.org/10.1016/J.PLIPRES.2013.07.002

Hu, H., Tian, M., Li, P., Bao, Y., Guan, X., Lian, Z., Yin, Y., Ding, C., & Yu, S. (2019). Brucella infection regulates peroxiredoxin-5 protein expression to facilitate intracellular survival by reducing the production of nitric oxide and reactive oxygen species. *Biochemical and Biophysical Research Communications*, *516*(1), 82–88. https://doi.org/10.1016/J.BBRC.2019.06.026

Hu, H., Tian, M., Li, P., Guan, X., Lian, Z., Yin, Y., Shi, W., Ding, C., & Yu, S. (2020a). Brucella Infection Regulates Thioredoxin-Interacting Protein Expression to Facilitate Intracellular Survival by Reducing the Production of Nitric Oxide and Reactive Oxygen Species . *The Journal of*

Immunology, *204*(3), 632–643. https://doi.org/10.4049/JIMMUNOL.1801550/-/DCSUPPLEMENTAL

Hu, H., Tian, M., Li, P., Guan, X., Lian, Z., Yin, Y., Shi, W., Ding, C., & Yu, S. (2020b). Brucella Infection Regulates Thioredoxin-Interacting Protein Expression to Facilitate Intracellular Survival by Reducing the Production of Nitric Oxide and Reactive Oxygen Species. *Journal of Immunology (Baltimore, Md. : 1950)*, *204*(3), 632–643. https://doi.org/10.4049/JIMMUNOL.1801550

J, P.-C., S, M., RG, P., G, van der G., A, S.-L., I, L.-G., E, M., & JP, G. (1998). Brucella abortus transits through the autophagic pathway and replicates in the endoplasmic reticulum of nonprofessional phagocytes. *Infection and Immunity*, *66*(12), 5711–5724. https://doi.org/10.1128/IAI.66.12.5711-5724.1998

Kämpfer, P., Wohlgemuth, S., & Scholz, H. (2013). The family Brucellaceae. *The Prokaryotes: Alphaproteobacteria and Betaproteobacteria*, 155–178. https://doi.org/10.1007/978-3-642-30197-1_299

Kang, Y.-X., Li, X.-M., Piao, D.-R., Tian, G.-Z., Jiang, H., Jia, E.-H., Lin, L., Cui, B.-Y., Chang, Y.-F., Guo, X.-K., & Zhu, Y.-Z. (2015). Typing Discrepancy Between Phenotypic and Molecular Characterization Revealing an Emerging Biovar 9 Variant of Smooth Phage-Resistant B. abortus Strain 8416 in China. *Frontiers in Microbiology*, *0*(DEC), 1375. https://doi.org/10.3389/FMICB.2015.01375

Kim, S. H., Kwon, D. Y., Kwak, J. H., Lee, S., Lee, Y. H., Yun, J., Son, T. G., & Jung, Y. S. (2018). Tunicamycin-Induced ER Stress is Accompanied with Oxidative Stress via Abrogation of Sulfur Amino Acids Metabolism in the Liver. *International Journal of Molecular Sciences 2018, Vol. 19, Page 4114*, *19*(12), 4114. https://doi.org/10.3390/IJMS19124114

Kim, S., Watarai, M., Suzuki, H., Makino, S. I., Kodama, T., & Shirahata, T. (2004). Lipid raft microdomains mediate class A scavenger receptor-dependent infection of Brucella abortus. *Microbial Pathogenesis*, *37*(1), 11–19. https://doi.org/10.1016/J.MICPATH.2004.04.002

Knight, M., & Stanley, S. (2019). HIF-1α as a central mediator of cellular resistance to intracellular pathogens. *Current Opinion in Immunology*, *60*, 111–116. https://doi.org/10.1016/J.COI.2019.05.005

Koh, M. Y., Spivak-Kroizman, T., Venturini, S., Welsh, S., Williams, R. R., Kirkpatrick, D. L., & Powis, G. (2008). Molecular mechanisms for the activity of PX-478, an antitumor inhibitor of the hypoxia-inducible factor-1α. *Molecular Cancer Therapeutics*, *7*(1), 90–100. https://doi.org/10.1158/1535-7163.MCT-07-0463

Koirala, S., Guo, Q., Kalia, R., Bui, H. T., Eckert, D. M., Frost, A., & Shaw, J. M. (2013a). Interchangeable adaptors regulate mitochondrial dynamin assembly for membrane scission. *Proceedings of the National Academy of Sciences of the United States of America*, *110*(15). https://doi.org/10.1073/PNAS.1300855110/-/DCSUPPLEMENTAL/PNAS.201300855SI.PDF

Koirala, S., Guo, Q., Kalia, R., Bui, H. T., Eckert, D. M., Frost, A., & Shaw, J. M. (2013b). Interchangeable adaptors regulate mitochondrial dynamin assembly for membrane scission. *Proceedings of the National Academy of Sciences of the United States of America*, *110*(15). https://doi.org/10.1073/PNAS.1300855110/-/DCSUPPLEMENTAL/PNAS.201300855SI.PDF

Kokame, K., Agarwal, K. L., Kato, H., & Miyata, T. (2000). Herp, a New Ubiquitin-like Membrane Protein Induced by Endoplasmic Reticulum Stress. *Journal of Biological Chemistry*, *275*(42), 32846–32853. https://doi.org/10.1074/JBC.M002063200

Kreymerman, A., Buickians, D. N., Nahmou, M. M., Tran, T., Galvao, J., Wang, Y., Sun, N., Bazik, L., Huynh, S. K., Cho, I. J., Boczek, T., Chang, K. C., Kunzevitzky, N. J., & Goldberg, J. L. (2019).

MTP18 is a Novel Regulator of Mitochondrial Fission in CNS Neuron Development, Axonal Growth, and Injury Responses. *Scientific Reports*, *9*(1). https://doi.org/10.1038/S41598-019-46956-5

Kroemer, G., Mariño, G., & Levine, B. (2010). Autophagy and the integrated stress response. *Molecular Cell*, *40*(2), 280–293. https://doi.org/10.1016/J.MOLCEL.2010.09.023

Kühlbrandt, W. (2015). Structure and function of mitochondrial membrane protein complexes. *BMC Biology 2015 13:1*, *13*(1), 1–11. https://doi.org/10.1186/S12915-015-0201-X

Kumar, H., Kawai, T., & Akira, S. (2009). Toll-like receptors and innate immunity. *Biochemical and Biophysical Research Communications*, *388*(4), 621–625. https://doi.org/10.1016/J.BBRC.2009.08.062

Kummer, E., & Ban, N. (2021). Mechanisms and regulation of protein synthesis in mitochondria. *Nature Reviews Molecular Cell Biology*, *22*(5), 307–325. https://doi.org/10.1038/s41580-021-00332-2

Landes, T., Leroy, I., Bertholet, A., Diot, A., Khosrobakhsh, F., Daloyau, M., Davezac, N., Miquel, M. C., Courilleau, D., Guillou, E., Olichon, A., Lenaers, G., Arnauné-Pelloquin, L., Emorine, L. J., & Belenguer, P. (2010). OPA1 (dys)functions. *Seminars in Cell & Developmental Biology*, *21*(6), 593–598. https://doi.org/10.1016/J.SEMCDB.2009.12.012

Landry, J. J. M., Pyl, P. T., Rausch, T., Zichner, T., Tekkedil, M. M., Stütz, A. M., Jauch, A., Aiyar, R. S., Pau, G., Delhomme, N., Gagneur, J., Korbel, J. O., Huber, W., & Steinmetz, L. M. (2013). The genomic and transcriptomic landscape of a hela cell line. *G3: Genes, Genomes, Genetics*, *3*(8), 1213–1224. https://doi.org/10.1534/G3.113.005777/-/DC1/FIGURES6.PDF

Lawrie, C. M., Sulistijo, E. S., & MacKenzie, K. R. (2010). Intermonomer hydrogen bonds enhance gxxxg-driven dimerization of the BNIP3 transmembrane domain: Roles for sequence context in helix-helix association in membranes. *Journal of Molecular Biology*, *396*(4), 924–936. https://doi.org/10.1016/j.jmb.2009.12.023

Lebeau, J., Saunders, J. M., Moraes, V. W. R., Madhavan, A., Madrazo, N., Anthony, M. C., & Wiseman, R. L. (2018). The PERK Arm of the Unfolded Protein Response Regulates Mitochondrial Morphology during Acute Endoplasmic Reticulum Stress. *Cell Reports*, *22*(11), 2827. https://doi.org/10.1016/J.CELREP.2018.02.055

Lee, J. J., Kim, D. H., Kim, D. G., Lee, H. J., Min, W., Rhee, M. H., Cho, J. Y., Watarai, M., & Kim, S. (2013). Toll-like receptor 4-linked janus kinase 2 signaling contributes to Internalization of Brucella abortus by macrophages. *Infection and Immunity*, *81*(7), 2448–2458. https://doi.org/10.1128/IAI.00403-13/SUPPL_FILE/ZII999090199SO3.PDF

Lee, K., & Kim, H. M. (2011). A novel approach to cancer therapy using PX-478 as a HIF-1α inhibitor. *Archives of Pharmacal Research*, *34*(10), 1583–1585. https://doi.org/10.1007/S12272-011-1021-3

Leitman, J., Shenkman, M., Gofmanb, Y., Shtern, N. O., Ben-Tal, N., Hendershot, L. M., & Lederkremer, G. Z. (2014). Herp coordinates compartmentalization and recruitment of HRD1 and misfolded proteins for ERAD. *Molecular Biology of the Cell*, *25*(7), 1050–1060. https://doi.org/10.1091/MBC.E13-06-0350

Li, D., Cai, Y., Teng, D., Li, W., Tang, Y., & Liu, G. (2019). Computational insights into the interaction mechanisms of estrogen-related receptor alpha with endogenous ligand cholesterol. *Chemical Biology & Drug Design*, *94*(1), 1316–1329. https://doi.org/10.1111/CBDD.13506

Li, Q., Xie, Y., Cui, Z., Huang, H., Yang, C., Yuan, B., Shen, P., & Shi, C. (2021). Activation of hypoxia-inducible factor 1 (Hif-1) enhanced bactericidal effects of macrophages to

Mycobacterium tuberculosis. *Tuberculosis*, *126*, 102044. https://doi.org/10.1016/J.TUBE.2020.102044

Lim, K. H., & Staudt, L. M. (2013). Toll-Like Receptor Signaling. *Cold Spring Harbor Perspectives in Biology*, *5*(1), a011247. https://doi.org/10.1101/CSHPERSPECT.A011247

Lin, Q., Li, S., Jiang, N., Jin, H., Shao, X., Zhu, X., Wu, J., Zhang, M., Zhang, Z., Shen, J., Zhou, W., Gu, L., Lu, R., & Ni, Z. (2020). Inhibiting NLRP3 inflammasome attenuates apoptosis in contrast-induced acute kidney injury through the upregulation of HIF1A and BNIP3-mediated mitophagy. *Autophagy*, *00*(00), 1–16. https://doi.org/10.1080/15548627.2020.1848971

Liu, L., Feng, D., Chen, G., Chen, M., Zheng, Q., Song, P., Ma, Q., Zhu, C., Wang, R., Qi, W., Huang, L., Xue, P., Li, B., Wang, X., Jin, H., Wang, J., Yang, F., Liu, P., Zhu, Y., … Chen, Q. (2012). Mitochondrial outer-membrane protein FUNDC1 mediates hypoxia-induced mitophagy in mammalian cells. *Nature Cell Biology*, *14*(2), 177–185. https://doi.org/10.1038/ncb2422

Liu, Z., Reba, S., Chen, W. D., Porwal, S. K., Boom, W. H., Petersen, R. B., Rojas, R., Viswanathan, R., & Devireddy, L. (2014). Regulation of mammalian siderophore 2,5-DHBA in the innate immune response to infection. *The Journal of Experimental Medicine*, *211*(6), 1197–1213. https://doi.org/10.1084/JEM.20132629

Lobet, E., Willemart, K., Ninane, N., Demazy, C., Sedzicki, J., Lelubre, C., de Bolle, X., Renard, P., Raes, M., Dehio, C., Letesson, J. J., & Arnould, T. (2018). Mitochondrial fragmentation affects neither the sensitivity to TNFα-induced apoptosis of Brucella-infected cells nor the intracellular replication of the bacteria. *Scientific Reports*, *8*(1), 1–17. https://doi.org/10.1038/s41598-018-23483-3

Lopez, J., & Tait, S. W. G. (2015). Mitochondrial apoptosis: killing cancer using the enemy within. *British Journal of Cancer 2015 112:6*, *112*(6), 957–962. https://doi.org/10.1038/bjc.2015.85

Luizet, J. B., Raymond, J., Lacerda, T. L. S., Barbieux, E., Kambarev, S., Bonici, M., Lembo, F., Willemart, K., Borg, J. P., Celli, J., Gérard, F. C. A., Muraille, E., Gorvel, J. P., & Salcedo, S. P. (2021). The Brucella effector BspL targets the ER-associated degradation (ERAD) pathway and delays bacterial egress from infected cells. *Proceedings of the National Academy of Sciences of the United States of America*, *118*(32). https://doi.org/10.1073/PNAS.2105324118/-/DCSUPPLEMENTAL

Luz, A. L., Rooney, J. P., Kubik, L. L., Gonzalez, C. P., Song, D. H., & Meyer, J. N. (2015). Mitochondrial Morphology and Fundamental Parameters of the Mitochondrial Respiratory Chain Are Altered in Caenorhabditis elegans Strains Deficient in Mitochondrial Dynamics and Homeostasis Processes. *PLOS ONE*, *10*(6), e0130940. https://doi.org/10.1371/JOURNAL.PONE.0130940

Mahla, R. S., Kumar, A., Tutill, H. J., Krishnaji, S. T., Sathyamoorthy, B., Noursadeghi, M., Breuer, J., Pandey, A. K., & Kumar, H. (2021). NIX-mediated mitophagy regulate metabolic reprogramming in phagocytic cells during mycobacterial infection. *Tuberculosis*, *126*, 102046. https://doi.org/10.1016/J.TUBE.2020.102046

Marchesini, M. I., Herrmann, C. K., Salcedo, S. P., Gorvel, J. P., & Comerci, D. J. (2011). In search of Brucella abortus type IV secretion substrates: screening and identification of four proteins translocated into host cells through VirB system. *Cellular Microbiology*, *13*(8), 1261–1274. https://doi.org/10.1111/J.1462-5822.2011.01618.X

Marim, F. M., Franco, M. M. C., Gomes, M. T. R., Miraglia, M. C., Giambartolomei, G. H., & Oliveira, S. C. (2017a). The role of NLRP3 and AIM2 in inflammasome activation during Brucella abortus infection. *Seminars in Immunopathology*, *39*(2), 215–223. https://doi.org/10.1007/S00281-016-0581-1/FIGURES/2

Marim, F. M., Franco, M. M. C., Gomes, M. T. R., Miraglia, M. C., Giambartolomei, G. H., & Oliveira, S. C. (2017b). The role of NLRP3 and AIM2 in inflammasome activation during Brucella abortus infection. *Seminars in Immunopathology*, *39*(2), 215–223. https://doi.org/10.1007/S00281-016-0581-1/FIGURES/2

Marinković, M., Šprung, M., & Novak, I. (2021). Dimerization of mitophagy receptor BNIP3L/NIX is essential for recruitment of autophagic machinery. *Autophagy*, *17*(5), 1232–1243. https://doi.org/10.1080/15548627.2020.1755120

Martínez-Reyes, I., & Chandel, N. S. (2020). Mitochondrial TCA cycle metabolites control physiology and disease. *Nature Communications 2020 11:1*, *11*(1), 1–11. https://doi.org/10.1038/s41467-019-13668-3

Masoud, G. N., & Li, W. (2015). HIF-1α pathway: Role, regulation and intervention for cancer therapy. *Acta Pharmaceutica Sinica B*, *5*(5), 378–389. https://doi.org/10.1016/j.apsb.2015.05.007

Mellado, M., Garcia, A. M., Arellano-Reynoso, B., Diaz-Aparicio, E., & Garcia, J. E. (2013). Milk yield and reproductive performance of brucellosis-vaccinated but seropositive Holstein cows. *Tropical Animal Health and Production 2013 46:2*, *46*(2), 391–397. https://doi.org/10.1007/S11250-013-0502-4

Miller, C. N., Smith, E. P., Cundiff, J. A., Knodler, L. A., Bailey Blackburn, J., Lupashin, V., & Celli, J. (2017). A Brucella Type IV effector targets the COG tethering complex to remodel host secretory traffic and promote intracellular replication. *Cell Host & Microbe*, *22*(3), 317. https://doi.org/10.1016/J.CHOM.2017.07.017

Mimouna, S., Bazin, M., Mograbi, B., Darfeuille-Michaud, A., Brest, P., Hofman, P., & Vouret-Craviari, V. (2014). HIF1A regulates xenophagic degradation of adherent and invasive Escherichia coli (AIEC). *Autophagy*, *10*(12), 2333–2345. https://doi.org/10.4161/15548627.2014.984275/SUPPL_FILE/KAUP_A_984275_SM3896.ZIP

Moreno, E., & Barquero-Calvo, E. (2020). The Role of Neutrophils in Brucellosis. *Microbiology and Molecular Biology Reviews*, *84*(4), 1–34. https://doi.org/10.1128/mmbr.00048-20

Mu, F.-T., Callaghan, J. M., Steele-Mortimer, O., Stenmark, H., Parton, R. G., Campbell, P. L., McCluskey, J., Yeo, J.-P., Tock, E. P. C., & Toh, B.-H. (1995). EEA1, an Early Endosome-Associated Protein.: EEA1 IS A CONSERVED α-HELICAL PERIPHERAL MEMBRANE PROTEIN FLANKED BY CYSTEINE “FINGERS” AND CONTAINS A CALMODULIN-BINDING IQ MOTIF ∗. *Journal of Biological Chemistry*, *270*(22), 13503–13511. https://doi.org/10.1074/JBC.270.22.13503

Muñoz-Sánchez, J., & Chánez-Cárdenas, M. E. (2019). The use of cobalt chloride as a chemical hypoxia model. In *Journal of Applied Toxicology* (Vol. 39, Issue 4, pp. 556–570). John Wiley and Sons Ltd. https://doi.org/10.1002/jat.3749

Muraille, E., Leo, O., & Moser, M. (2014). Th1/Th2 Paradigm Extended: Macrophage Polarization as an Unappreciated Pathogen-Driven Escape Mechanism? *Frontiers in Immunology*, *0*, 603. https://doi.org/10.3389/FIMMU.2014.00603

Murray, P. J. (2017). Macrophage Polarization. *Http://Dx.Doi.Org/10.1146/Annurev-Physiol-022516-034339*, *79*, 541–566. https://doi.org/10.1146/ANNUREV-PHYSIOL-022516-034339

Myeni, S., Child, R., Ng, T. W., Kupko, J. J., Wehrly, T. D., Porcella, S. F., Knodler, L. A., & Celli, J. (2013). Brucella Modulates Secretory Trafficking via Multiple Type IV Secretion Effector Proteins. *PLOS Pathogens*, *9*(8), e1003556. https://doi.org/10.1371/JOURNAL.PPAT.1003556

Naeem, S., Qi, Y., Tian, Y., & Zhang, Y. (2020). NIX compensates lost role of parkin in cd-induced mitophagy in HeLa cells through phosphorylation. *Toxicology Letters*, *326*, 1–10. https://doi.org/10.1016/j.toxlet.2020.03.001

Nagano, M., Toshima, J. Y., Siekhaus, D. E., & Toshima, J. (2019). Rab5-mediated endosome formation is regulated at the trans-Golgi network. *Communications Biology 2019 2:1*, *2*(1), 1–12. https://doi.org/10.1038/s42003-019-0670-5

Nandi, D., Farid, N. S. S., Karuppiah, H. A. R., & Kulkarni, A. (2021). Imaging Approaches to Monitor Inflammasome Activation. *Journal of Molecular Biology*, 167251. https://doi.org/10.1016/J.JMB.2021.167251

Narendra, D., Tanaka, A., Suen, D. F., & Youle, R. J. (2008). Parkin is recruited selectively to impaired mitochondria and promotes their autophagy. *Journal of Cell Biology*, *183*(5), 795–803. https://doi.org/10.1083/jcb.200809125

Neta, A. V. C., Mol, J. P. S., Xavier, M. N., Paixão, T. A., Lage, A. P., & Santos, R. L. (2010). Pathogenesis of bovine brucellosis. *The Veterinary Journal*, *184*(2), 146–155. https://doi.org/10.1016/J.TVJL.2009.04.010

Neta, A. V. C., Stynen, A. P. R., Paixão, T. A., Miranda, K. L., Silva, F. L., Roux, C. M., Tsolis, R. M., Everts, R. E., Lewin, H. A., Adams, L. G., Carvalho, A. F., Lage, A. P., & Santos, R. L. (2008). Modulation of the Bovine Trophoblastic Innate Immune Response by Brucella abortus. *Infection and Immunity*, *76*(5), 1897. https://doi.org/10.1128/IAI.01554-07

Neupert, W., & Herrmann, J. M. (2007). Translocation of proteins into mitochondria. *Annual Review of Biochemistry*, *76*, 723–749. https://doi.org/10.1146/ANNUREV.BIOCHEM.76.052705.163409

Ney, P. A. (2015). Mitochondrial autophagy: Origins, significance, and role of BNIP3 and NIX. In *Biochimica et Biophysica Acta - Molecular Cell Research* (Vol. 1853, Issue 10, pp. 2775–2783). Elsevier. https://doi.org/10.1016/j.bbamcr.2015.02.022

Nkengfac, B., Pouyez, J., Bauwens, E., Vandenhaute, J., Letesson, J. J., Wouters, J., & de Bolle, X. (2012). Structural analysis of Brucella abortus RicA substitutions that do not impair interaction with human Rab2 GTPase. *BMC Biochemistry*, *13*(1), 16. https://doi.org/10.1186/1471-2091-13-16

Novak, I., Kirkin, V., McEwan, D. G., Zhang, J., Wild, P., Rozenknop, A., Rogov, V., Löhr, F., Popovic, D., Occhipinti, A., Reichert, A. S., Terzic, J., Dötsch, V., Ney, P. A., & Dikic, I. (2010). Nix is a selective autophagy receptor for mitochondrial clearance. *EMBO Reports*, *11*(1), 45–51. https://doi.org/10.1038/EMBOR.2009.256

O'Callaghan, D. (2020). Human brucellosis: recent advances and future challenges. *Infectious Diseases of Poverty 2020 9:1*, *9*(1), 1–2. https://doi.org/10.1186/S40249-020-00715-1

Ohba, Y., MacVicar, T., & Langer, T. (2020). Regulation of mitochondrial plasticity by the i-AAA protease YME1L. *Biological Chemistry*, *401*(6–7), 877–890. https://doi.org/10.1515/HSZ-2020-0120/PDF

Pei, J., Ding, X., Fan, Y., Rice-Ficht, A., & Ficht, T. A. (2012). Toll-like receptors are critical for clearance of Brucella and play different roles in development of adaptive immunity following aerosol challenge in mice. *Frontiers in Cellular and Infection Microbiology*, *2*, 115. https://doi.org/10.3389/FCIMB.2012.00115/BIBTEX

Pfanner, N., Warscheid, B., & Wiedemann, N. (2019). Mitochondrial proteins: from biogenesis to functional networks. *Nature Reviews Molecular Cell Biology 2018 20:5*, *20*(5), 267–284. https://doi.org/10.1038/s41580-018-0092-0

Pigino, G., Morfini, G. A., & Brady, S. T. (2012). Intracellular Trafficking. *Basic Neurochemistry*, 119–145. https://doi.org/10.1016/B978-0-12-374947-5.00007-9

Pitt, A. S., & Buchanan, S. K. (2021). A Biochemical and Structural Understanding of TOM Complex Interactions and Implications for Human Health and Disease. *Cells*, *10*(5). https://doi.org/10.3390/CELLS10051164

Proikas-Cezanne, T., Takacs, Z., Dönnes, P., & Kohlbacher, O. (2015). WIPI proteins: Essential PtdIns3P effectors at the nascent autophagosome. *Journal of Cell Science*, *128*(2), 207–217. https://doi.org/10.1242/JCS.146258/259897/AM/WIPI-PROTEINS-ESSENTIAL-PTDINS3P-EFFECTORS-AT-THE

Schaible, B., McClean, S., Selfridge, A., Broquet, A., Asehnoune, K., Taylor, C. T., & Schaffer, K. (2013). Hypoxia Modulates Infection of Epithelial Cells by Pseudomonas aeruginosa. *PLOS ONE*, *8*(2), e56491. https://doi.org/10.1371/JOURNAL.PONE.0056491

Schuerwegh, A. J., Stevens, W. J., Bridts, C. H., & de Clerck, L. S. (2001). Evaluation of monensin and brefeldin A for flow cytometric determination of interleukin-1 beta, interleukin-6, and tumor necrosis factor-alpha in monocytes. *Cytometry*, *46*(3), 172–176. https://doi.org/10.1002/CYTO.1102

Schweers, R. L., Zhang, J., Randall, M. S., Loyd, M. R., Li, W., Dorsey, F. C., Kundu, M., Opferman, J. T., Cleveland, J. L., Miller, J. L., & Ney, P. A. (2007). NIX is required for programmed mitochondrial clearance during reticulocyte maturation. *Proceedings of the National Academy of Sciences of the United States of America*, *104*(49), 19500–19505. https://doi.org/10.1073/pnas.0708818104

Shadel, G. S., & Horvath, T. L. (2015). Mitochondrial ROS Signaling in Organismal Homeostasis. *Cell*, *163*(3), 560–569. https://doi.org/10.1016/J.CELL.2015.10.001

Shirane-Kitsuji, M., & Nakayama, K. I. (2014). Mitochondria: FKBP38 and mitochondrial degradation. *The International Journal of Biochemistry & Cell Biology*, *51*(1), 19–22. https://doi.org/10.1016/J.BIOCEL.2014.03.007

Shires, S. E., Quiles, J. M., Najor, R. H., Leon, L. J., Cortez, M. Q., Lampert, M. A., Mark, A., & Gustafsson, Å. B. (2020). Nuclear Parkin Activates the ERRα Transcriptional Program and Drives Widespread Changes in Gene Expression Following Hypoxia. *Scientific Reports*, *10*(1), 1–15. https://doi.org/10.1038/s41598-020-65438-7

Simpson, C. L., Tokito, M. K., Uppala, R., Sarkar, M. K., Gudjonsson, J. E., & Holzbaur, E. L. F. (2021a). NIX initiates mitochondrial fragmentation via DRP1 to drive epidermal differentiation. *Cell Reports*, *34*(5), 108689. https://doi.org/10.1016/J.CELREP.2021.108689/ATTACHMENT/36CFB28F-7D9D-4A5E-BC88-667F5C4E0BB3/MMC1.PDF

Simpson, C. L., Tokito, M. K., Uppala, R., Sarkar, M. K., Gudjonsson, J. E., & Holzbaur, E. L. F. (2021b). NIX initiates mitochondrial fragmentation via DRP1 to drive epidermal differentiation. *Cell Reports*, *34*(5). https://doi.org/10.1016/J.CELREP.2021.108689

Sinha, S., & Aradhyam, G. K. (2019). Identification and characterization of signal peptide of Mitofusin1 (Mfn1). *Biochemical and Biophysical Research Communications*, *509*(3), 707–712. https://doi.org/10.1016/J.BBRC.2018.12.165

Sonoda, J., Laganière, J., Mehl, I. R., Barish, G. D., Chong, L. W., Li, X., Scheffler, I. E., Mock, D. C., Bataille, A. R., Robert, F., Lee, C. H., Giguère, V., & Evans, R. M. (2007). Nuclear receptor ERRα and coactivator PGC-1β are effectors of IFN-γ-induced host defense. *Genes & Development*, *21*(15), 1909. https://doi.org/10.1101/GAD.1553007

Starr, T., Ng, T. W., Wehrly, T. D., Knodler, L. A., & Celli, J. (2008). Brucella Intracellular Replication Requires Trafficking Through the Late Endosomal/Lysosomal Compartment. *Traffic*, *9*(5), 678–694. https://doi.org/10.1111/J.1600-0854.2008.00718.X

Stranahan, L. W., & Arenas-Gamboa, A. M. (2021). When the Going Gets Rough: The Significance of Brucella Lipopolysaccharide Phenotype in Host–Pathogen Interactions. *Frontiers in Microbiology*, *0*, 1956. https://doi.org/10.3389/FMICB.2021.713157

Suárez-Esquivel, M., Chaves-Olarte, E., Moreno, E., & Guzmán-Verri, C. (2020). Brucella Genomics: Macro and Micro Evolution. *International Journal of Molecular Sciences 2020, Vol. 21, Page 7749*, *21*(20), 7749. https://doi.org/10.3390/IJMS21207749

Sulistijo, E. S., Jaszewski, T. M., & MacKenzie, K. R. (2003a). Sequence specific Dimerization of the Transmembrane Domain of the "BH3-only" Protein BNIP3 in Membranes and Detergent. *Journal of Biological Chemistry*, *278*(51), 51950–51956. https://doi.org/10.1074/jbc.M308429200

Sulistijo, E. S., Jaszewski, T. M., & MacKenzie, K. R. (2003b). Sequence-specific dimerization of the transmembrane domain of the "BH3-only" protein BNIP3 in membranes and detergent. *The Journal of Biological Chemistry*, *278*(51), 51950–51956. https://doi.org/10.1074/JBC.M308429200

Sulistijo, E. S., & MacKenzie, K. R. (2006). Sequence Dependence of BNIP3 Transmembrane Domain Dimerization Implicates Side-chain Hydrogen Bonding and a Tandem GxxxG Motif in Specific Helix-Helix Interactions. *Journal of Molecular Biology*, *364*(5), 974–990.

Sulkshane, P., Ram, J., Thakur, A., Reis, N., Kleifeld, O., & Glickman, M. H. (2021). Ubiquitination and receptor-mediated mitophagy converge to eliminate oxidation-damaged mitochondria during hypoxia. *Redox Biology*, *45*, 102047. https://doi.org/10.1016/J.REDOX.2021.102047

Sztal, T. E., & Stainier, Y. R. (2020). Transcriptional adaptation: A mechanism underlying genetic robustness. *Development (Cambridge)*, *147*(15). https://doi.org/10.1242/DEV.186452/143912

Tiku, V., Tan, M. W., & Dikic, I. (2020). Mitochondrial Functions in Infection and Immunity. *Trends in Cell Biology*, *30*(4), 263–275. https://doi.org/10.1016/j.tcb.2020.01.006

Tilokani, L., Nagashima, S., Paupe, V., & Prudent, J. (2018). Mitochondrial dynamics: overview of molecular mechanisms. *Essays in Biochemistry*, *62*(3), 341–360. https://doi.org/10.1042/EBC20170104

van der Bliek, A. M., Sedensky, M. M., & Morgan, P. G. (2017). Cell Biology of the Mitochondrion. *Genetics*, *207*(3), 843–871. https://doi.org/10.1534/GENETICS.117.300262

Velásquez, L. N., Delpino, M. V., Ibañez, A. E., Coria, L. M., Miraglia, M. C., Scian, R., Cassataro, J., Giambartolomei, G. H., & Barrionuevo, P. (2012). Brucella abortus induces apoptosis of human T lymphocytes. *Microbes and Infection*, *14*(7–8), 639–650. https://doi.org/10.1016/J.MICINF.2012.02.004

Wai, T., & Langer, T. (2016a). Mitochondrial Dynamics and Metabolic Regulation. *Trends in Endocrinology & Metabolism*, *27*(2), 105–117. https://doi.org/10.1016/J.TEM.2015.12.001

Wai, T., & Langer, T. (2016b). Mitochondrial Dynamics and Metabolic Regulation. *Trends in Endocrinology & Metabolism*, *27*(2), 105–117. https://doi.org/10.1016/J.TEM.2015.12.001

Wang, L., Deng, A., Zhang, Y., Liu, S., Liang, Y., Bai, H., Cui, D., Qiu, Q., Shang, X., Yang, Z., He, X., & Wen, T. (2018). Efficient CRISPR-Cas9 mediated multiplex genome editing in yeasts. *Biotechnology for Biofuels*, *11*(1), 1–16. https://doi.org/10.1186/S13068-018-1271-0/FIGURES/6

Wang, T., Liu, H., Lian, G., Zhang, S. Y., Wang, X., & Jiang, C. (2017a). HIF1 α -Induced Glycolysis Metabolism Is Essential to the Activation of Inflammatory Macrophages. *Mediators of Inflammation*, *2017*. https://doi.org/10.1155/2017/9029327

Wang, T., Liu, H., Lian, G., Zhang, S. Y., Wang, X., & Jiang, C. (2017b). HIF1 α -Induced Glycolysis Metabolism Is Essential to the Activation of Inflammatory Macrophages. *Mediators of Inflammation*, *2017*. https://doi.org/10.1155/2017/9029327

Wei, P., Cui, G., Lu, Q., Yang, L., Guan, Z., Sun, W., Zhao, Y., Wang, S., & Peng, Q. (2015). A20 promotes Brucella intracellular growth via inhibition of macrophage cell death and activation. *Veterinary Microbiology*, *175*(1), 50–57. https://doi.org/10.1016/J.VETMIC.2014.11.006

Weidemann, A., & Johnson, R. S. (2008). Biology of HIF-1α. *Cell Death and Differentiation*, *15*(4), 621–627. https://doi.org/10.1038/cdd.2008.12

Weinberg, S. E., Sena, L. A., & Chandel, N. S. (2015). Mitochondria in the regulation of innate and adaptive immunity. In *Immunity* (Vol. 42, Issue 3, pp. 406–417). Cell Press. https://doi.org/10.1016/j.immuni.2015.02.002

West, A. P., Brodsky, I. E., Rahner, C., Woo, D. K., Erdjument-Bromage, H., Tempst, P., Walsh, M. C., Choi, Y., Shadel, G. S., & Ghosh, S. (2011). TLR signalling augments macrophage bactericidal activity through mitochondrial ROS. *Nature*, *472*(7344), 476–480. https://doi.org/10.1038/NATURE09973

West, A. P., Shadel, G. S., & Ghosh, S. (2011). Mitochondria in innate immune responses. *Nature Reviews. Immunology*, *11*(6), 389–402. https://doi.org/10.1038/NRI2975

Wong, Y. C., Ysselstein, D., & Krainc, D. (2018). Mitochondria–lysosome contacts regulate mitochondrial fission via RAB7 GTP hydrolysis. *Nature 2018 554:7692*, *554*(7692), 382–386. https://doi.org/10.1038/nature25486

Wu, J., Chen, S., Liu, H., Zhang, Z., Ni, Z., Chen, J., Yang, Z., Nie, Y., & Fan, D. (2018). Tunicamycin specifically aggravates ER stress and overcomes chemoresistance in multidrug-resistant gastric cancer cells by inhibiting N-glycosylation. *Journal of Experimental and Clinical Cancer Research*, *37*(1), 1–12. https://doi.org/10.1186/S13046-018-0935-8/FIGURES/6

Xavier, M. N., Winter, M. G., Spees, A. M., den Hartigh, A. B., Nguyen, K., Roux, C. M., Silva, T. M. A., Atluri, V. L., Kerrinnes, T., Keestra, A. M., Monack, D. M., Luciw, P. A., Eigenheer, R. A., Bäumler, A. J., Santos, R. L., & Tsolis, R. M. (2013). PPARγ-Mediated Increase in Glucose Availability Sustains Chronic Brucella abortus Infection in Alternatively Activated Macrophages. *Cell Host & Microbe*, *14*(2), 159–170. https://doi.org/10.1016/J.CHOM.2013.07.009

Xu, Y., Shen, J., & Ran, Z. (2019). Emerging views of mitophagy in immunity and autoimmune diseases. *Https://Doi.Org/10.1080/15548627.2019.1603547*, *16*(1), 3–17. https://doi.org/10.1080/15548627.2019.1603547

Y, T., K, I., M, K., A, U., D, N., S, H.-O., R, K., F, K., & M, M. (2015). Yip1A, a novel host factor for the activation of the IRE1 pathway of the unfolded protein response during Brucella infection. *PLoS Pathogens*, *11*(3), 1–28. https://doi.org/10.1371/JOURNAL.PPAT.1004747

Yamashita, S. I., Jin, X., Furukawa, K., Hamasaki, M., Nezu, A., Otera, H., Saigusa, T., Yoshimori, T., Sakai, Y., Mihara, K., & Kanki, T. (2016). Mitochondrial division occurs concurrently with autophagosome formation but independently of Drp1 during mitophagy. *Journal of Cell Biology*, *215*(5), 649–665. https://doi.org/10.1083/JCB.201605093

Yan, C., Duanmu, X., Zeng, L., Liu, B., & Song, Z. (2019). Mitochondrial DNA: Distribution, Mutations, and Elimination. *Cells 2019, Vol. 8, Page 379*, *8*(4), 379. https://doi.org/10.3390/CELLS8040379

Yoo, S. M., & Jung, Y. K. (2018a). A Molecular Approach to Mitophagy and Mitochondrial Dynamics. *Molecules and Cells*, *41*(1), 18–26. https://doi.org/10.14348/MOLCELLS.2018.2277

Yoo, S. M., & Jung, Y. K. (2018b). A Molecular Approach to Mitophagy and Mitochondrial Dynamics. *Moleucles and Cells*, *41*(1), 18–26. https://doi.org/10.14348/MOLCELLS.2018.2277

Yoo, S. M., Yamashita, S. ichi, Kim, H., Na, D. H., Lee, H., Kim, S. J., Cho, D. H., Kanki, T., & Jung, Y. K. (2020). FKBP8 LIRL-dependent mitochondrial fragmentation facilitates mitophagy under stress conditions. *The FASEB Journal*, *34*(2), 2944–2957. https://doi.org/10.1096/FJ.201901735R

Youle, R. J., Bliek, A. M. van der, Complementation, F. P., Mitochondria, B. D., Fusion, M., & Proteins, F. (2012). *REVIEW Mitochondrial Fission, Fusion, and Stress*. *337*(August), 1062–1066.

Youle, R. J., & Narendra, D. P. (2011). Mechanisms of mitophagy. *Nature Reviews Molecular Cell Biology*, *12*(1), 9–14. https://doi.org/10.1038/nrm3028

Yu, R., Jin, S., Lendahl, U., Nistér, M., & Zhao, J. (2019). Human Fis1 regulates mitochondrial dynamics through inhibition of the fusion machinery. *The EMBO Journal*, *38*(8). https://doi.org/10.15252/EMBJ.201899748

Zhang, J., & Ney, P. A. (2009). Role of BNIP3 and NIX in cell death, autophagy, and mitophagy. *Cell Death and Differentiation*, *16*(7), 939–946. https://doi.org/10.1038/cdd.2009.16

Zhang, Y., Liu, D., Hu, H., Zhang, P., Xie, R., & Cui, W. (2019). HIF-1α/BNIP3 signaling pathway-induced-autophagy plays protective role during myocardial ischemia-reperfusion injury. *Biomedicine & Pharmacotherapy = Biomedecine & Pharmacotherapie*, *120*. https://doi.org/10.1016/J.BIOPHA.2019.109464

Zhou, D., Zhi, F. J., Qi, M. Z., Bai, F. R., Zhang, G., Li, J. M., Liu, H., Chen, H. T., Lin, P. F., Tang, K. Q., Liu, W., Jin, Y. P., & Wang, A. H. (2018a). Brucella induces unfolded protein response and inflammatory response via GntR in alveolar macrophages. *Oncotarget*, *9*(4), 5184. https://doi.org/10.18632/ONCOTARGET.23706

Zhou, D., Zhi, F. J., Qi, M. Z., Bai, F. R., Zhang, G., Li, J. M., Liu, H., Chen, H. T., Lin, P. F., Tang, K. Q., Liu, W., Jin, Y. P., & Wang, A. H. (2018b). Brucella induces unfolded protein response and inflammatory response via GntR in alveolar macrophages. *Oncotarget*, *9*(4), 5184. https://doi.org/10.18632/ONCOTARGET.23706

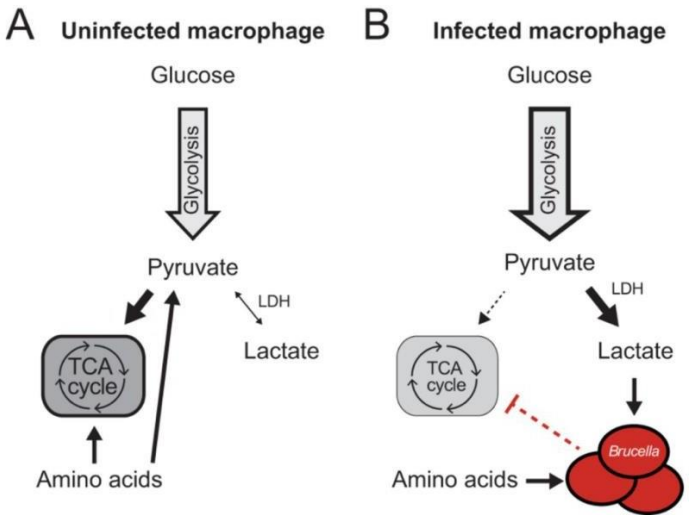

Figure 11: The Warburg shift in host metabolism upon *Brucella* infection (Czyż et al., 2017).
This model suggests that *Brucella*-induced inhibition of tricarboxylic acid cycle (TCA) metabolism prevents the host cell from moving towards amino acid catabolism and shift to lactic acid production.
(A) In uninfected macrophages, glucose is converted to pyruvate via glycolysis and is used, indirectly, by the Krebs cycle as a carbon source (in the form of acetyl-CoA). (B) During infection with *Brucella abortus*, glucose can be converted to pyruvate. Pyruvate is converted to lactate by the lactate dehydrogenase and this metabolite, together with amino acids, are used as a carbon source by the bacteria.

Université de Namur
FACULTE DES SCIENCES
Secrétariat du Département de Biologie
Rue de Bruxelles 61 - 5000 NAMUR
Téléphone: + 32(0)81.72.44.18 - Téléfax: + 32(0)81.72.44.20
E-mail: joelle.jonet@unamur.be - http://www.unamur.be

Study of the putative role of HIF-1alpha and BNIP3L in the biology of mitochondria in *Brucella abortus*-infected cells

MARTIN Lisa

ABSTRACT :

Brucella abortus are facultative intracellular pathogen, causing Brucellosis, known for their interactions and the subversion of multiple organelles in infected host cells, including mitochondria. The mitochondrion is a dynamic organelle that plays a central role in the cell, involving ATP production, cellular immunity, many syntheses and degradation pathways, regulation of calcium homeostasis and the integration of life-or-death signals. These important roles of mitochondria in the regulation of many biological processes also make the mitochondria an important target for pathogens. *B. abortus* is able to corrupt several functions of the mitochondria to its advantage. Indeed, a glycolytic shift, the fragmentation of the mitochondrial population and induction of mitophagy are observed in both myeloid and non-myeloid *B. abortus*-infected cells. More recently, in the host laboratory, a nuclear accumulation of HIF-1α correlated with Parkin translocation have been observed in *Brucella*-infected HeLa cells or macrophages. In addition, at 48 h post-infection (p.i) time, the induction of mitophagy correlates with the expression of the HIF-1α-target gene encoding BNIP3L was demonstrated.

The major aim of the master thesis was therefore to better understand the putative role of these molecular actors/effectors (HIF-1α, Parkin and BNIP3L) in the induction of mitochondrial fragmentation and/or mitophagy in *B. abortus*-infected HeLa and macrophages.

In this work, we observed a decrease in CFU numbers in macrophages in which HIF-1α is stabilised by a chemical hypoxia ($CoCl_2$ treatment) when the stabilisation of the transcription factor occurs prior to or during the early phase of infection. These observations suggest that the entry and/or survival of the bacteria may be disrupted even if the response is not observed for HeLa infected cells. We also show that the translocation of Parkin in the nucleus of *Brucella*-infected cells is not a robust phenotype while a knock-down of BNIP3L expression in *B. abortus*-infected HeLa cells prevent, at least partially, but significantly, the fragmentation of mitochondria observed in *Brucella*-infected cells. A protective effect of BNIP3L expression silencing was also observed on *B. abortus*-induced mitophagy as assessed by a decreased co-localisation between LC3 and TOM20 in *B. abortus*-infected HeLa cells. Finally, we focused on the erUPR response potentially involved in the upregulation of autophagic/mitaphagic pathways. We found that activation of the IRE1 pathway occurs in HeLa cells infected with *B. abortus* at 24 and 48 h p.i. However, the use of siRNA directed against IRE1 did not have any effect on the induction of BNIP3L nor on mitochondrial fragmentation induced by *B. abortus* in HeLa cells.

In conclusion, in this work, we showed that the mitochondrial fragmentation and mitophagy triggered by *Brucella* during its intracellular trafficking in the host cells might be mediated by BNIP3L but not Parkin.

Mémoire de master 120 en biochimie et biologie moléculaire et cellulaire

Janvier 2022

Promoteur: Thierry Arnould

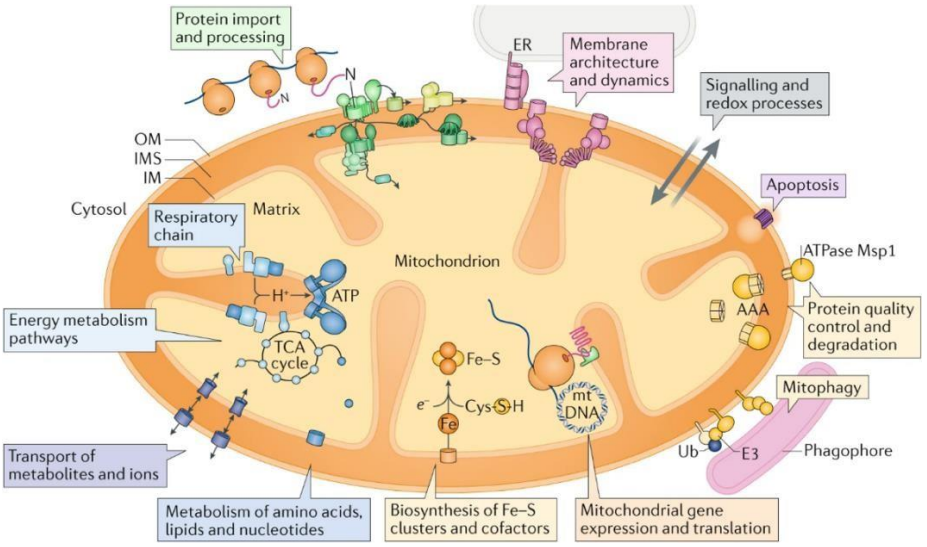

Figure 10: Overview of mitochondrial functions (Pfanner et al., 2019).
A range of functions has been attributed to the mitochondria thanks to the number of proteins and protein complexes that are found in its membranes. The different functions are energy metabolism with respiration and production of ATP; metabolism of amino acids, lipids and nucleotides; biosynthesis of iron–sulfur (Fe–S) clusters and cofactors; expression of the mitochondrial genome; quality control and contribution to the degradation processes including mitophagy and apoptosis; signalling and redox processes; membrane architecture and dynamics. Complexes will also allow the entry and processing of precursors that have been translated by cytosolic ribosomes.
AAA, ATP-dependent proteases of the inner membrane; E3, ubiquitin-protein ligase; ER, endoplasmic reticulum; mtDNA, mitochondrial DNA; TCA, tricarboxylic acid; Ub, ubiquitin.

REMERCIEMENT

C'est en arrivant au bout de ces 10 mois que l'on arrive à prendre un peu de recul pour observer tout ce beau chemin parcouru. Il n'a certes pas toujours été bien plat mais c'est ce qui en fait sa beauté. Tout au long de ce cheminement, j'ai été accompagné par de belles personnes qui laisseront à tout jamais une trace indélébile.

Je souhaite tout d'abord remercier l'ensemble des professeurs de l'URBC pour l'accueil chaleureux au sein de leur laboratoire. Je tiens également à remercier tout particulièrement mon promoteur Thierry Arnould pour ses conseils précieux, ses nombreuses corrections, son soutien, ses encouragements et son exigence scientifique qui m'ont permis d'évoluer dans le monde de la recherche bien plus que ce que je n'aurai pu imaginer en commençant. Je tiens à remercier également mon co-promoteur Xavier De Bolle, pour m'avoir accueilli dans son labo en URBM.

Aucun merci ne pourra être à la hauteur, pour remercier Jérémy Verbeke, mon tuteur. Il a pu m'accompagner tout au long de ce parcours avec une extrême gentillesse, une générosité et une disponibilité sans faille. Il nous a fait découvrir le magnifique monde de la recherche, nous a transmis son savoir en toute humilité et nous a merveilleusement soutenu tout au long de ce parcours. J'espère avoir été à la hauteur de tes attentes. Merci pour tout.

Ensuite, la team *Brucella* ne serait pas une team sans mon super, fidèle compatriote, collègue et ami Youri Fayt. Il a été d'une aide et d'un soutien précieux tout au long de ce mémoire. Je tiens également à le féliciter pour son travail, sa détermination et ses innombrables lectures d'article qui m'ont toujours beaucoup impressionné. Nous avons formé une belle équipe de choc, alors merci.

J'aimerai ensuite remercier l'ensemble des Doctorants pour leur soutien, leur conseil mais également tous ses moments partagés tout au long de ce mémoire. Ces moments de sérieux, ou non, qui ont contribués à rendre ce mémoire beaucoup plus pétillant.

Et puis sans oublier l'ensemble des mémorants qui ont été ma petite famille pendant ces 10 mois. Merci pour ces moments de rire, de fou rire, de joie, de stress partagé, de consolation et j'en passe. Vous avez été de véritable pilier pour cette belle aventure. Vous occupez tous une place toute particulière dans mon petit cœur et j'espère vivre de nombreuses et belles aventures avec vous dans les années à venir.

Enfin j'aimerai remercier l'ensemble de mes amis et de ma famille pour m'avoir soutenue, encouragée, d'avoir accepté ces moments d'éloignement, d'avoir effacé les moments de doutes.

Merci à vous pour tous les gestes et moments qui ont contribué d'une manière ou d'une autre à ce mémoire.